

Universität
Rostock



Traditio et Innovatio

Synthesis and Characterisation of Cyclic Polyphosphanes

Cumulative Dissertation

to acquire the academic degree
doctor rerum naturalium (Dr. rer. nat.)
of the Faculty of Mathematics and Natural Sciences
at the University of Rostock

submitted by Jonas Bresien, born on 1 February 1988 in Schwerin
Rostock, 01 March 2016

The present work was accomplished at the Department of Chemistry of the University of Rostock, at the chair for Inorganic Chemistry in the work group of Professor Dr Axel Schulz during the period from October 2013 to March 2016.

Reviewer #1: Professor Dr Axel Schulz, Universität Rostock

Reviewer #2: Professor Dr Manfred Scheer, Universität Regensburg

Reviewer #3: Professor Dr Christian Müller, Freie Universität Berlin

Date of thesis defence: 14 June 2016

Statement of Authorship

Ich versichere hiermit an Eides statt, dass ich die vorliegende Arbeit selbstständig angefertigt und ohne fremde Hilfe verfasst habe. Dazu habe ich keine außer den von mir angegebenen Hilfsmitteln und Quellen verwendet und die den benutzten Werken inhaltlich und wörtlich entnommenen Stellen habe ich als solche kenntlich gemacht.

I hereby affirm that I have written the present work by myself without outside assistance. No resources were utilised other than those stated. All references as well as verbatim extracts were quoted and all sources of information were specifically acknowledged.

Rostock, 01 March 2016

Jonas Bresien

Acknowledgements

I am especially indebted to **Professor Dr Axel Schulz** for the exciting and challenging topic of my work, for the extensive scientific freedom I could enjoy in the lab, for plenty helpful and informative discussions, and not least for the opportunity to attend lots of highly fascinating conferences on main group chemistry! Likewise, I would like to express my gratitude for Axel's outstanding lectures, which have engaged my interest in inorganic chemistry and all its aspects; without that, surely I could not have realised this work.

Special thanks are also due to **Dr Alexander Villinger** for training me on the X-ray diffractometer and teaching me how to solve and refine crystal structures. This was certainly one of the most interesting and helpful aspects of my PhD period. Moreover, I am equally thankful to Alex for teaching me how to work thoroughly and scientifically, as well as for his inspiring advice that has certainly had a great influence on this work.

I wish to thank **Kirill Faust**, who did outstanding work under my supervision and thus contributed greatly to the development of my research. Similarly, I would like to thank **Richy Hauptmann** for continuing the zinc phosphides project which is not part of this work.

I would like to express my thanks to my former co-workers **Dr Christian Hering-Junghans**, **Dr Fabian Reiß**, and **Dr Alexander Hinz** for their advice and interest in my work, for training me on our analytical equipment, as well as for a great time in the lab! Furthermore, I thank **Dr Ronald Wustrack** for technical support with our computer equipment. I am grateful to **Sören Arlt**, **Kerstin Bohn**, **Dr Jörg Harloff**, **René Labbow**, **Anne-Kristin Rölke**, **Kati Rosenstengel**, **Julia Rothe**, **Alrik Stoffers**, and **Max Thomas** for an excellent working atmosphere. Likewise, I wish to thank all members of the work group for good collaboration and mutual assistance in the laboratory.

I am indebted to the analytical department for the acquisition of a plethora of data that were required to fully characterise all reported compounds. I would like to thank **Isabel Schicht** for her assistance with X-ray measurements, **Dr Dirk Michalik**, **Brigitte Goronzi**, and **Heike Borgwaldt** for the acquisition of NMR spectra according to all my wishes, **Petra Duncker** for the measurement of CHN analyses, as well as **Dr Christine Fischer** and **Sigrun Roßmeisl** for the acquisition of mass spectra.

Special thanks also go to the work group's secretary **Nadja Kohlmann**, the department's mechanics **Peter Kumm** and **Martin Riedel**, the electrician **Thomas Kröger**, as well as the glassblowers **Roland Weihs** and **Patrick Quade**.

I would like to thank **Malte Willert** and **Matthias Linke** of the ITMZ for their assistance concerning the cluster computer and for continuously answering all my questions about the API of the queuing system.

Last but not least I wish to thank **all my family** for their unconditional support, love and care. I am grateful beyond measure that I was given the opportunity to attend university and follow my own interests during my studies.

Elisa, thank you for your patience and for giving me the strength to accomplish this work! Your love and support have been a vital contribution to the success of my PhD thesis, and our wonderful time together is and has always been a great source of motivation!

Thanks to everyone who contributed to the success of my work!

Summary

This dissertation reports on the synthesis and reactivity of the novel cyclotetraphosphane $[\text{ClP}(\mu\text{-PMes}^*)]_2$. Its synthesis could be accomplished by treating Mes^*PH_2 with PCl_3 in the presence of NEt_3 . The cyclophosphane proved to be a versatile reagent in phosphorus chemistry, since its Cl-functionalised P_4 backbone could be used as a building block in a variety of reactions with Lewis acids, bases as well as reducing agents. Hence, it was possible to find access to a novel bicyclic phosphino-phosphonium framework, a tricyclic hexaphosphane, a dinuclear silver complex as well as new approaches to the selective synthesis of bicyclic tetraphosphanes. The rearrangement of P–P bonds as well as a 1,2-Cl shift were identified as common reaction pathways to stabilise the products. All synthesised compounds were fully characterised, including experimental and theoretical methods.

Zusammenfassung

Die vorliegende Dissertation beschäftigt sich mit der Synthese und Reaktivität des neuartigen Cyclotetraphosphans $[\text{ClP}(\mu\text{-PMes}^*)]_2$. Dessen Synthese konnte durch die Umsetzung von Mes^*PH_2 mit PCl_3 in Gegenwart von NEt_3 realisiert werden. Das Cyclophosphan stellte sich als vielseitiges Reagenz in der Phosphorchemie heraus, da sein Cl-funktionalisiertes P_4 -Rückgrat als Baustein in einer Vielzahl von Reaktionen mit Lewis-Säuren und -Basen sowie Reduktionsmitteln Anwendung finden konnte. Derart war es möglich, Zugang zu einem neuartigen bicyclischen Phosphino-Phosphonium-Gerüst, tricyclischen Hexaphosphan sowie dinuklearen Silberkomplex zu finden und neue Methoden zur selektiven Herstellung von bicyclischen Tetraphosphanen zu entwickeln. Die Umlagerung von P–P-Bindungen sowie eine 1,2-Cl-Umlagerung wurden als typische Reaktionspfade zur Stabilisierung der Produkte identifiziert. Alle hergestellten Verbindungen wurden vollständig charakterisiert, sowohl mittels experimenteller als auch theoretischer Methoden.

To Elisa

Table of Contents

1	Target and Motivation	1
2	Introduction	3
2.1	Pnictogen-Nitrogen Ring Systems	3
2.2	Cyclic Phosphanes.....	5
2.3	Computational Details	9
3	Results and Discussion	13
3.1	Synthesis of $[\text{ClP}(\mu\text{-PMes}^*)]_2$	13
3.2	Reactivity Towards GaCl_3	19
3.3	Reactivity Towards $\text{Ag}[\text{WCA}]$	22
3.4	Reactivity Towards Lewis Bases	25
3.5	Reactivity Towards Reducing Agents.....	28
3.6	Further Syntheses of Bicyclic Tetraphosphanes	32
4	Summary and Outlook.....	35
5	References	37
6	Selected Publications.....	45
6.1	Dimers and Trimers of Diphosphanes: A Wealth of Cyclophosphanes.....	46
6.2	Low-Temperature Isolation of the Bicyclic Phosphinophosphonium Salt $[\text{Mes}^*_2\text{P}_4\text{Cl}][\text{GaCl}_4]$	56
6.3	Low-Temperature Isolation of a Dinuclear Silver Complex of the Cyclotetraphosphane $[\text{ClP}(\mu\text{-PMes}^*)]_2$	62
6.4	A Tricyclic Hexaphosphane	67
6.5	Synthetic Strategies to Bicyclic Tetraphosphanes using P_1 , P_2 and P_4 Building Blocks	72
7	Appendix	83
7.1	$[\text{ClP}(\mu\text{-PMes}^*)]_2$ – A Versatile Reagent in Phosphorus Chemistry.....	83
7.2	Source Code of the Submission Script.....	91

List of Abbreviations

AO	atomic orbital	LP	lone pair of electrons
approx.	approximately	LUMO	lowest-lying unoccupied MO
<i>ca.</i>	circa	<i>m</i>	meta
CAAC	cyclic alkylaminocarbene	μ -	bridging group (in formulae)
calcd.	calculated	Mes	mesityl (2,4,6-trimethylphenyl)
cat.	catalyst	Mes*	supermesityl (2,4,6-tri- <i>tert</i> -butylphenyl)
<i>cf.</i>	compare (lat. <i>conferre</i>)	MO	molecular orbital
cov.	covalent	NBO	natural bond orbital
Cp	cyclopentadienyl	NHC	<i>N</i> -heterocyclic carbene
Cp*	pentamethylcyclopentadienyl	NLMO	natural localised MO
Cy	cyclohexyl	NMR	nuclear magnetic resonance
DBU	1,8-diazabicyclo[5.4.0]undec- 7-ene	NPA	natural population analysis
DFT	density functional theory	<i>o</i>	ortho
dmap	4-dimethylaminopyridine	<i>p</i>	para
dmb	dimethylbutadiene	ref.	reference
Dmp	2,6-dimethylphenyl	R ^F	hexafluoroisopropyl (CH(CF ₃) ₂)
<i>e.g.</i>	for example (lat. <i>exempli gratia</i>)	RT	room temperature
ELF	electron localisation function	sim.	simulated
equiv.	equivalent	<i>t</i> -Bu	<i>tert</i> -butyl
<i>et al.</i>	and others (lat. <i>et alii/aliae</i>)	Ter	terphenyl (2,6-dimesitylphenyl)
exptl.	experimental	Ter'	2,6-bis(2,6-diisopropylphenyl)- phenyl
GIAO	gauge-independent AO	Tf	triflyl (CF ₃ SO ₂)
HOMO	highest-lying occupied MO	THF	tetrahydrofuran
<i>i.e.</i>	that is (lat. <i>id est</i>)	TMEDA	tetramethylethylenediamine
<i>i</i> -Pr	isopropyl	vdW	van der Waals
IR	infrared spectroscopy	WCA	weakly coordinating anion
LA	Lewis acid	xs	excess
LB	Lewis base		

Units of Measurement

The International System of Units (SI) is utilised throughout this work to measure experimental or theoretical quantities. All derived units and their expression in terms of the SI base units are given below:

Quantity	Unit	Name	Conversion to SI base units
Frequency	MHz	Megahertz	$1 \text{ MHz} = 1 \times 10^6 \text{ s}^{-1}$
	Hz	Hertz	$1 \text{ Hz} = 1 \text{ s}^{-1}$
Length	Å	Ångström	$1 \text{ Å} = 1 \times 10^{-10} \text{ m}$
Power	mW	Milliwatt	$1 \text{ mW} = 1 \times 10^{-3} \text{ kg m}^2 \text{ s}^{-1}$
Temperature	°C	Degree Celsius	$T/K = T/^\circ\text{C} - 273.15$
Volume	mL	Millilitre	$1 \text{ mL} = 1 \text{ cm}^3 = 1 \times 10^{-6} \text{ m}^3$
Energy	kJ	Kilojoule	$1 \text{ kJ} = 1 \times 10^3 \text{ m}^2 \text{ kg s}^{-2}$
Wavenumber	cm^{-1}	Reciprocal centimetre	$1 \text{ cm}^{-1} = 100 \text{ m}^{-1}$
Time	d	Day	$1 \text{ d} = 8.64 \times 10^4 \text{ s}$
	h	Hour	$1 \text{ h} = 3.6 \times 10^3 \text{ s}$
	min	Minute	$1 \text{ min} = 60 \text{ s}$

1 Target and Motivation

The objective of this work was to develop a suitable lab scale synthesis for halo-substituted cyclophosphanes, especially cyclotetraphosphanes of the type $[\text{XP}(\mu\text{-PR})]_2$ (X = (pseudo)halogen, R = organic substituent; Scheme 1), and investigate their chemistry. The latter can be regarded as homologues of the well-studied cyclodipnictadiazanes $[\text{XE}(\mu\text{-NR})]_2$ (E = P, As, Sb, Bi), thus the similarities and differences in their respective reactivities were of interest, in particular with respect to abstraction or substitution of the halogen substituents. By this means, possible application of these ring systems as formal R-PP^+ synthon was to be evaluated.



Scheme 1. Whereas the chemistry of dihalo-substituted cyclodipnictadiazanes (left) is well investigated, little is known about the homologous cyclotetraphosphanes of the type $[\text{XP}(\mu\text{-PR})]_2$ (right).

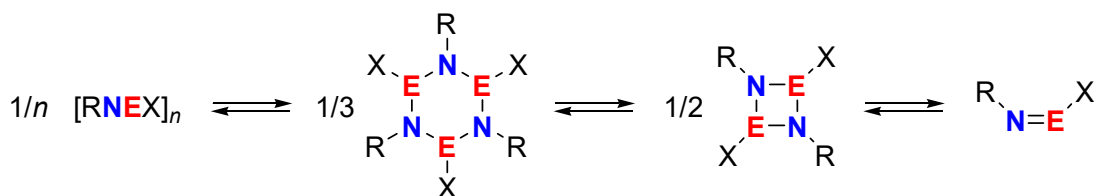
Furthermore, the synthesis of polycyclic phosphane scaffolds was of interest. Such systems are often derived from white phosphorus, which is, however, hard to obtain commercially. Moreover, the product distribution of P_4 activation processes is often difficult to control, so alternative reaction pathways from other precursors were desirable. To this end, P_1 precursors such as PCl_3 and R-PH_2 were to be utilised, as well as functionalised ring systems that might allow a selective synthesis of polycyclic scaffolds.

All synthesised compounds were to be fully characterised by single crystal X-ray diffraction, vibrational spectroscopy (IR, Raman) and NMR spectroscopy. Moreover, DFT calculations were intended to give insight into the chemical bonding and electronic structure of the compounds to improve the understanding of their chemical reactivity. For this purpose, the *Gaussian 09* program suite was supposed to be installed on the new compute cluster of the university. A scripted interface to the *SLURM* workload manager was to be developed, so all parameters needed for the allocation of computer resources could be automatically derived from the Gaussian input, and to facilitate easy submission of *Gaussian* jobs using a simple command line keyword.

2 Introduction

2.1 Pnictogen-Nitrogen Ring Systems

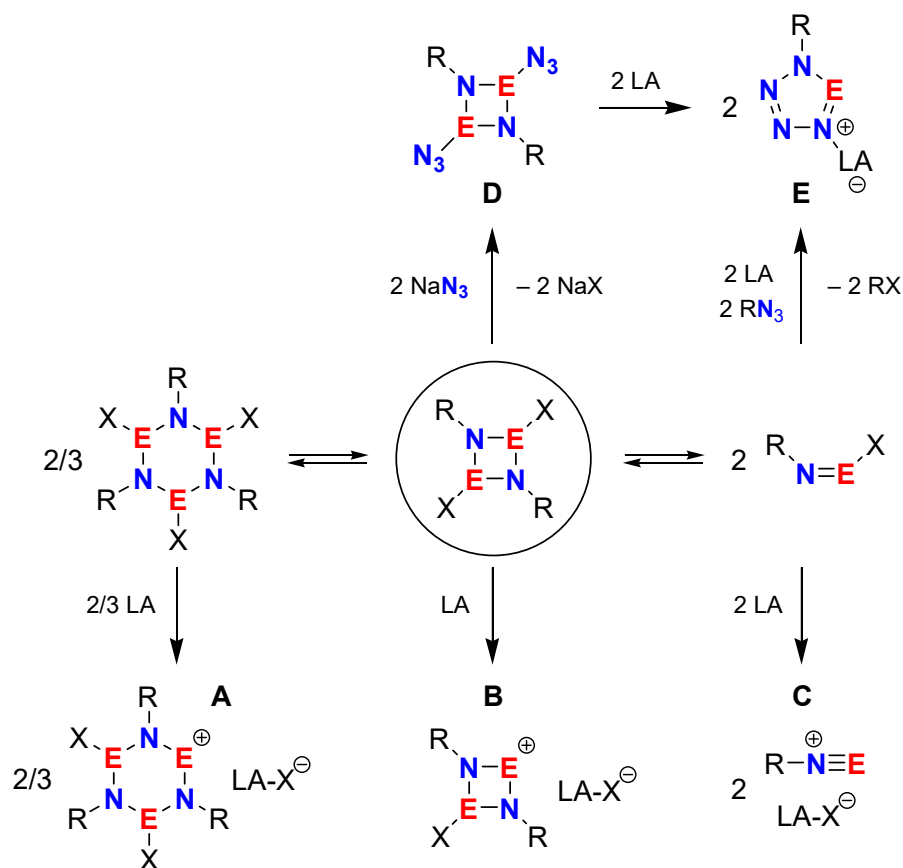
The synthesis and reactivity of pnictogen-nitrogen ring systems is a fascinating and by now thoroughly investigated field of main group chemistry.^[1-5] Starting in 1894 with Michaelis' and Schroeter's report on the synthesis of "phosphazobenzene chloride",^[6] pnictogen-nitrogen cycles have been in the focus of chemical research until today. Especially for synthetic chemistry, cyclodipnictadiazanes of the type $[\text{XE}(\mu\text{-NR})]_2$ (E = P, As, Sb, Bi; X = (pseudo)halogen; R = sterically demanding substituent) are of great interest due to their versatile reactivity: Depending on the size of the substituent R, a formal equilibrium between the monomeric unit $\text{RN}=\text{EX}$, the dimeric four-membered ring system $[\text{XE}(\mu\text{-NR})]_2$, the trimeric six-membered ring system $[\text{XE}(\mu\text{-NR})]_3$ and higher oligomers $[\text{XE}(\mu\text{-NR})]_n$ can be discussed (Scheme 2),^[7-10] giving rise to a variety of different reaction channels.



Scheme 2. Formal equilibrium between oligomeric and monomeric iminopnictanes depending on the sterical demand of the substituent R (E = P, As, Sb, Bi; X = (pseudo)halogen; R = sterically demanding substituent).

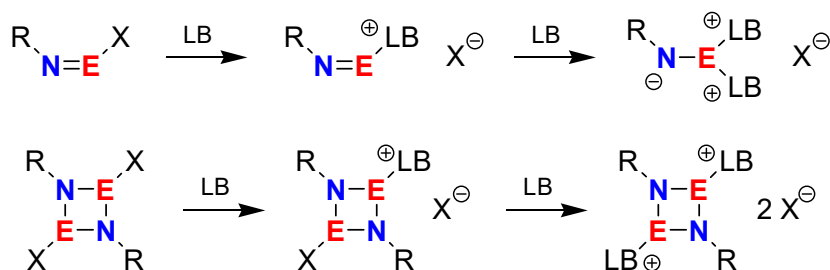
For example, the halogen substituents can be abstracted by treatment with Lewis acids such as GaCl_3 , leading to the formation of cyclic, cationic pnictazenes (**A** and **B** in Scheme 3)^[9,11-15] or even acyclic pnicta-diazonium cations with an N–E triple bond, of which the phosphorus and arsenic derivatives are known to date (**C** in Scheme 3).^[16-22] Treatment with azides results in the generation of five membered ring systems (**E** in Scheme 3), e.g. by [3+2] cycloaddition or ring expansion reactions (*via D*).^[11,22-26] The concept of [3+2] cycloaddition can also be applied to so-called “disguised” dipolarophiles and 1,3-dipoles, *i.e.* the reactive species are formed *in*

situ from a suitable precursor molecule such as (Me₃Si)₂N–N(SiMe₃)–PCl₂. In this vein, different five membered ring systems, such as triazadiphospholes, are accessible.^[12,24,27,28]



Scheme 3. Cyclodipnictadiazanes as prototypical building blocks in pnictogen-nitrogen chemistry. Reaction with Lewis acids (LA).

Upon substitution of cyclodipnictadiazanes or iminopnictanes with good leaving groups such as the triflate moiety (*i.e.* X = OTf), the reaction with Lewis bases yields base stabilised adduct cations, demonstrating the possibility of nucleophilic substitution at the pnictogen centre (Scheme 4).^[19,21,29,30]

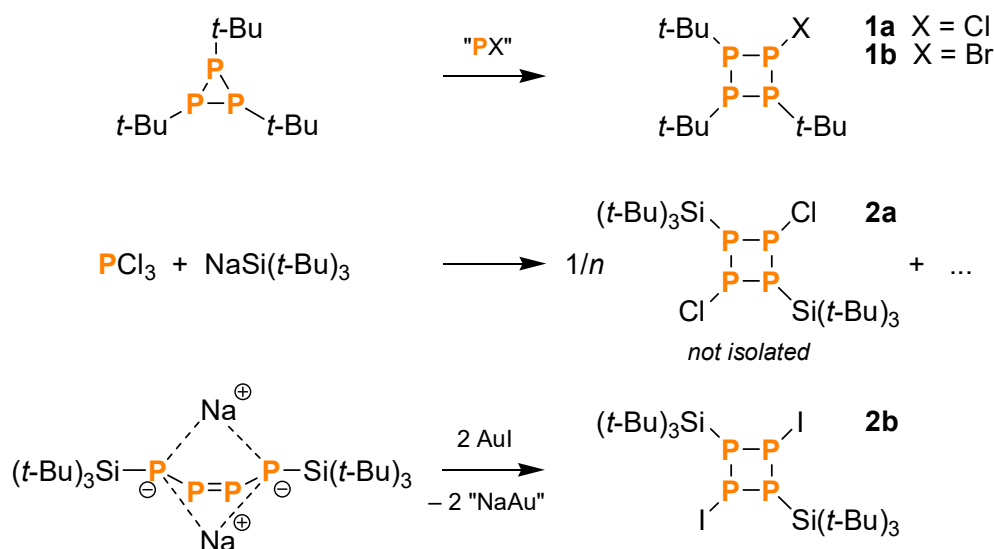


Scheme 4. Cyclodipnictadiazanes as prototypical building blocks in pnictogen-nitrogen chemistry. Reaction with Lewis bases (LB).

Typically, cyclodipnictadiazanes can be prepared in good yields starting from R–NH₂ and ECl₃ by a two-step elimination reaction *via* R–N(H)–ECl₂.^[4,7,25,31–33] Thus being easily accessible, they can be regarded as prototypical building blocks in pnictogen-nitrogen chemistry. Therefore, we aimed at a systematic development of the chemistry of the homologous cyclotetraphosphanes of the type [XP(μ-PR)]₂, which have been barely studied so far, and, by analogy with the pnictogen-nitrogen systems, might prove to be versatile reagents in phosphorus chemistry.

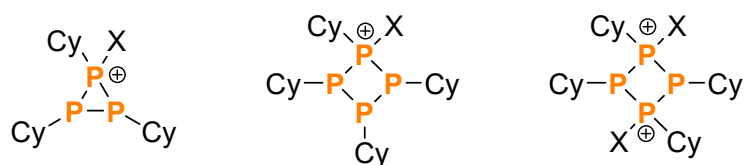
2.2 Cyclic Phosphanes

While the chemistry of phosphorus ring systems with organic, silyl or amino substituents is well investigated,^[34–36] functionalised cyclophosphanes with halogen substituents, in particular four membered ring systems, are rather rare. The only previous reports date back to the last three decades: The ring system (t-BuP)₃PX (**1a**, **b**; X = Cl, Br) was first observed spectroscopically by Baudler *et al.* in the 1980s,^[37,38] before it could be isolated and fully characterised by Binder *et al.* in 1994/95 (Scheme 5, top).^[39,40] Differently substituted derivatives containing an R₃P₄Cl scaffold were also reported within the same timeframe.^[41] Additionally, two dihalo-cyclotetraphosphanes of the type [XP(μ-PR)]₂ were reported by the groups of Wiberg and Lerner in the last decade; however, the compound [ClP(μ-PSi(t-Bu)₃)]₂ (**2a**; Scheme 5, middle) could only be detected by NMR spectroscopy and was not isolated,^[42] whereas the iodo derivative [IP(μ-PSi(t-Bu)₃)]₂ (**2b**; Scheme 5, bottom) was fully characterised seven years later.^[43]



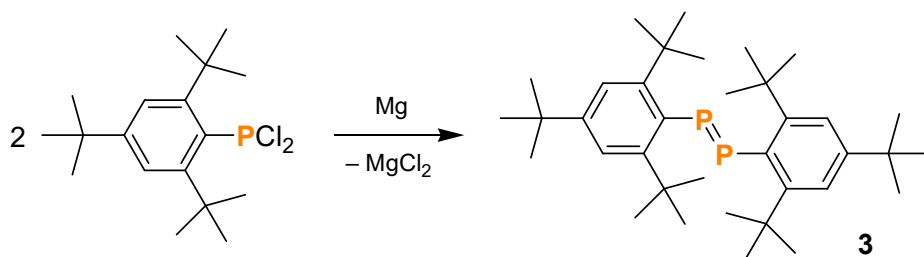
Scheme 5. Literature reported halo-substituted cyclotetraphosphanes.

Furthermore, some three-membered ring systems with halogen substituents were synthesised in the 1980s; however, these systems were mainly characterised on the basis of NMR spectroscopy and structural evidence is missing.^[38,44,45] Apart from those neutral species, Weigand, Burford and co-workers also reported on cationic, cyclic phosphino-phosphonium frameworks incorporating a halo-substituted phosphonium centre (Scheme 6).^[46]



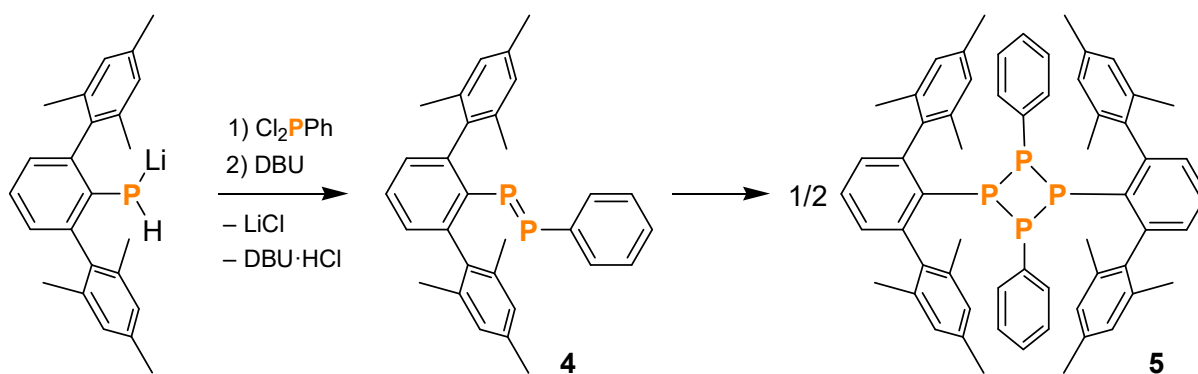
Scheme 6. Examples of halo-substituted phosphino-phosphonium frameworks (X = Cl, I).

By analogy with iminopnictanes, diphosphenes can be regarded as formal monomeric units of cyclotetraphosphanes. Similarly, the P–P double bond can only be stabilised by sterically demanding substituents, as demonstrated by the work of Yoshifuji *et al.*, who were able to isolate and characterise the first diphosphene $\text{Mes}^*\text{P}=\text{PMes}^*$ (**3**; $\text{Mes}^* = 2,4,6\text{-tri-}t\text{-butylphenyl}$, Scheme 7) in 1981.^[47,48] Even though Köhler and Michaelis had already reported on “phosphobenzene” ($\text{PhP}=\text{PPh}$) in 1877,^[49] this compound was later identified as cyclic $(\text{PhP})_n$ ($n = 4, 5$),^[50] which can be attributed to the lack of kinetic protection.



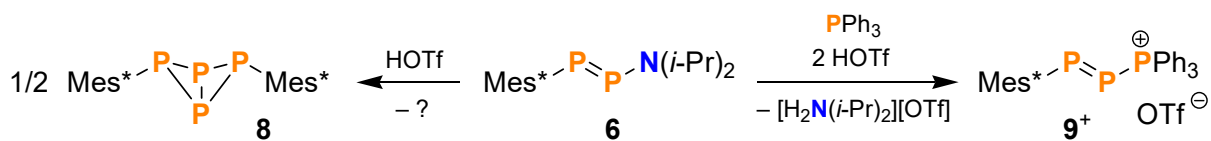
Scheme 7. Synthesis of the diphosphene **3** bearing the bulky Mes^* group that prevents dimerisation.

More diphosphenes with different sterically demanding substituents such as Cp^* (pentamethylcyclopentadienyl) or Ter (2,6-dimesitylphenyl) were reported,^[51–61] including a study on the diphosphene $\text{TerP}=\text{PPh}$ (**4**), which could be observed in solution but underwent rapid dimerisation to the cyclotetraphosphane $[\text{PhP}(\mu\text{-PTer})]_2$ (**5**, Scheme 8).^[60] In this respect, diphosphenes can be regarded as suitable precursors for the synthesis of cyclotetraphosphanes, as the formation of one or the other depends on the size of the (sterically demanding) substituent R, comparable to the analogous pnictogen-nitrogen compounds.



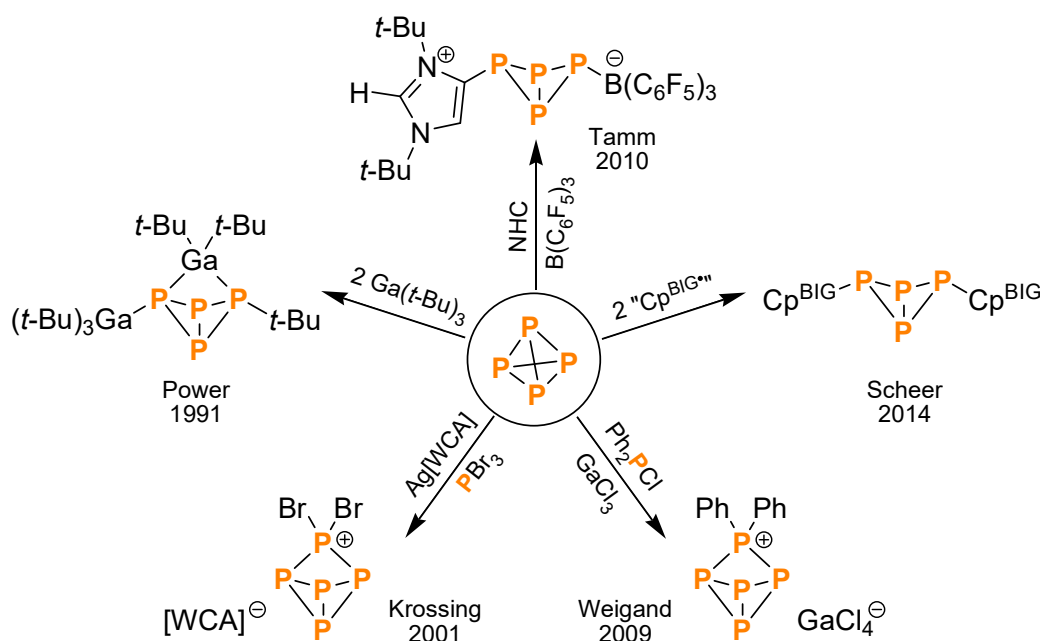
Scheme 8. The diphosphene **4** is substituted by a sterically demanding Ter and a small Ph group. Dimerisation leads to the cyclotetraphosphane **5** (DBU = 1,8-diazabicyclo[5.4.0]undec-7-ene).

Most interesting in this concern are two reports by Romanenko *et al.*, wherein the authors describe the reactivity of the diphosphene Mes*P=PN(*i*-Pr)₂ (**6**) towards Brønsted acids: Upon treatment of **6** with HCl (2 equiv.) at low temperatures, the diphosphene Mes*P=PCl (**7**) was generated *in situ*; however, no analytical data was given to prove its existence.^[54] On the other hand, when reacting **6** with HOTf (1 equiv.), the bicyclic tetraphosphanes Mes*P₄Mes* (**8**) and, allegedly, Mes*P₄N(*i*-Pr)₂ were obtained, the former of which had previously been described by Fluck *et al.*^[62] The exact reaction pathway, especially the fate of the missing electrons from the overall equation, remains unclear, though (Scheme 9, left).^[63] Intriguingly, when **6** was treated with HOTf (2 equiv.) in the presence of PPh₃, the unusual cation [Mes*P=P(PPh₃)]⁺ (**9**⁺) was obtained, which was described as a base stabilised diphospha-diazonium cation (Scheme 9, right).^[63]

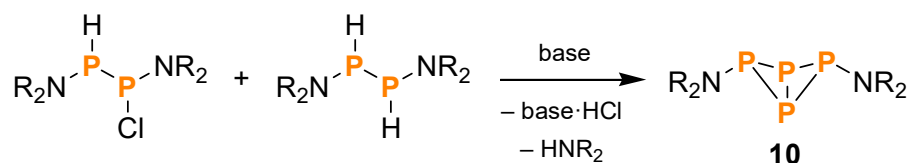


Scheme 9. Reactions of Mes*P=PN(*i*-Pr)₂ (**6**) with HOTf.

Polycyclic phosphanes similar to compound **8** are not uncommon in phosphorus chemistry. In most cases, such systems were synthesised by direct activation of white phosphorus, *e.g.* by use of Lewis acids and bases, metals, radicals, or singlet carbenes (Scheme 10).^[5,35,36,64–72] Syntheses starting from P_n (*n* = 1, 2, 4) precursor molecules, however, are rather unusual. The first bicyclic tetraphosphane, (Me₃Si)₂N–P₄–N(SiMe₃)₂ (**10**), which was reported by Niecke *et al.* in 1982, is one of the rare examples that was not derived from P₄, but from a diphosphane precursor (Scheme 11).^[73]

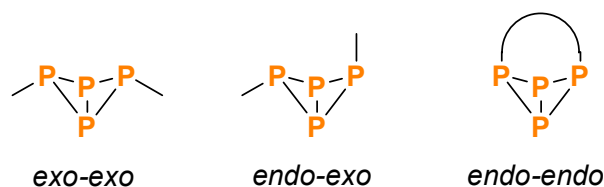


Scheme 10. Some examples of P₄ activation leading to polycyclic structures (NHC = *N*-heterocyclic carbene, Cp^{BIG} = pentakis(4-*n*-butylphenyl)-cyclopentadienyl, WCA = [Al(OC(CF₃)₃)₄]⁻).



Scheme 11. Synthesis of the first bicyclic tetraphosphane **10** (R = SiMe₃).

Due to their rigid P₄ backbone, bicyclic tetraphosphanes typically display two different arrangements of the substituents, namely the *exo-exo* and *endo-exo* isomers (Scheme 12). Owing to the generally large substituents, the unusual *endo-endo* arrangement could only be realised by bridging groups so far.^[13,68,74] Most commonly found are *exo-exo* substituted tetraphosphabicyclobutanes, indicating that they are energetically favoured.



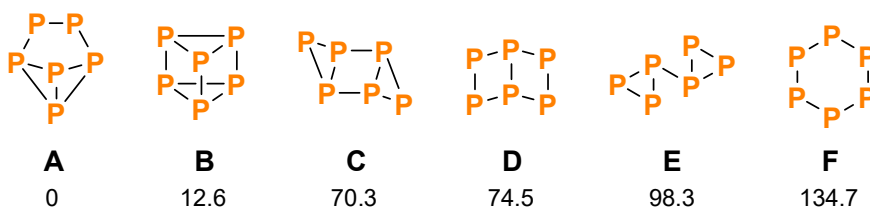
Scheme 12. Isomers of tetraphosphabicyclobutanes. The *exo-exo* substitution pattern is most common.

For instance, an *endo-endo*-type structure is incorporated in the tricyclic hexaphosphane Cp*₂P₆ (**11**, Scheme 13),^[74] which was reported by Jutzi and co-workers in 1989.^[75,76] It is a rare

example of a polycyclic hexaphosphane,^[71,77,78] even though a variety of structural motifs have been predicted for neutral P₆ (A-F in Scheme 14)^[79] that indicate possible structural motifs for substituted phosphanes of the type R_nP_m ($m > n$).



Scheme 13. Structure of Cp*₂P₆ (**11**, left). The P₆ scaffold resembles the structure of benzvalene (right).



Scheme 14. Computed minimum structures of P₆ in the gas phase. Relative energies given in kJ/mol.^[79]

Compound **11** was synthesised by reductive elimination of Cp* substituents from *cyclo*-(Cp*P)₃, indicating that this method might be a viable way to synthesise polycyclic phosphanes from cyclophosphane precursors. Consequently, the investigation of this kind of reactivity concerning systems of the type [XP(μ -PR)]₂ was also of interest in this work.

2.3 Computational Details

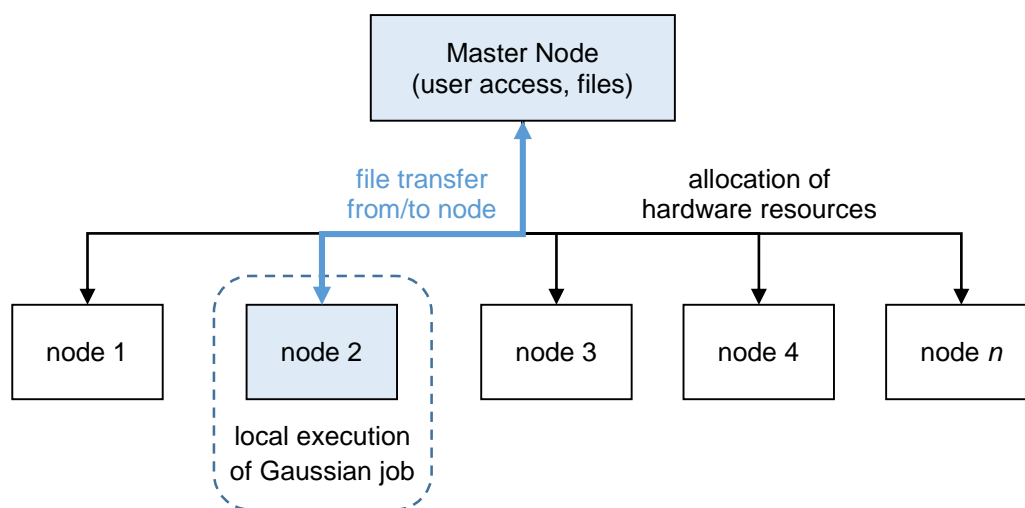
All computations were carried out using the *Gaussian 09* program suite^[80] and the standalone version of *NBO 6.0*.^[81] The Kohn-Sham orbitals were calculated using the hybrid DFT functional PBE0^[82–84] and different types of basis sets according to the problem (usually 6-31G(d,p) or aug-cc-pVDZ;^[85–100] notation PBE0/6-31G(d,p) or PBE0/aug-cc-pVDZ). For energy calculations, the core electrons of heavy atoms (third period or up) were described by an effective core potential. All structures were fully optimised and confirmed as minima by frequency analyses; the calculated frequencies were scaled by appropriate scaling factors.^[101] Partial charges were derived by Natural Population analysis using the NBO program. Chemical shifts and coupling constants were derived by the GIAO method,^[102–106] the calculated absolute shifts ($\sigma_{\text{calc},X}$) were referenced to the experimental absolute shift of 85 % H₃PO₄ in the gas phase ($\sigma_{\text{ref},1} = 328.35$ ppm),^[107] using PH₃ ($\sigma_{\text{ref},2} = 594.45$ ppm) as a secondary standard:^[108]

$$\begin{aligned}\delta_{\text{calc},X} &= (\sigma_{\text{ref},1} - \sigma_{\text{ref},2}) - (\sigma_{\text{calc},X} - \sigma_{\text{calc},\text{PH}_3}) \\ &= \sigma_{\text{calc},\text{PH}_3} - \sigma_{\text{calc},X} - 266.1 \text{ ppm}\end{aligned}$$

The calculated absolute shift of PH₃ ($\sigma_{\text{calc},\text{PH}_3}$) amounted to +604.92 ppm (PBE0/6-31G(d,p)) or +633.04 ppm (PBE0/aug-cc-pVDZ).

To efficiently calculate all electronic properties of the synthesised compounds, the *Gaussian 09* software suite had to be installed on the cluster computer. As indicated in chapter 1, this involved the development of a submission script that would automatically determine the hardware resources needed for the calculation from the *Gaussian* input file. Additionally, all file operations had to be handled by the script, *i.e.* copying the input and checkpoint files to the local hard drive of the cluster node before job execution and saving the output files to the user's storage space afterwards (Scheme 15).

On the old cluster system, the amount of memory and CPU cores had to be manually specified when submitting a new *Gaussian* job. Additional file operations had to be carried out using a manually edited script file, which was obviously prone to errors. Therefore, the new script was intended to be used by a simple command line keyword, so other members of the work group and the department would also benefit from the easy and robust submission process.



Scheme 15. Simplified scheme of the cluster setup.

The script was written in *bash*, as it easily allows the interpretation of text files using a variety of commands such as *grep* or *sed*. In the first step, the *Gaussian* input is evaluated with respect to the *%mem* and *%nprocs* commands; thus, the requested hardware resources are obtained. This information is stored in a small instruction file for *SLURM* (Simple Linux Utility for

Resource Management), which controls the allocation of hardware resources. In the second step, *i.e.* when the *Gaussian* job is executed on a cluster node, the script interprets the file related *Link0* commands in the *Gaussian* input (*%chk*, *%rwf* and *%nosave*) and copies the requested files onto the local hard drive of the cluster node. (Otherwise, the files would be located on a network storage, which reduces performance.) Additionally, the script stores the information which of these files should be discarded after job completion (*%nosave*).

As soon as the *Gaussian* job finishes successfully, all files are copied back to their original destination. If, however, the time limit of the cluster (72 h) is exceeded beforehand, the checkpoint and read-write files are saved and the job is automatically re-queued for continuation using *Gaussian*'s *restart* keyword. The necessary input is generated automatically from the initial input file. This is repeated until the *Gaussian* job finishes successfully (or else aborts with an error). Especially for frequency analyses on large molecules, this proved to be rather convenient. The behaviour of the submission script can additionally be influenced by optional switches. An overview is given in Scheme 16. The complete source code can be found in the appendix (chapter 7.2).

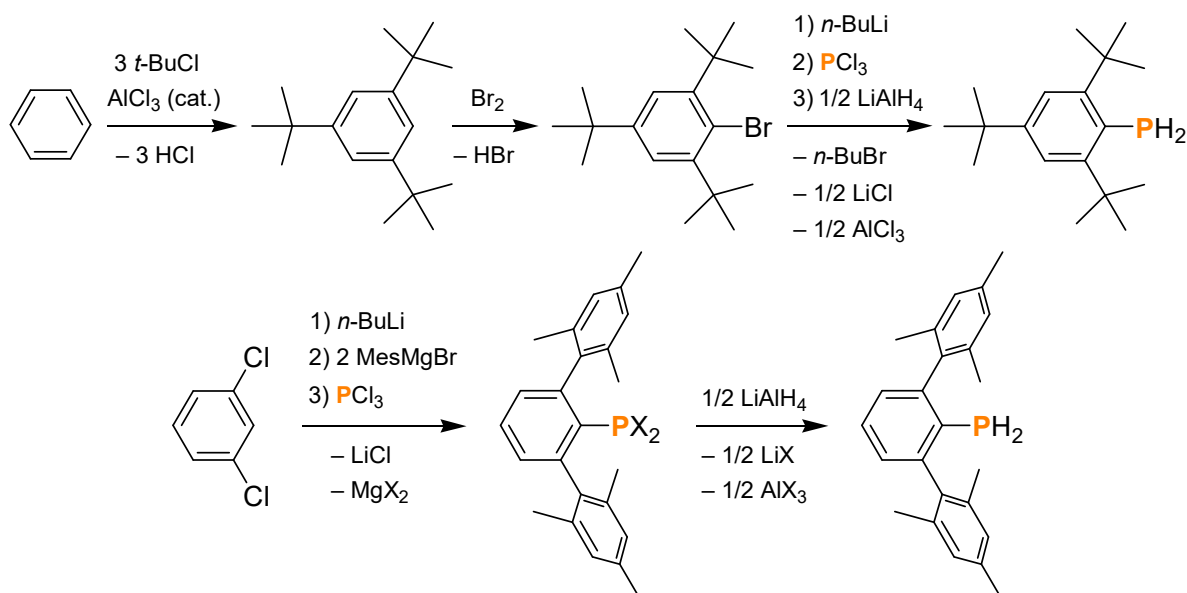
```
run_g09 [-option] input_file
-e Specifies the e-mail address which should be used for status
  updates. The address may also be stored in ~/email_addr
-t CPU time in hours (max. 72)
-s Checkpointing time in minutes (default: 20)
-a Specifies that a job should only be executed after successful
  completion of another job with the specified ID
Example: run_g09 -t24 input.com
```

Scheme 16. Usage of the input script on the command line.

3 Results and Discussion

3.1 Synthesis of $[\text{ClP}(\mu\text{-PMes}^*)]_2$

To begin with, a suitable lab scale synthesis for dihalocyclotetraphosphanes needed to be developed. By analogy with the synthesis of cyclodipnictadiazanes, a reaction starting from Mes^*PH_2 or TerPH_2 and PCl_3 was targeted. Both phosphanes could be synthesised in larger quantities using modified literature procedures, starting from readily available chemicals: Mes^*H was generated on a 200 g scale in a Friedel-Crafts alkylation from benzene and $t\text{-BuCl}$ using AlCl_3 as catalyst. It was subsequently brominated and then converted to the phosphane *via* lithiation, treatment with PCl_3 , and hydrogenation (Scheme 17, top).^[109,110] TerPH_2 could be synthesised starting from 2,6-dichlorobenzene and MesBr according to a modified Hart reaction,^[111] which was quenched with PCl_3 . Afterwards, the resulting dihalophosphanes (TerPCl_2 , TerPClBr , TerPBr_2) were hydrogenated (Scheme 17, bottom).^[112–114]



Scheme 17. Synthesis of Mes^*PH_2 (top) and TerPH_2 (bottom, X = Cl, Br).

In previous studies, the reactivity of silylated phosphanes had been explored with respect to the synthesis of cyclotetraphosphanes; however, this method had not proven successful to that

end.^[115] Therefore, an approach similar to the synthesis of Mes*NPCl was chosen.^[16] Upon treatment of Mes*PH₂ with PCl₃ in the presence of NEt₃, a dark red solution was obtained. By *in situ* ³¹P NMR spectroscopy, the colour could be attributed to the formation of the tetraphosphene Mes*P=PP(Mes*)PCl₂ (**12**). It featured an ABCD spin system (Figure 1) with chemical shifts and coupling constants indicative of a diphosphene moiety ($\delta = +587.0, +463.2$ ppm, $^1J = -578$ Hz)^[48,51,52,60,116] as well as a PCl₂ unit ($\delta = +209.5$ ppm).^[38,117–119] Comparison with calculated NMR data (PBE0/6-31g(d,p)) for compound **12** showed reasonable agreement.

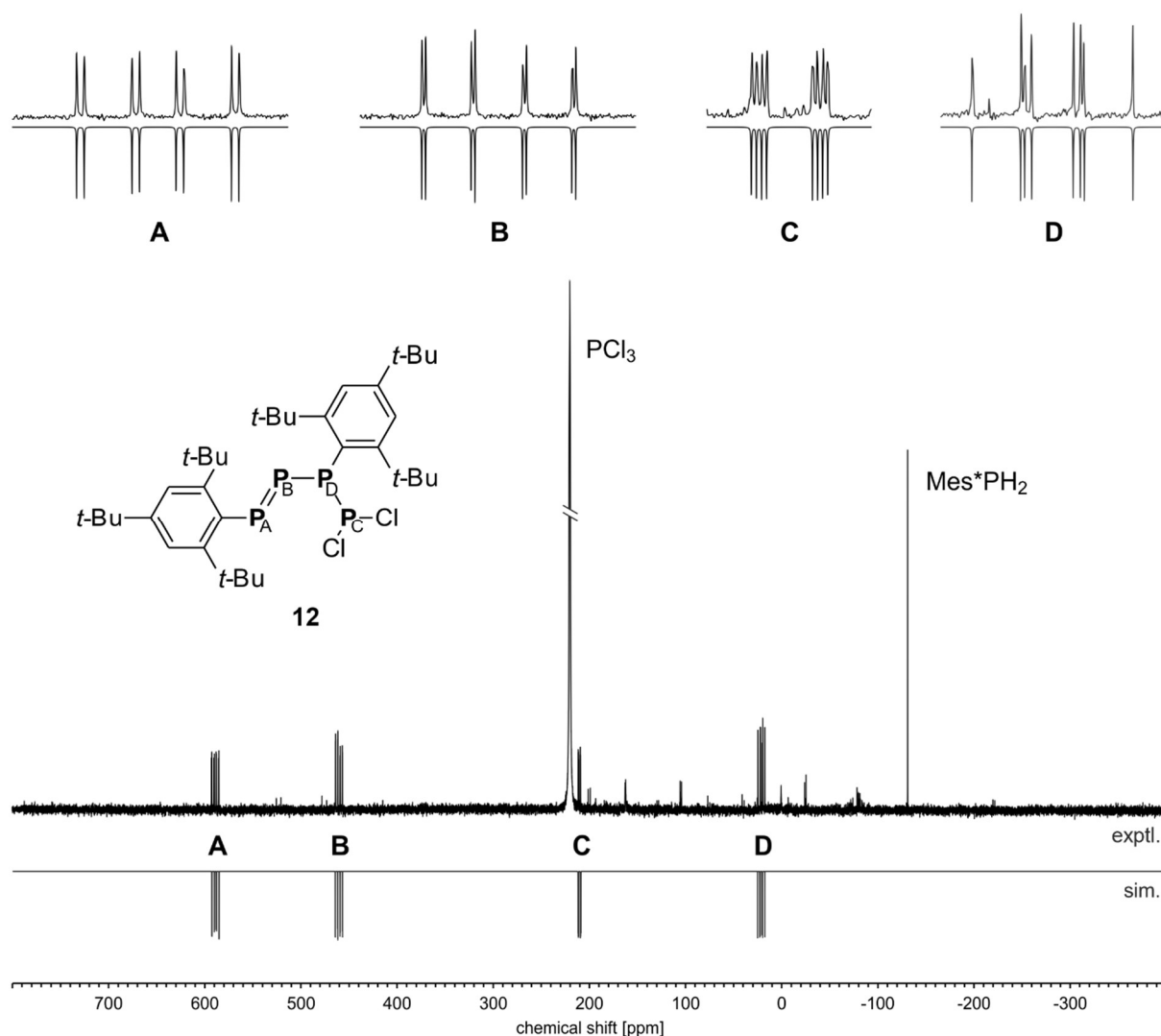
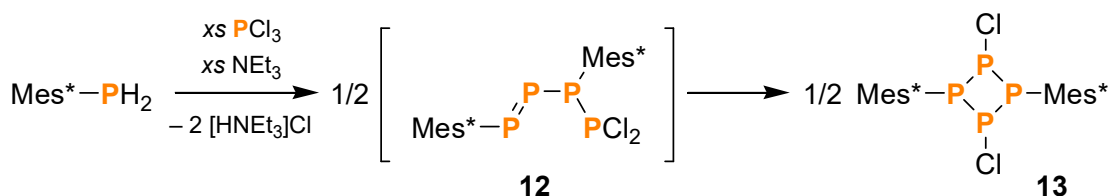


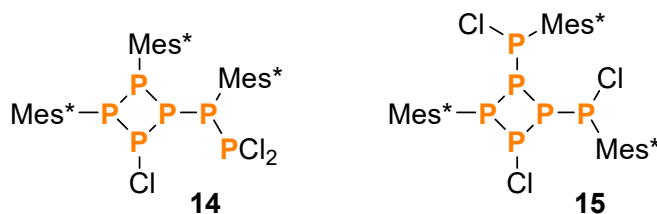
Figure 1. *In situ* ³¹P NMR spectrum of the reaction of Mes*PH₂ with PCl₃ in the presence of NEt₃ after 12 hours of reaction time. The simulated NMR spectrum of compound **12** is shown at the bottom.

Attempts to crystallise and isolate **12** were unsuccessful. Nonetheless, the constitutionally isomeric cyclotetraphosphane [CIP(μ -PMes*)]₂ (**13**, Scheme 18) could be obtained in moderate

yield (*ca.* 30 %), indicating the rearrangement of one Cl substituent, accompanied by P–P bond formation. Moreover, two different cyclotetraphosphane species with phosphanyl side chains could be identified as side products (**14**, **15**; Scheme 19). All discussed products comply with the general sum formula $[\text{Mes}^*\text{PPCl}]_n$ ($n = 2, 3$) and can therefore be regarded as formal dimers and trimers of the diphosphene $\text{Mes}^*\text{P}=\text{PCl}$ (**7**).



Scheme 18. Synthesis of $[\text{ClP}(\mu\text{-PMes}^*)]_2$ (**13**) via tetraphosphene **12**.



Scheme 19. The side products **14** and **15** are formal trimers of Mes^*PPCl (**7**)

In the ^{31}P NMR spectrum, compound **13** featured an A_2X_2 spin system (-8.1 ppm, $+131.1$ ppm; $^1J = -217$ Hz), which again compared well to calculated NMR data (-1.6 ppm, $+119.9$ ppm; $^1J = -166$ Hz) and previously reported NMR shifts of the related compounds **2a** and **2b**.^[42,43]

The cyclotetraphosphane **13** could be crystallised in two different crystal modifications and as fluorobenzene solvate depending on the crystallisation conditions. The molecular structure (Figure 2, left) revealed a folded P_4 ring system with four P–P single bonds; all substituents were arranged in equatorial positions. The Mes^* moiety connected to P3 was twisted by *ca.* 60° around the P–C axis compared with the position of the other Mes^* moiety. Clearly, this conformation displayed four inequivalent phosphorus nuclei, in contrast to the A_2X_2 pattern observed by solution NMR spectroscopy. To shed light on this discrepancy, detailed structural calculations were performed, showing that the C_1 symmetric conformer observed in the solid state (**13A**) was indeed thermodynamically favoured. However, a C_2 symmetric conformer (**13B**) was only 24.3 kJ/mol higher in energy, with a rotational barrier of approx. 58 kJ/mol, indicating that the A_2X_2 pattern was likely caused by dynamic rotation of the Mes^* substituents in solution (Figure 3).

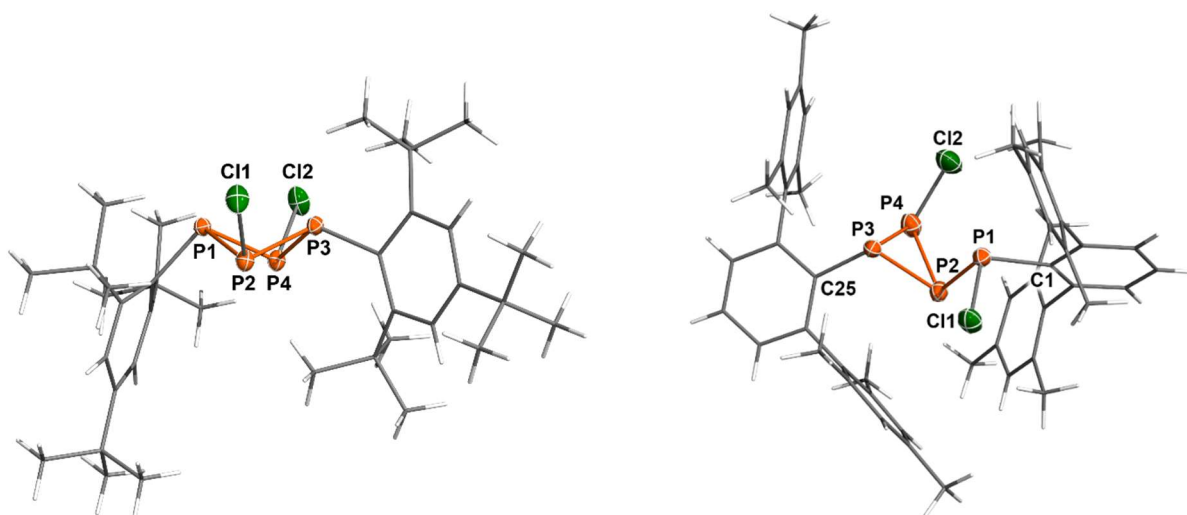


Figure 2. Molecular structures of **13** (left) and **17** (right) in the crystal. Thermal ellipsoids are set at 50 % probability (173 K).

To further elaborate on this dynamic behaviour, temperature dependent ^{31}P NMR spectra were recorded. Upon cooling to $-80\text{ }^\circ\text{C}$, the signal assigned to the Mes* substituted P nuclei was split in two broad resonances in agreement with the minimum structure **13A**; however, the dynamic effect could not be entirely resolved, so the contribution of other dynamic behaviour could not be excluded (Figure 3).

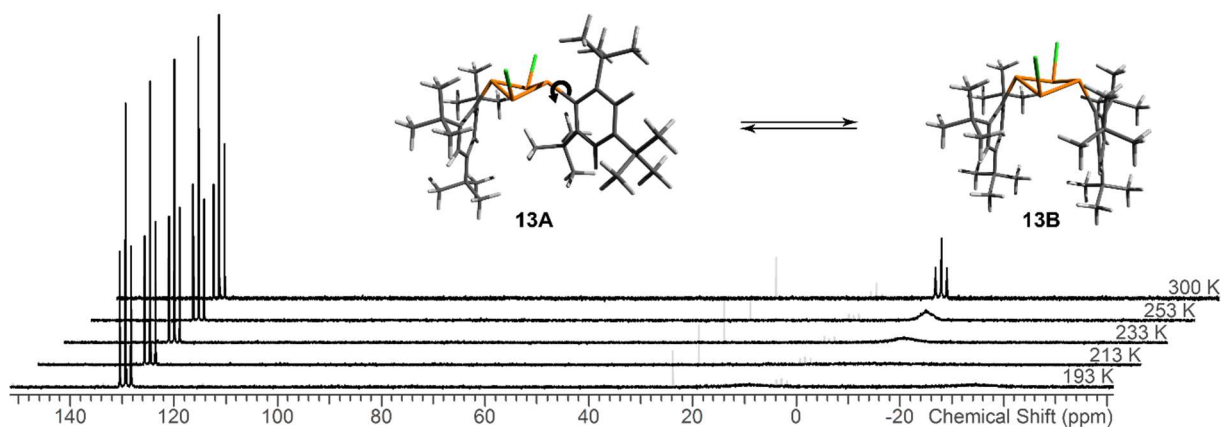
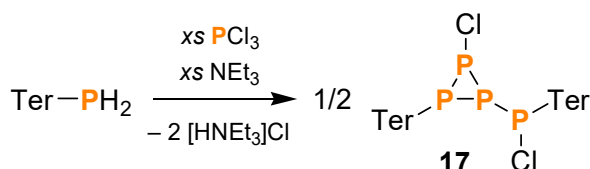


Figure 3. Top: The calculated rotamers **13A** and **13B** are minimum structures of compound **13**. The rotamer **B** is 24 kJ/mol higher in energy, the rotational barrier is approx. 58 kJ/mol (gas phase). Bottom: Temperature dependent ^{31}P NMR spectra of **13** (impurities are greyed out).

The synthesis of **13** could be further improved during the timespan of this work. First of all, NMR experiments indicated that the choice of a polar solvent such as CH_2Cl_2 for the rearrangement reaction of **12** to **13** significantly enhanced the selectivity. Moreover, the separation of $[\text{HNET}_3]\text{Cl}$ proved to be a crucial step; washing the salt thoroughly with *n*-pentane

by repeated back-condensation was found to be necessary to extract the product quantitatively. For increased purity (> 99 %), the raw product was additionally recrystallised from fluorobenzene. In this vein, the overall yield of **13** could be improved to 50 % based on Mes*PH₂, allowing synthesis on a 10–20 g scale.

When using TerPH₂ instead of Mes*PH₂ as starting material, an unexpected reaction outcome was observed: Due to H/Cl scrambling, as indicated by the presence of TerPH₂, TerPHCl, and TerPCl₂ in the reaction mixture, only small amounts of the desired cyclophosphane [ClP(μ-Pter)]₂ (**16**) had formed. Instead, a tricyclic phosphane with an exocyclic phosphanyl group could be isolated (**17**, Scheme 20), which was a constitutional isomer of **16**. Furthermore, no intermediate analogous to the tetraphosphane **12** could be detected.



Scheme 20. Synthesis of the tricyclic phosphane TerP₃(Cl)P(Cl)Ter (**17**).

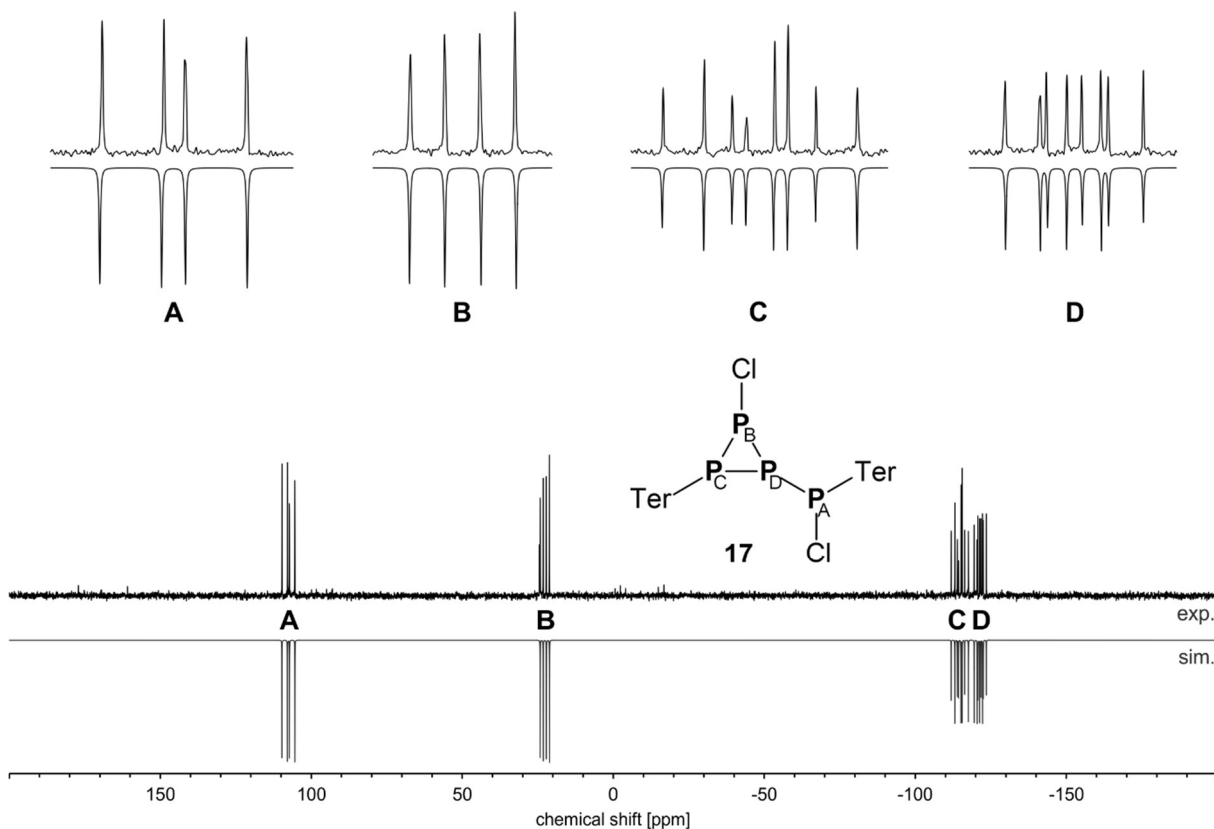


Figure 4. Experimental (up) and simulated (down) ³¹P NMR spectrum of compound **17**.

In the ^{31}P NMR spectrum, compound **17** displayed an ABCD spin system (Figure 4), which compares to previously reported NMR data for similar systems.^[38,44,45] The molecular structure was established by single crystal X-ray diffraction (Figure 2, right). The P_3 ring system adopted the shape of an almost equilateral triangle with typical P–P single bond lengths (*cf.* $\Sigma r_{\text{cov}} = 2.22 \text{ \AA}$).^[120] The substituents were found in a *trans* arrangement in relation to the Ter group connected directly to the ring. Both Ter moieties effectively shielded the P_4Cl_2 scaffold by their *ortho*-mesityl groups.

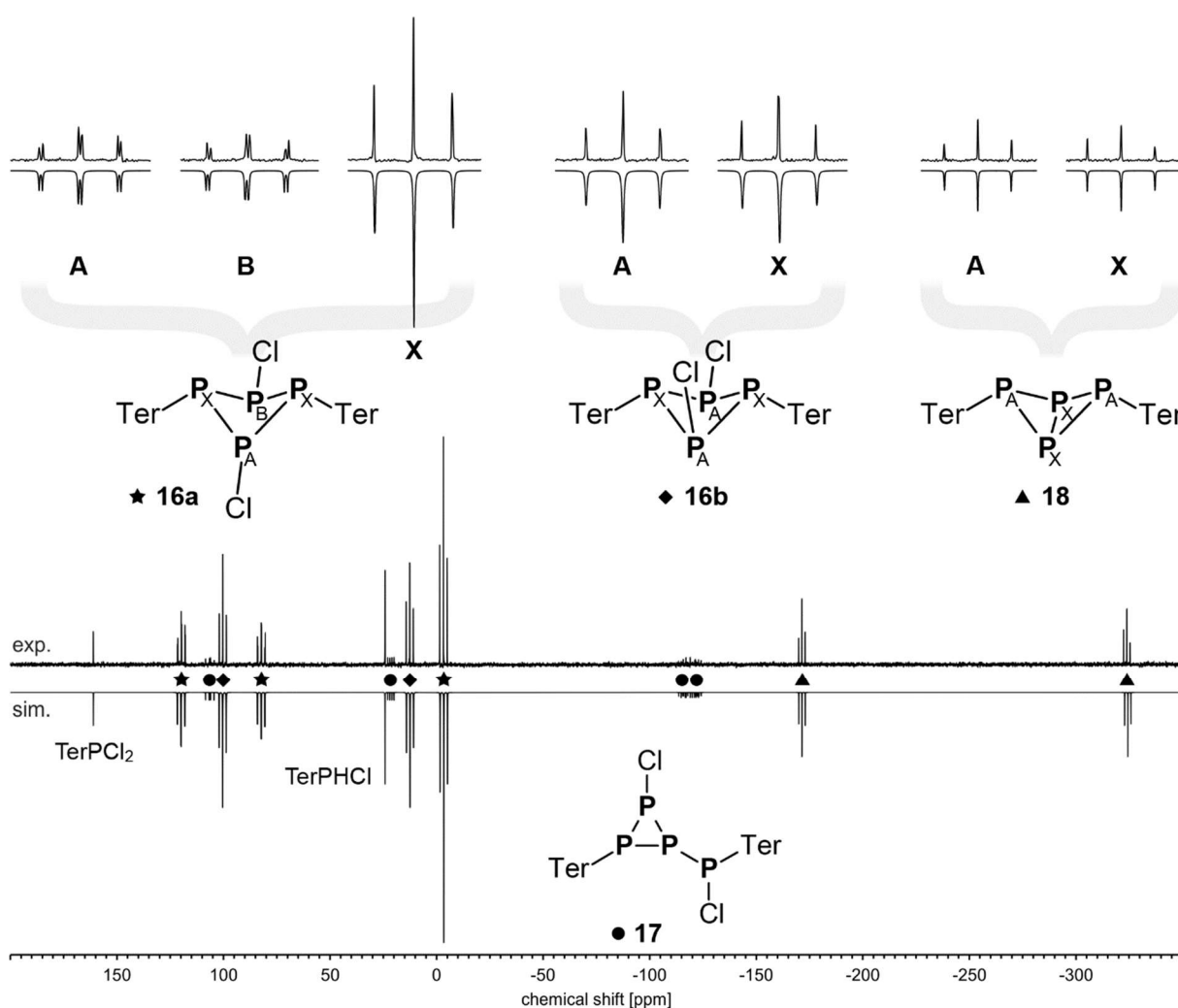


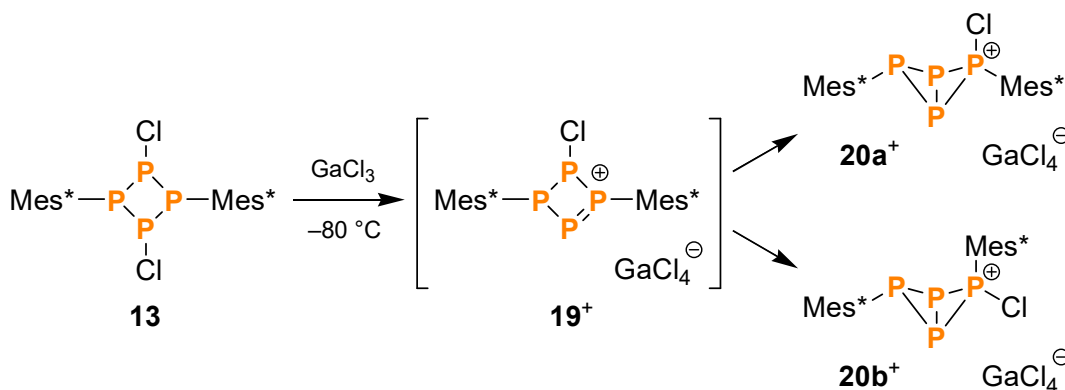
Figure 5. ^{31}P NMR spectrum of the isomerisation of **17** after 27 days. The starting material (●) is almost consumed. Main products are **16a** (*trans*, ★) and **16b** (*cis*, ◆).

Since compound **17** was a constitutional isomer of the cyclotetraphosphane **16**, the relative energies of these species were of interest. DFT calculations showed that the cyclotetraphosphane **16** is in fact energetically favoured. This could also be verified experimentally by heating a solution of **17** in THF to 75 °C. The starting material was slowly consumed according

to a first order reaction, leading mainly to the formation of the *cis* and *trans* isomers of **16** (Figure 5). The *exo-exo* bicycle TerP₄Ter (**18**) as well as the phosphanes TerPHCl and TerPCl₂ were observed as side products (< 20 mol %) of the isomerisation reaction, possibly due to thermal decomposition. However, due to the long reaction time, this approach was not deemed feasible for synthetic use.

3.2 Reactivity Towards GaCl₃

In a next series of experiments, the reactivity of the cyclophosphane [ClP(μ -PMes*)]₂ (**13**) towards the Lewis acid GaCl₃ was investigated. By analogy with the synthesis of cyclic dipnictadiazenium salts,^[9,11–15] the formation of a cyclic tetraphosphenium ion could be expected. In fact, when treating a colourless solution of **13** with GaCl₃ at –80 °C, an instant colour change to dark red was observed. *In situ* ³¹P NMR spectroscopy revealed the formation of a P₄ ring system, as indicated by an AM₂X spin system. The significant downfield shift as well as two rather large ¹J coupling constants implied significant double bond character in agreement with the expected product. DFT/GIAO computations further confirmed the identity of the observed species, which was characterised as the cyclotetraphosphenium ion **19**⁺ (Scheme 21).



Scheme 21. The synthesis of the bicyclic phosphino-phosphonium salt **20**[GaCl₄] occurs via the cyclic tetraphosphenium intermediate **19**⁺.

The computed gas phase minimum structure of **19**⁺ was found to be chiral, incorporating a two-coordinate phosphorus atom as well as a planar, three-coordinate phosphorus centre bearing a Mes* substituent. Due to a dynamic equilibrium between both enantiomers, the two Mes* substituted P nuclei were equivalent on the NMR timescale, which accounted for the broadened AM₂X spin system (Figure 6).

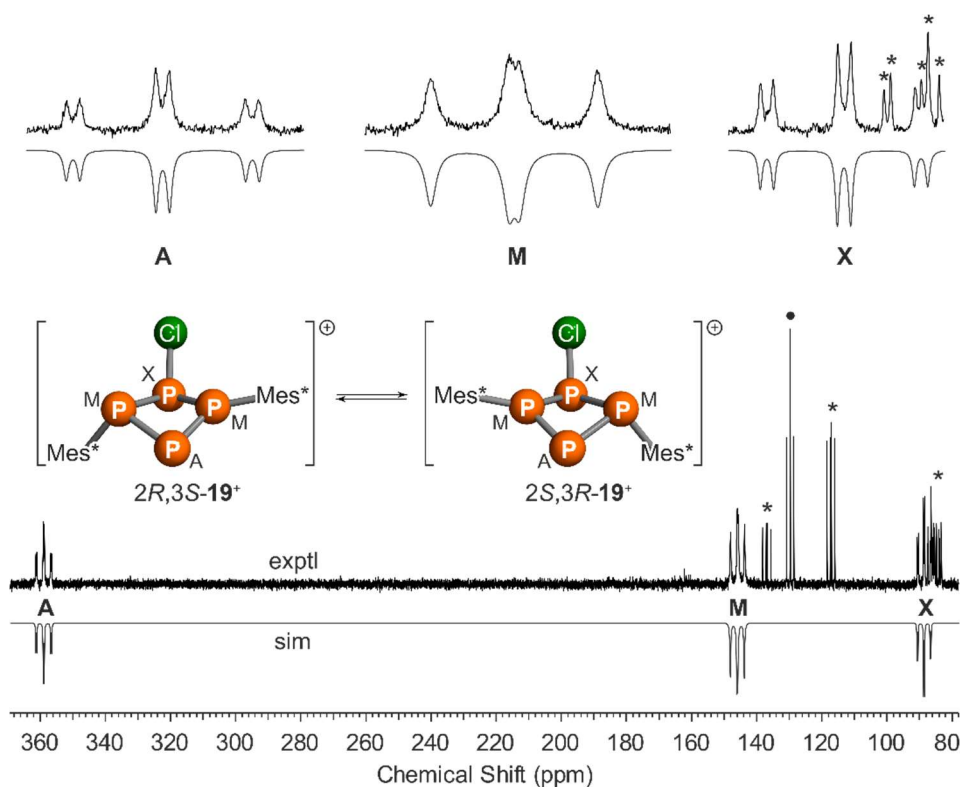


Figure 6. *In situ* ^{31}P NMR spectrum of the reaction of **13** and GaCl_3 at $-60\text{ }^\circ\text{C}$. The simulated spectrum of **19** $^+$ is depicted at the bottom, including dynamic exchange between both enantiomers (computed structures). Labelled signals are caused by the starting material (\bullet) and other intermediates (\star).

The signals of the intermediate disappeared upon heating to $-60\text{ }^\circ\text{C}$, and the colour of the solution faded. As revealed by ^{31}P NMR spectroscopy, two main products were formed, which could be identified as the *exo-exo* (**20a** $^+$) and *endo-exo* isomer (**20b** $^+$) of the bicyclic phosphino-phosphonium salt $[\text{Mes}^*\text{P}_4(\text{Cl})\text{Mes}^*][\text{GaCl}_4]$ (Scheme 21). Intriguingly, the product cation incorporated a tetracoordinate phosphonium centre. With respect to the constitutionally isomeric intermediate **19** $^+$, its formation can be rationalised by a formal 1,2-Cl shift. Accordingly, DFT calculations indicated that the isomers **20a** $^+$ and **20b** $^+$ are energetically favoured by 46.3 and 45.3 kJ/mol, respectively. Still, both isomers are thermally labile and started to decompose above $-30\text{ }^\circ\text{C}$.

In the ^{31}P NMR spectrum, both **20a** $^+$ and **20b** $^+$ featured an AMX_2 spin system, in agreement with computed NMR data. The bridgehead nuclei were observed in the typical upfield range (-214.5 , -226.4 ppm, respectively), whereas the tetracoordinate phosphonium centre was shifted significantly downfield ($+51.1$, $+9.0$ ppm), which is quite unusual for bicyclic tetraphosphanes.^[62,64,67,69,70,121–125] Therefore, NBO analyses were performed to investigate the electronic structure of the bicyclic P_4 scaffold, revealing that the positive charge was mostly localised at the phosphonium centre ($+0.76 e$) but also resided at the tricoordinate, Mes^*

substituted P atom (+0.37 e). The overall charge of the P₄ scaffold amounted to +1.37 e , which is rather high in comparison with other bicyclic systems, such as Mes*P₄Mes* (+0.54 e) or even the dication [(Ph₃As)P₄(AsPh₃)]²⁺ (+0.12 e).^[124] A similar picture was obtained by the electrostatic potential map (Figure 7, right), which shows areas of repulsive potential around the P atoms that can be attributed to low electron density.

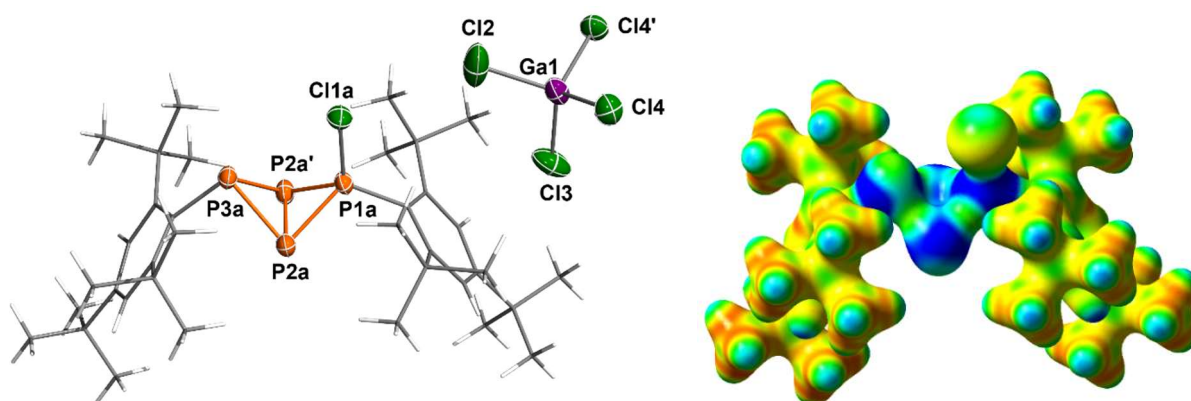
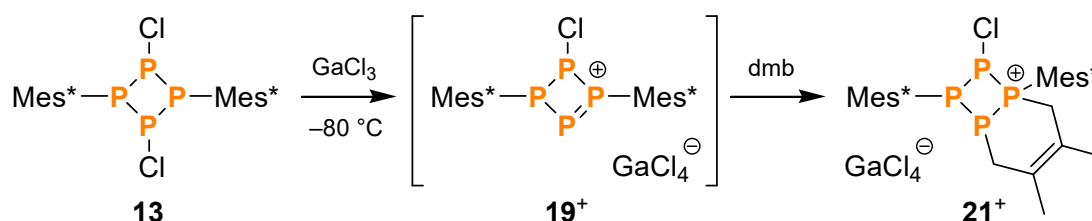


Figure 7. Left: Molecular structure of **20a**[GaCl₄] in the crystal. Thermal ellipsoids are set at 50 % probability (173 K). Right: Electrostatic potential of **20a**⁺ mapped onto the electron density. Blue areas indicate repulsive, red areas attractive potential.

At -80 °C, **20a**[GaCl₄] could be crystallised as CH₂Cl₂/PhF solvate. The molecular structure was determined by single crystal X-ray diffraction (Figure 7, left). All P–P bond lengths corresponded to typical P–P single bonds (*cf.* $\Sigma r_{\text{cov}} = 2.22$ Å),^[120] although those to the tetracoordinate atom P1a were somewhat shortened due to bond polarisation. P1a was located in a distorted tetrahedral coordination environment, that is comparable to tetracoordinate P atoms in cyclic phosphino-phosponium cations or the bicyclic Lewis acid adduct TerP₄Me·B(C₆F₅)₃.^[46,64] The fold angle of the bicyclic system (101.7°) lied in the expected range.^[62,69,121]

In the presence of dimethylbutadiene (dmb) as trapping reagent, the reaction of **13** with GaCl₃ led to the quantitative formation of a bicyclic tetraphosphaoctenium cation (**21**⁺, Scheme 22), which can be regarded as [4+2] cycloaddition product between the intermediate **19**⁺ and dmb. Hence, compound **21**⁺ represented further chemical evidence for the identity of the intermediate. In the ³¹P NMR spectrum, **21**⁺ was characterised by four broad resonances, likely due to hindered rotation of the Mes* or *t*-Bu groups. Upon heating, it began to decompose, whereas cooling to -80 °C resolved a dynamic exchange between several rotamers. The steric strain within the molecule became apparent in the molecular structure (Figure 8, left), as one of

the Mes* moieties was highly bent out of planarity to avoid the neighbouring P₂C₄ ring system. The angle between the P1–C1 axis and the least squares plane of the phenyl ring amounted to 52.1°, as opposed to an idealised value of 0° that would be expected for substituents at an aromatic ring system. According to NBO analysis, the positive charge was mainly localised at the phosphonium centre (+0.92 *e*), supporting its description as a bicyclic phosphonium ion.

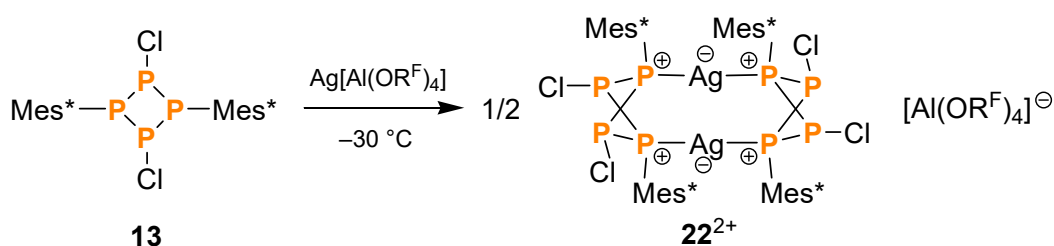


Scheme 22. In the presence of dmb, the intermediate **19⁺** could be trapped by [4+2] cycloaddition, leading to the formation of a bicyclic tetraphosphaoctenium cation (**21⁺**).

When treating the bicyclic phosphino–phosphonium cation **20a⁺** or **20b⁺** with dmb, no reaction occurred. Therefore, this reaction pathway could be excluded as a possible source of **21⁺**, giving further proof that the latter was indeed formed by [4+2] cycloaddition between dmb and the intermediate **19⁺**.

3.3 Reactivity Towards Ag[WCA]

As weakly coordinating anions (WCAs) are known for their ability to stabilise reactive cations,^[126,127] the reaction of the tetraphospane **13** with Ag[Al(OR^F)₄] (R^F = CH(CF₃)₂) and Ag[B(C₆F₅)₄] was investigated. However, no colouration of the reaction mixture was observed (even at low temperature), which might have indicated the formation of the previously detected tetraphosphenium cation **19⁺**. In case of Ag[Al(OR^F)₄], all solids dissolved upon warming to -30 °C and a clear solution was obtained.



Scheme 23. Synthesis of the silver complex **22²⁺**.

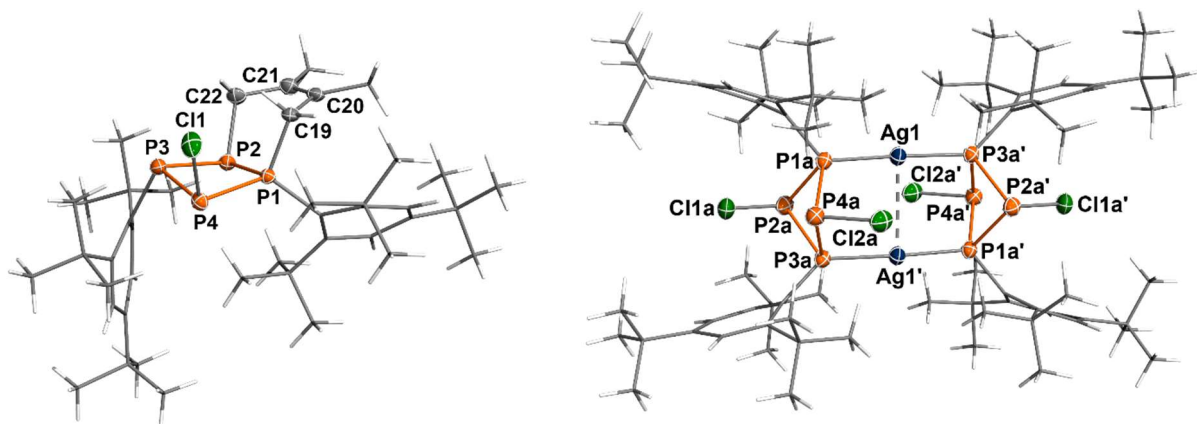


Figure 8. Molecular structures of **21⁺** (left) and **22²⁺** (right) in the crystal. Thermal ellipsoids are set at 50 % probability (173 K).

Crystallisation at $-80\text{ }^{\circ}\text{C}$ yielded a dinuclear silver complex of **13**, which was capped by two cyclophosphane moieties (**22²⁺**, Scheme 23). Its molecular structure was elucidated by single crystal X-ray diffraction (Figure 8, right). Interestingly, the centrosymmetric structure revealed two configurationally inverted P atoms (P2a, P2a'), however, none of the Cl atoms were abstracted. Still, two $\text{Ag}\cdots\text{Cl}$ contacts were significantly shorter than the sum of van der Waals radii ($\text{Ag1}-\text{Cl2a}$ 3.496(1) Å, $\text{Ag1}-\text{Cl2a}'$ 3.641(2) Å; *cf.* $\Sigma r_{\text{vdW}} = 4.35$ Å).^[128]

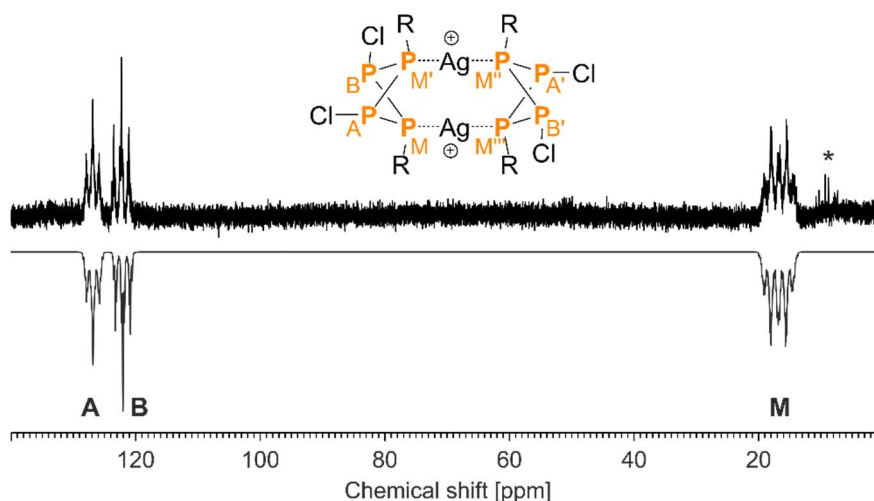
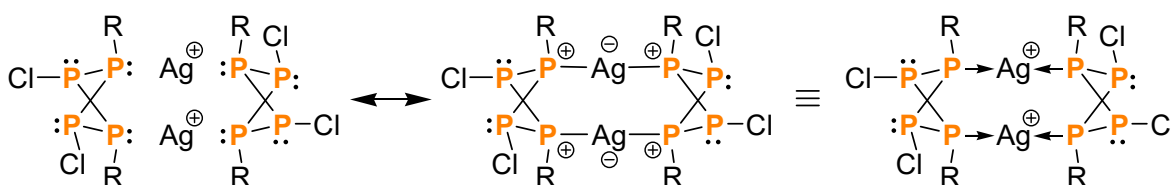


Figure 9. Experimental (up) and simulated (down) ^{31}P NMR spectrum of **22²⁺**. The starred signal is caused by incipient formation of **20b⁺** due to slow elimination of AgCl even at low temperatures (see below).

The ^{31}P NMR spectrum revealed a complex AA'BB'MM'M''M'''XX' spin system (Figure 9) due to coupling between the ^{31}P nuclei within the ring system and the NMR active ^{107}Ag and ^{109}Ag nuclei. The A and B part were assigned to the inequivalent, Cl substituted P atoms,

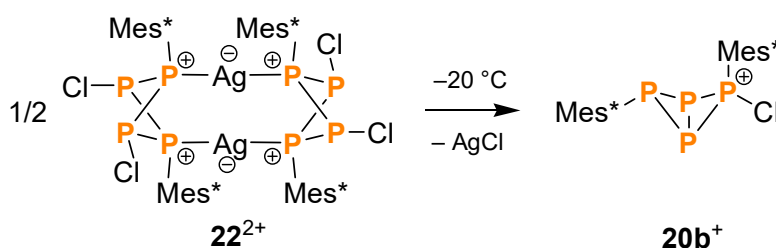
whereas the M part was attributed to the Mes* substituted P atoms and the X part to the Ag nuclei. The $^1J(^{31}\text{P}, ^{107}\text{Ag})$ coupling constant (J_{MX}) was -468 Hz, which compares to reported coupling constants of two-coordinate, linear silver complexes.^[129,130]

NBO analysis indicated that the P–Ag interaction can be described as a classical dative bond, *i.e.* the resonance between two neutral cyclophosphane moieties and two distinct Ag^+ cations as well as a bonding situation with formal positive charges at phosphorus and formal negative charges at Ag (Scheme 24). Electron density is donated from the lone pairs (LPs) at phosphorus into the empty *s*-orbital at Ag.



Scheme 24. Canonical Lewis representations of $\mathbf{22}^{2+}$ which describe the P–Ag dative bond.

When either the reaction mixture of **13** and $\text{Ag}[\text{Al}(\text{OR}^{\text{F}})_4]$ or a solution of $\mathbf{22}[\text{Al}(\text{OR}^{\text{F}})_4]_2$ was allowed to warm to ambient temperatures, precipitation of a white solid was observed, accompanied by the formation of the bicyclic phosphino-phosphonium cation $\mathbf{20b}^+$ (Scheme 25) as well as minor amounts of $\mathbf{20a}^+$. In this respect, $\mathbf{22}[\text{Al}(\text{OR}^{\text{F}})_4]_2$ can be viewed as an isolable intermediate of an intramolecular AgCl elimination process.

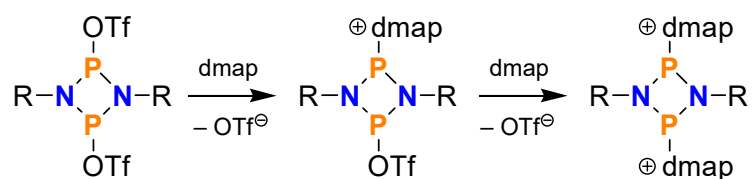


Scheme 25. Above -30 °C, the complex $\mathbf{22}^{2+}$ eliminated silver chloride, leading to the formation of $\mathbf{20b}^+$.

When the cyclophosphane **13** was treated with $\text{Ag}[\text{B}(\text{C}_6\text{F}_5)_4]$, precipitation of AgCl was observed even at low temperatures and again the cationic species $\mathbf{20a}^+$ and $\mathbf{20b}^+$ were formed. However, the unusual cyclotetraphosphenium cation $\mathbf{19}^+$ could not be observed in any of these reactions.

3.4 Reactivity Towards Lewis Bases

In a next series of experiments, the reactivity of $[\text{ClP}(\mu\text{-PMes}^*)]_2$ (**13**) towards Lewis bases was investigated. Substitution of a (formal) chloride by a neutral nucleophile was intended to give rise to cationic, four membered ring systems, in which the positive charge should be stabilised by the Lewis base. In particular, this was supposed to prevent the previously observed rearrangement to bicyclic phosphino-phosphonium cations (**20a**⁺, **20b**⁺).



Scheme 26. Synthesis of base-stabilised, cyclic PN cations (R = Dmp).

A similar concept was used to generate cations from $[\text{TfOP}(\mu\text{-NDmp})]_2$ (Dmp = 2,6-dimethylphenyl, Scheme 26).^[131] Nevertheless, upon treatment of **13** with dimethylaminopyridine (dmap), the *in situ* ³¹P NMR spectrum displayed an ABMX spin system that was indicative of a three-membered ring system with an exocyclic phosphanyl substituent rather than a four-membered cycle. With the aid of comprehensive DFT studies, the signals could be assigned to $[\text{Mes}^*\text{P}_3(\text{dmap})\text{P}(\text{Cl})\text{Mes}^*]^+$ (**23**⁺, Figure 10).

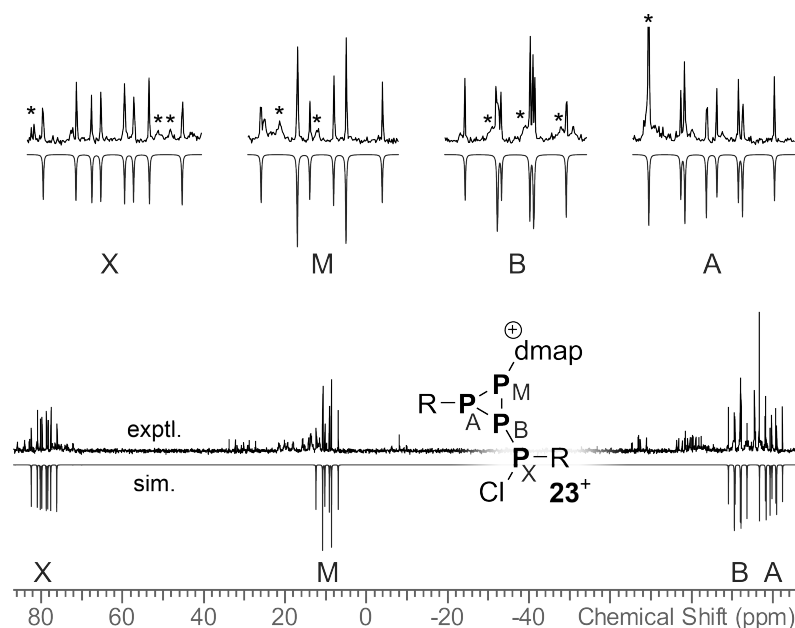
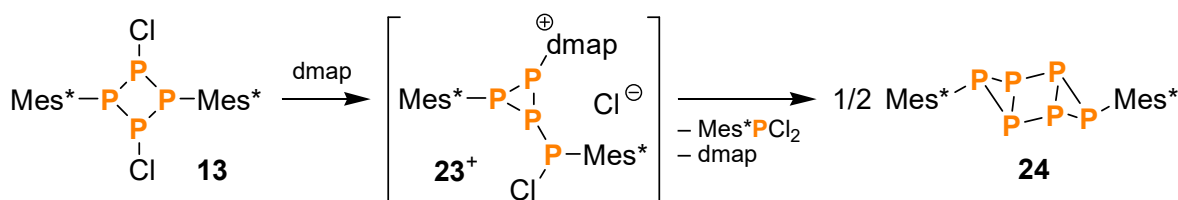


Figure 10. *In situ* ³¹P NMR spectrum of the reaction of **13** and dmap after five hours of reaction time. The simulated spectrum of the intermediate **23**⁺ is depicted at the bottom.

Notably, the calculated structure of 23^+ resembled the structure of $\text{TerP}_3(\text{Cl})\text{P}(\text{Cl})\text{Ter}$ (**17**), which had previously been obtained by reacting TerPH_2 with PCl_3 in the presence of NEt_3 (cf. chapter 3.1). Its formation can be understood in terms of a formal 1,2-Cl shift and rearrangement of one P–P bond with respect to the starting material. Again, this is congruent with previously observed reactivity of **13** and might imply that this kind of rearrangement is part of a more general reaction behaviour.



Scheme 27. The tricyclic hexaphosphane **24** was formed *via* a base induced ring expansion reaction.

Unfortunately, all attempts to isolate 23Cl failed, since it was found to be a transient species. ^{31}P NMR spectroscopy indicated extrusion of Mes^*PCl_2 , which was accompanied by the formation of the highly symmetric, tricyclic hexaphosphane $\text{Mes}^*\text{P}_6\text{Mes}^*$ (**24**, Scheme 27). The latter was identified in the NMR spectrum by an $\text{AA}'\text{BB}'\text{B}''\text{B}'''$ spin system (Figure 11), which corresponds nicely to calculated NMR data.

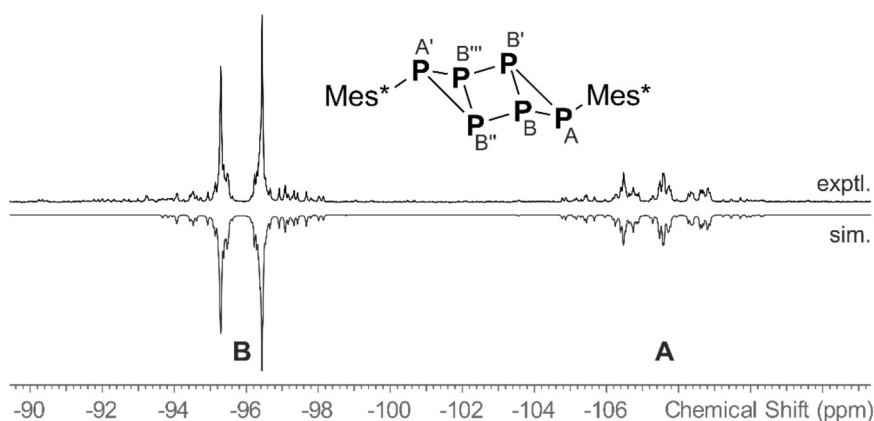


Figure 11. Experimental (up) and simulated (down) ^{31}P NMR spectrum of **24** ($\text{AA}'\text{BB}'\text{B}''\text{B}'''$ spin system).

The molecular structure of **24** was determined by single crystal X-ray diffraction (Figure 12, left). It comprised an unprecedented, chair-like six-membered ring system with two transannular bonds and a flat P_4 ring system in the middle. All P–P bond lengths corresponded to typical single bonds, which was supported by DFT calculations. The electron localisation function (ELF; Figure 12, right) as well as NBO analysis indicated that the electron density was

distributed asymmetrically around the line of nuclear centres, especially in case of the three-membered ring systems. This situation is comparable to the so-called “banana bonds” within tetrahedral P_4 .^[132] In the solid-state Raman spectrum of compound **24**, three prominent bands at 414, 442 and 537 cm^{-1} could be assigned to different vibrational modes of the P_6 scaffold. Interestingly, the tricyclic hexaphosphane was found to be stable towards air and moisture.

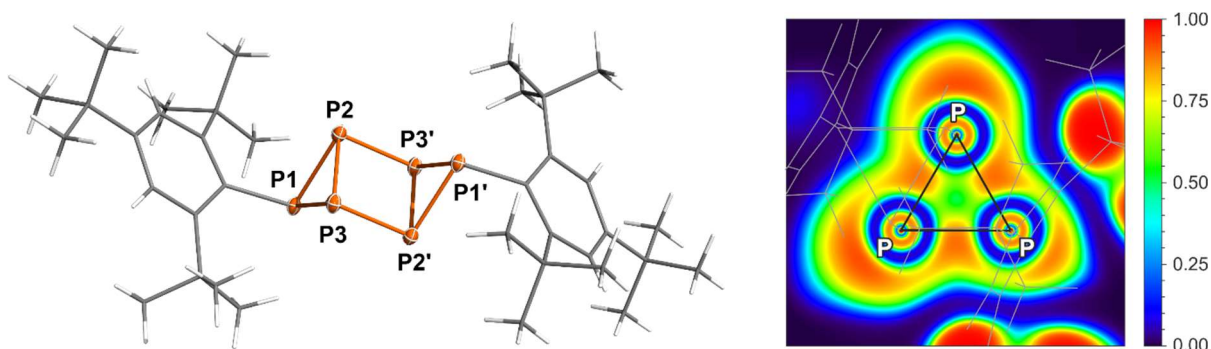
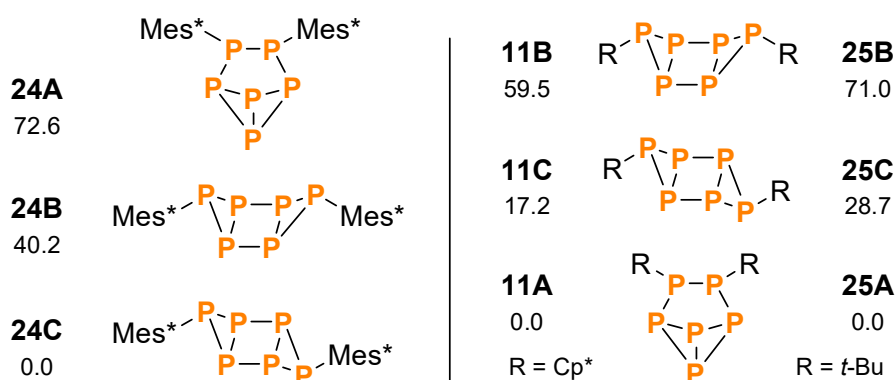


Figure 12. Left: Molecular structure of **24** in the crystal. Thermal ellipsoids are set at 50 % probability (123 K). Right: Depiction of the ELF through the three-membered ring plane, showing the P–P bonding system and the LPs at the P atoms.

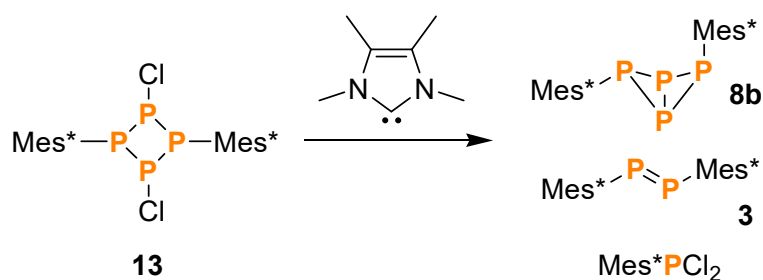
Furthermore, computations were carried out to compare the relative stabilities of different R_2P_6 isomers (A–C in Scheme 28). In agreement with experimental findings,^[74] calculations showed that the smaller Cp^* or *t*-Bu moieties favoured a benzvalene-type structure (A), whereas the large Mes^* substituent stabilised the tricyclic scaffold of type C.



Scheme 28. Relative energies of R_2P_6 isomers (ΔG_{298} in kJ/mol).

When treating the cyclophosphane **13** with other Lewis bases such as PPh_3 or tetramethylethylenediamine (TMEDA), consumption of the starting material could only be detected in the ^{31}P NMR spectrum after an extended reaction time. In case of PPh_3 , trace amounts of **24** were

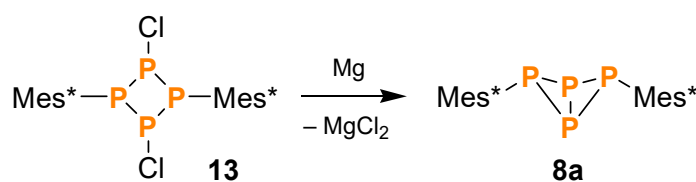
observed after nine days. The reaction of **13** with the NHC tetramethylimidazolyldene, on the other hand, led to degradation of the P₄ ring system. Main products were the hitherto unknown *endo-exo* isomer of the bicyclic tetraphosphane Mes*P₄Mes* (**8b**, cf. chapter 3.5) as well as the previously reported diphosphene Mes*PPMes* (**3**) and dichlorophosphane Mes*PCl₂ (5:1:7 ratio, Scheme 29).^[47,48]



Scheme 29. Formation of the *endo-exo* isomer of Mes*P₄Mes* (**8b**) among other products.

3.5 Reactivity Towards Reducing Agents

The corresponding *exo-exo* isomer of Mes*P₄Mes* (**8a**), which was first reported by Fluck and co-workers,^[62] could be selectively obtained in good yields (73 %) by reduction of **13** with Mg turnings (Scheme 30). This new procedure proved highly advantageous for synthetic use, as the yield reported for the original synthesis (from P₄, Mes*Br and Mes*Li) was very low (5 %).



Scheme 30. The *exo-exo* isomer of Mes*P₄Mes* (**8a**) can be synthesised selectively by reduction of **13**.

Both isomers were fully characterised, including single crystal X-ray diffraction, NMR and vibrational spectroscopy. The molecular structures displayed a typically folded “butterfly” conformation (Figure 13). In case of the rare *endo-exo* substitution, one Mes* substituent fully shielded the top side of the P₄ scaffold; hence, the fold angle was about 10° larger in this case. The P–P bond lengths corresponded to typical single bonds. In the ³¹P NMR spectrum, compound **8a** displayed an A₂X₂ spin system, whereas **8b** featured an A₂MX pattern. The bridgehead atoms were observed at characteristic upfield shifts (**8a**: –273.2 ppm, **8b**:

–220.4 ppm). The P₄ scaffold exhibited characteristic bands in the Raman spectrum, which allowed to distinguish between *endo-exo* and *exo-exo* substitution. Most easily, the substitution pattern could be recognised by the position of the in-phase A₁ mode (“breathing mode”) of the P₄ scaffold, which was observed at 592 (**8a**) or 568 cm⁻¹ (**8b**).

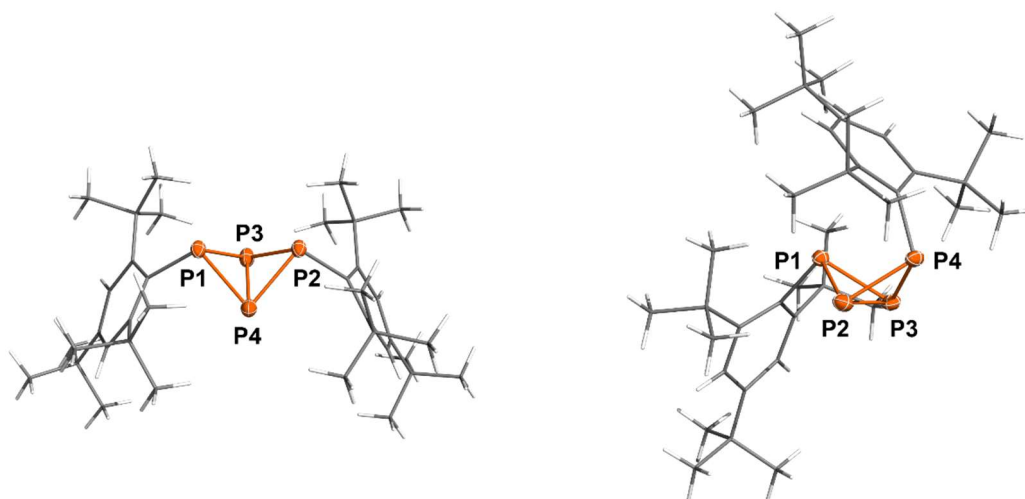
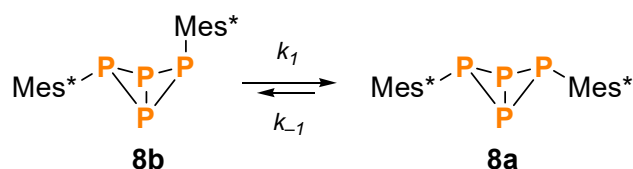


Figure 13. Molecular structures of **8a** (left) and **8b** (right) in the crystal. Thermal ellipsoids are set at 50 % probability (173 K).

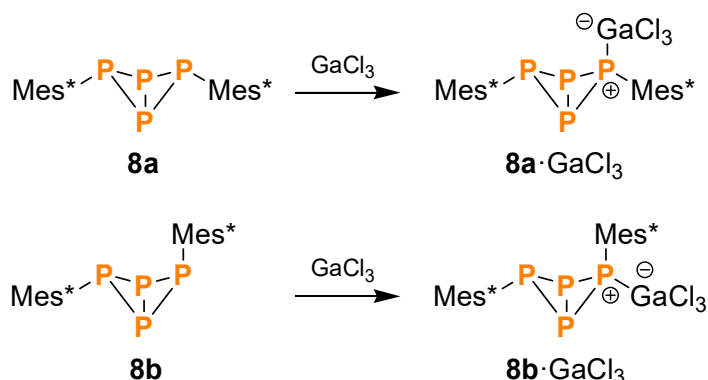
According to DFT calculations, the *exo-exo* isomer was thermodynamically more stable ($\Delta G_{298} = 8.8$ kJ/mol). Hence, it was of interest whether the *endo-exo* isomer could be isomerised at elevated temperatures. Indeed, when heating a solution of **8b** in THF to 75 °C, slow conversion to **8a** was observed in the ³¹P NMR spectrum (Scheme 31). After *ca.* 20 days, a stationary point was reached, indicating an equilibrium between both isomers. The process was modelled as first order kinetics; the equilibrium constant was found to be 9.3 in good agreement with the calculated Gibbs energies.



Scheme 31. A slow equilibrium between both isomers was experimentally confirmed.

The bonding situation within **8a** and **8b** was investigated by NBO analysis. Comparable to the bonding in the tricyclic hexaphosphane **24**, the electron density was found to be bent out of the line of nuclear centres, as expected for cyclic P₃ subunits with bond angles near 60°. The lone

pairs at P indicated Lewis basicity, which could be confirmed by the formation of Lewis acid adducts with GaCl₃ (Scheme 32).



Scheme 32. The reaction of **8a** and **8b** with GaCl₃ yielded the respective Lewis acid-base adducts.

In contrast to the tricyclic hexaphosphane **24**, the bicyclic tetraphosphanes **8a** and **8b** were stable towards GaCl₃ and the respective adducts could be isolated and fully characterised. The molecular structures (Figure 14) with a tetracoordinate P atom were similar to the structures of the bicyclic phosphino-phosphonium cations **20a**⁺ and **20b**⁺ as well as the Lewis acid-base adduct TerP₄Me·B(C₆F₅)₃.^[64] The fold angles of the P₄ systems changed only slightly upon coordination; however, the P–P bond lengths between the tetracoordinate P atoms and the bridgehead atoms were shortened in both isomers. The P–Ga bond lengths were somewhat longer than the sum of covalent radii ($\Sigma r_{\text{cov}} = 2.35 \text{ \AA}$)^[120] due to Pauli repulsion between the *o-t*-Bu groups of the Mes* substituents and the GaCl₃ units.

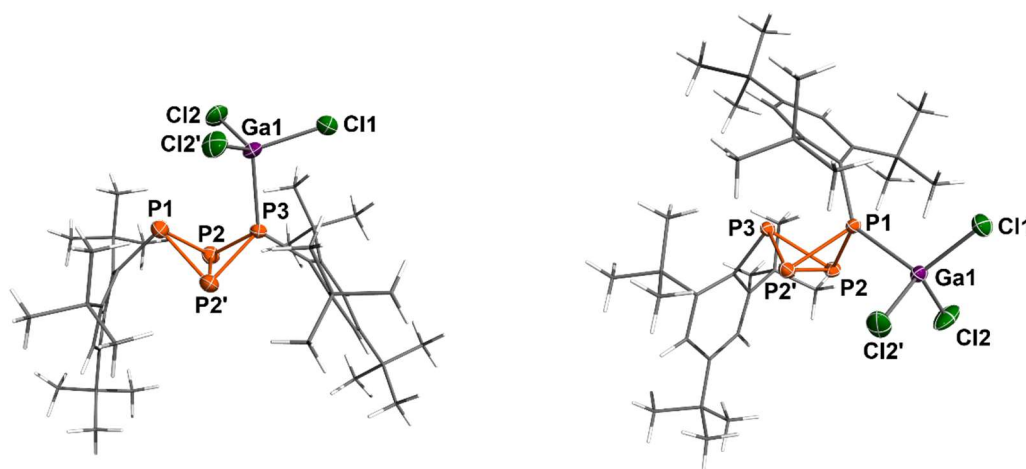
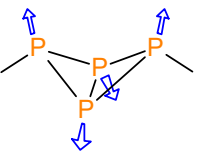
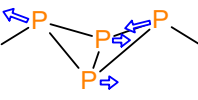
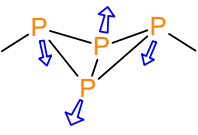
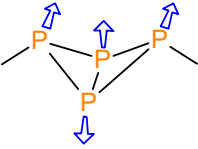


Figure 14. Molecular structures of **8a**·GaCl₃ (left) and **8b**·GaCl₃ (right) in the crystal. Thermal ellipsoids are set at 50 % probability (173 K).

Like the free phosphanes **8a** and **8b**, the adducts **8a**·GaCl₃ and **8b**·GaCl₃ were nicely distinguishable in the solid state Raman spectrum. A summary of important vibrational modes of the P₄ scaffold is given in Table 1.

Table 1: Main vibrational modes of bicyclic tetraphosphanes in the Raman spectrum. Assignment of the symmetries based on approximate C_{2v} symmetry of the P₄ scaffold.

Vibration mode	Description	Wavenumber [cm ⁻¹]
	symmetrical valence “breathing mode” (A ₁ mode, in phase)	8a : 592 8b : 568 8a ·GaCl ₃ : 597 8b ·GaCl ₃ : 567
	peripheral bond stretch (B ₁ mode)	8a : 447 8b : 500 8a ·GaCl ₃ : 497 8b ·GaCl ₃ : 518
	transannular bond stretch (A ₁ mode, out of phase)	8a : 412 8b : – 8a ·GaCl ₃ : 436 8b ·GaCl ₃ : –
	peripheral bond stretch (B ₂ mode)	8a : 412 8b : 412 8a ·GaCl ₃ : 451 8b ·GaCl ₃ : 438

NBO analysis revealed that the charge distribution only changed slightly upon coordination and that the P₄ bonding system basically remained unchanged. The P–Ga interaction can be described as a dative bond between a LP at the phosphorus atom and an empty *p*-type orbital at the Ga atom; the electron density is strongly polarised towards phosphorus. Again, the *exo-exo* isomer **8a**·GaCl₃ was calculated to be thermodynamically favoured (8.0 kJ/mol).

In the ³¹P NMR spectrum of **8a**·GaCl₃, dynamic exchange of the GaCl₃ moiety was detected (Figure 15). Variable temperature NMR experiments revealed that the exchange could be attributed to an intramolecular as well as intermolecular process (*i.e.* fast swapping of the GaCl₃ moiety between both bridging P atoms and a slower dissociation equilibrium). The temperature dependent rate constants of both processes could be determined by line-shape analysis and the activation barriers were derived using the Eyring theory (39.5, 30.9 kJ/mol, respectively). In case of **8b**·GaCl₃, no intramolecular exchange was observed due to the arrangement of the Mes* substituents. Nonetheless, dynamic exchange between the free phosphane and the adduct was

detected, which was likely caused by a bimolecular exchange reaction of the type $8b \cdot GaCl_3 + 8b' \rightleftharpoons 8b + 8b' \cdot GaCl_3$.

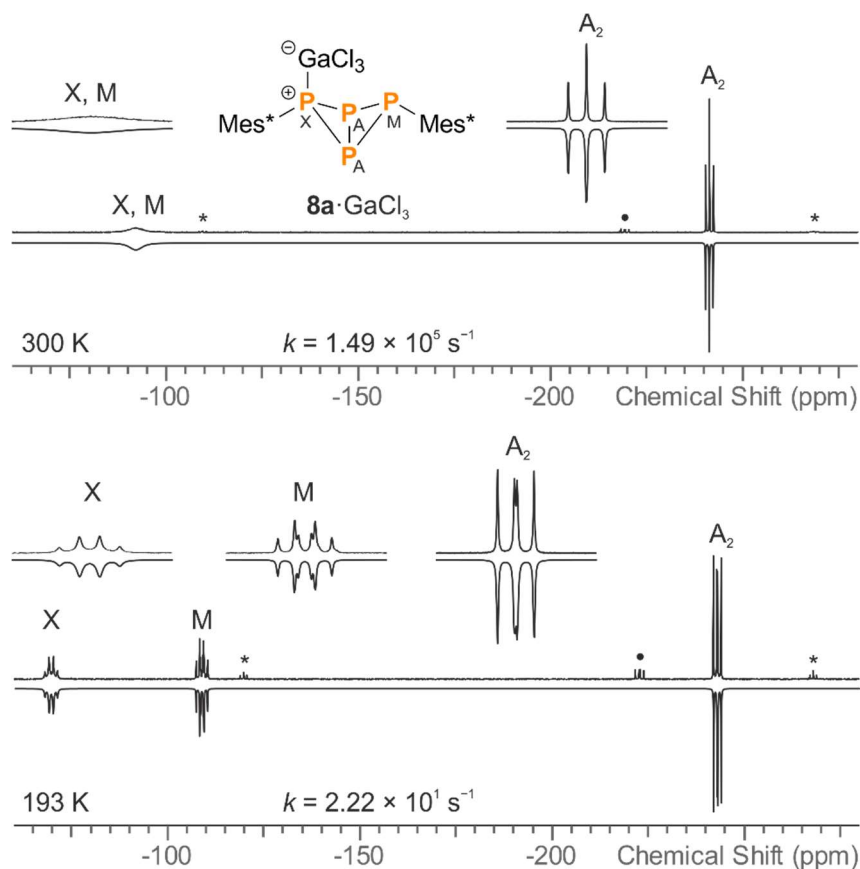


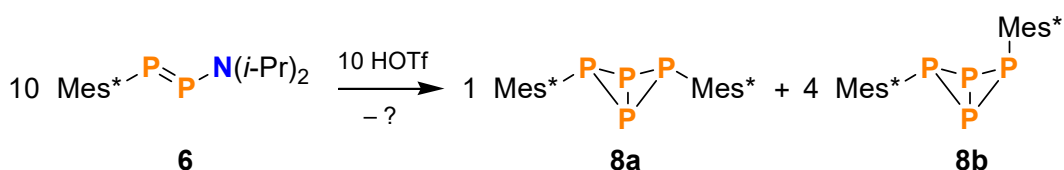
Figure 15. Experimental (up) and simulated (down) ^{31}P NMR spectra of $8a \cdot GaCl_3$ at 27 °C (top) and -80 °C (bottom) demonstrating the dynamic exchange of the $GaCl_3$ moiety in solution. The free phosphane (\star) was added in slight excess so it was detectable in the NMR spectrum (\bullet = impurity).

Analogously to the free phosphanes, the adducts $8a \cdot GaCl_3$ and $8b \cdot GaCl_3$ could be isomerised in solution. They were found to interconvert slowly even at room temperature. The establishment of equilibrium was monitored by ^{31}P NMR spectroscopy over a period of several weeks. The equilibrium constant for the reaction $8b \cdot GaCl_3 \rightleftharpoons 8a \cdot GaCl_3$ was found to be 1.6, hence the relative stability of the *endo-exo* isomer was increased upon coordination to $GaCl_3$.

3.6 Further Syntheses of Bicyclic Tetraphosphanes

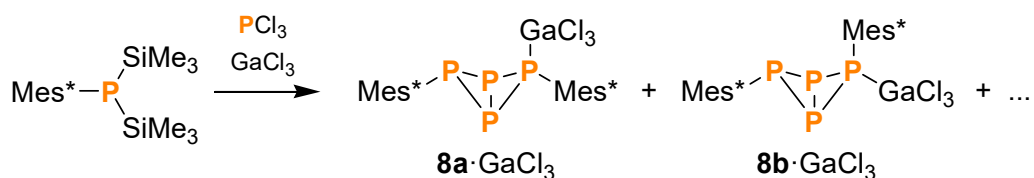
In the context of the studies concerning bicyclic tetraphosphanes, the previously reported reaction of $Mes^*P=PN(i-Pr)_2$ (**6**) and HOTf was of interest.^[63] Reportedly, it yielded $Mes^*P_4Mes^*$ (**8**) and the unusual, asymmetrically substituted bicycle $Mes^*P_4N(i-Pr)_2$;

however, the configuration of these systems remained undefined. In fact, when trying to reproduce the previous findings, the *exo-exo* and *endo-exo* isomer of Mes*P₄Mes* (**8a**, **8b**) were obtained in a 1:4 ratio (Scheme 33). Probably, the analytical data were misinterpreted in the original publication. Since a mixture of both isomers was obtained, separation was difficult and only achievable for small amounts of substance. The reduction of **13** or its reaction with tetramethylimidazolydene proved to be more suitable for the preparation of pure **8a** or **8b**, as described above.



Scheme 33. In contrast to previous reports, the reaction of **6** and HOTf yielded **8a** and **8b** in a 1:4 ratio.

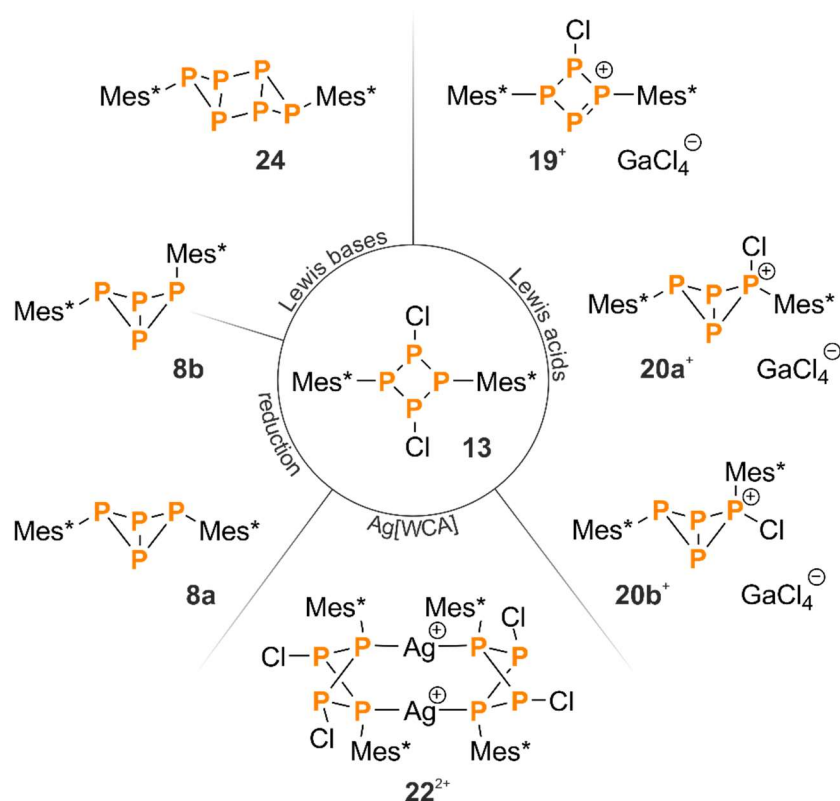
Upon reaction of Mes*P(SiMe₃)₂^[133] with PCl₃ in the presence of GaCl₃, the adducts **8a**·GaCl₃ and **8b**·GaCl₃ were obtained (7:5 ratio, Scheme 34) among other side products. Depending on the choice of solvent, either isomer could be crystallised selectively. Hence, this reaction can be regarded as another example of “self-assembly” from P₁ building blocks, similar to the synthesis of the cyclotetraphosphane [ClP(μ-PMes*)]₂ (**13**).



Scheme 34. Direct synthesis of **8a**·GaCl₃ and **8b**·GaCl₃ from P₁ building blocks.

4 Summary and Outlook

In conclusion, it was possible to develop a practical synthesis for the cyclophosphane $[\text{ClP}(\mu\text{-PMes}^*)]_2$ (**13**), by which it could be obtained in quantities of 10–20 g. Its reactivity towards Lewis acids and bases as well as reducing agents was studied, demonstrating that the formation of bicyclic P_4 scaffolds represents a general type of reactivity in phosphorus chemistry. This is especially interesting in view of the fact that comparable structural motifs can also be observed in degradation processes of white phosphorus;^[35,36] however, the examples presented in this work were formed from a functionalised cyclophosphane, which again was generated from P_1 precursors. (Scheme 35).



Scheme 35. Overview of the product scope of the cyclotetraphosphane **13**.

Particularly, the first bicyclic triphosphino-phosphonium framework (**20a⁺**, **20b⁺**) as well as the first $[3.1.0.0^{2,4}]$ -tricyclic hexaphosphane (**24**) could be synthesised, which add missing fragments to the chemistry of polycyclic phosphanes. Furthermore, similarities and differences

to homologous pnictogen-nitrogen ring systems were shown: although cationic phosphonium ions can be generated, these are barely stabilised by the neighbouring P atoms and thus only stable at low temperatures. Therefore, such systems undergo rearrangement reactions to form additional P–P bonds to stabilise the low-coordinate P centres. Likewise, 1,2-Cl shifts were repeatedly observed, which can be attributed to the same cause.

Additionally, it was possible to synthesise bicyclic tetraphosphanes directly from P₁ and P₂ precursors. These systems were thoroughly investigated, including some thermodynamic and kinetic data concerning the stabilities and interconversion of different isomers.

Future studies will involve reactions of **13** with (frustrated) Lewis pairs. Preliminary results show that it is possible to replace the Cl substituents using this approach, leading to the formation of differently substituted ring systems, or – depending on the sterical demand of the Lewis base – even diphosphene species by formal [2+2] cycloreversion. However, further studies are needed to refine this method and to collect sufficient data for complete characterisation of the products.

5 References

- [1] M. S. Balakrishna, V. S. Reddy, S. S. Krishnamurthy, J. F. Nixon, J. C. T. R. B. St. Laurent, *Coord. Chem. Rev.* **1994**, *129*, 1–90.
- [2] L. Stahl, *Coord. Chem. Rev.* **2000**, *210*, 203–250.
- [3] G. G. Briand, T. Chivers, M. Krahn, *Coord. Chem. Rev.* **2002**, *233-234*, 237–254.
- [4] M. S. Balakrishna, D. J. Eisler, T. Chivers, *Chem. Soc. Rev.* **2007**, *36*, 650–664.
- [5] G. He, O. Shynkaruk, M. W. Lui, E. Rivard, *Chem. Rev.* **2014**, *114*, 7815–7880.
- [6] A. Michaelis, G. Schroeter, *Ber. Dtsch. Chem. Ges.* **1894**, *27*, 490–497.
- [7] N. Burford, T. S. Cameron, C. L. B. Macdonald, K. N. Robertson, R. W. Schurko, D. Walsh, R. McDonald, R. E. Wasylshen, *Inorg. Chem.* **2005**, *44*, 8058–8064.
- [8] M. Lehmann, A. Schulz, A. Villinger, *Struct. Chem.* **2010**, *22*, 35–43.
- [9] N. Burford, T. S. Cameron, K. D. Conroy, B. Ellis, M. D. Lumsden, C. L. B. Macdonald, R. McDonald, A. D. Phillips, P. J. Ragona, R. W. Schurko, D. Walsh, R. E. Wasylshen, *J. Am. Chem. Soc.* **2002**, *124*, 14012–14013.
- [10] E. W. Abel, D. A. Armitage, G. R. Willey, *J. Chem. Soc.* **1965**, 57–61.
- [11] D. Michalik, A. Schulz, A. Villinger, N. Weding, *Angew. Chem. Int. Ed.* **2008**, *47*, 6465–6468.
- [12] R. Kuzora, A. Schulz, A. Villinger, R. Wustrack, *Dalton Trans.* **2009**, 9304–9311.
- [13] M. H. Holthausen, J. J. Weigand, *J. Am. Chem. Soc.* **2009**, *131*, 14210–14211.
- [14] A. Schulz, A. Villinger, *Inorg. Chem.* **2009**, *48*, 7359–7367.
- [15] M. Lehmann, A. Schulz, A. Villinger, *Angew. Chem. Int. Ed.* **2012**, *51*, 8087–8091.
- [16] E. Niecke, M. Nieger, F. Reichert, *Angew. Chem. Int. Ed. Engl.* **1988**, *27*, 1715–1716.
- [17] R. D. Curtis, M. J. Schriver, R. E. Wasylshen, *J. Am. Chem. Soc.* **1991**, *113*, 1493–1498.
- [18] G. David, E. Niecke, M. Nieger, V. von der Gönna, W. W. Schoeller, *Chem. Ber.* **1993**, *126*, 1513–1517.

- [19] N. Burford, T. S. Cameron, J. A. C. Clyburne, K. Eichele, K. N. Robertson, S. Sereda, R. E. Wasylishen, W. A. Whitla, *Inorg. Chem.* **1996**, *35*, 5460–5467.
- [20] N. Burford, J. A. C. Clyburne, D. Silvert, S. Warner, W. A. Whitla, K. V. Darvesh, *Inorg. Chem.* **1997**, *36*, 482–484.
- [21] N. Burford, H. A. Spinney, M. J. Ferguson, R. McDonald, *Chem. Commun.* **2004**, *2*, 2696–2697.
- [22] M. Kuprat, A. Schulz, A. Villinger, *Angew. Chem. Int. Ed.* **2013**, *52*, 7126–7130.
- [23] A. Villinger, P. Mayer, A. Schulz, *Chem. Commun.* **2006**, 1236–1238.
- [24] H. Brand, A. Schulz, A. Villinger, *Z. Anorg. Allg. Chem.* **2007**, *633*, 22–35.
- [25] A. Schulz, A. Villinger, *Angew. Chem. Int. Ed.* **2008**, *47*, 603–606.
- [26] M. Lehmann, A. Schulz, A. Villinger, *Angew. Chem. Int. Ed.* **2011**, *50*, 5221–5224.
- [27] S. Herler, P. Mayer, J. Schmedt auf der Günne, A. Schulz, A. Villinger, J. J. Weigand, *Angew. Chem. Int. Ed.* **2005**, *44*, 7790–7793.
- [28] I. Mayer, *J. Comput. Chem.* **2007**, *28*, 204–221.
- [29] N. Burford, J. A. C. Clyburne, P. K. Bakshi, T. S. Cameron, *Organometallics* **1995**, *14*, 1578–1585.
- [30] N. Burford, T. Stanley Cameron, K. N. Robertson, A. D. Phillips, H. A. Jenkins, *Chem. Commun.* **2000**, 2087–2088.
- [31] F. Reiß, A. Schulz, A. Villinger, N. Weding, *Dalton Trans.* **2010**, *39*, 9962–9972.
- [32] M. Lehmann, A. Schulz, A. Villinger, *Eur. J. Inorg. Chem.* **2010**, *2010*, 5501–5508.
- [33] D. Michalik, A. Schulz, A. Villinger, *Angew. Chem. Int. Ed.* **2010**, *49*, 7575–7577.
- [34] M. Baudler, K. Glinka, *Chem. Rev.* **1993**, *93*, 1623–1667.
- [35] M. Scheer, G. Balázs, A. Seitz, *Chem. Rev.* **2010**, *110*, 4236–4256.
- [36] N. A. Giffin, J. D. Masuda, *Coord. Chem. Rev.* **2011**, *255*, 1342–1359.
- [37] M. Baudler, J. Hellmann, *Z. Anorg. Allg. Chem.* **1981**, *480*, 129–141.
- [38] M. Baudler, B. Makowka, *Z. Anorg. Allg. Chem.* **1985**, *528*, 7–21.
- [39] B. Riegel, A. Pfitzner, G. Heckmann, E. Fluck, H. Binder, *Phosphorus Sulfur* **1994**, *93*, 173–176.

- [40] B. Riegel, A. Pfitzner, G. Heckmann, H. Binder, E. Fluck, *Z. Anorg. Allg. Chem.* **1995**, *621*, 1365–1372.
- [41] G. Fritz, T. Vaahs, M. Jarmer, *Z. Anorg. Allg. Chem.* **1990**, *586*, 61–72.
- [42] N. Wiberg, A. Wörner, H.-W. Lerner, K. Karaghiosoff, *Z. Naturforsch. B* **2002**, *57*, 1027–1035.
- [43] A. Lorbach, A. Nadj, S. Tüllmann, F. Dornhaus, F. Schödel, I. Sängler, G. Margraf, J. W. Bats, M. Bolte, M. C. Holthausen, M. Wagner, H.-W. Lerner, *Inorg. Chem.* **2009**, *48*, 1005–1017.
- [44] G. Fritz, J. Härer, *Z. Anorg. Allg. Chem.* **1983**, *500*, 14–22.
- [45] G. Fritz, T. Vaahs, M. Jarmer, *Z. Anorg. Allg. Chem.* **1990**, *589*, 12–22.
- [46] J. J. Weigand, N. Burford, R. J. Davidson, T. S. Cameron, P. Seelheim, *J. Am. Chem. Soc.* **2009**, *131*, 17943–53.
- [47] M. Yoshifuji, I. Shima, N. Inamoto, K. Hirotsu, T. Higuchi, *J. Am. Chem. Soc.* **1981**, *103*, 4587–4589.
- [48] M. Yoshifuji, I. Shima, N. Inamoto, K. Hirotsu, T. Higuchi, *J. Am. Chem. Soc.* **1982**, *104*, 6167.
- [49] H. Köhler, A. Michaelis, *Ber. Dtsch. Chem. Ges.* **1877**, *10*, 807–814.
- [50] J. J. Daly, L. Maier, *Nature* **1964**, *203*, 1167–1168.
- [51] A. H. Cowley, J. E. Kilduff, T. H. Newman, M. Pakulski, *J. Am. Chem. Soc.* **1982**, *104*, 5820–5821.
- [52] P. Jutzi, U. Meyer, B. Krebs, M. Dartmann, *Angew. Chem. Int. Ed. Engl.* **1986**, *25*, 919–921.
- [53] P. Jutzi, U. Meyer, *J. Organomet. Chem.* **1987**, *326*, C6–C8.
- [54] L. N. Markovski, V. D. Romanenko, A. V. Ruban, *Phosphorus Sulfur* **1987**, *30*, 447–450.
- [55] L. Weber, G. Meine, R. Boese, N. Niederprün, *Z. Naturforsch. B* **1988**, *43*, 415–721.
- [56] A. H. Cowley, P. C. Knueppel, C. M. Nunn, *Organometallics* **1989**, *8*, 2490–2492.
- [57] E. Niecke, B. Kramer, M. Nieger, *Angew. Chem. Int. Ed. Engl.* **1989**, *28*, 215–217.
- [58] E. Urnéžius, J. D. Protasiewicz, *Main Group Chem.* **1996**, *1*, 369–372.

- [59] S. Shah, T. Concolino, A. L. Rheingold, J. D. Protasiewicz, *Inorg. Chem.* **2000**, *39*, 3860–3867.
- [60] R. C. Smith, E. Urnezis, K.-C. Lam, A. L. Rheingold, J. D. Protasiewicz, *Inorg. Chem.* **2002**, *41*, 5296–5299.
- [61] J. D. Protasiewicz, M. P. Washington, V. B. Gudimetla, J. L. Payton, M. C. Simpson, *Inorg. Chim. Acta* **2010**, *364*, 39–45.
- [62] R. Riedel, H.-D. Hausen, E. Fluck, *Angew. Chem. Int. Ed. Engl.* **1985**, *24*, 1056–1057.
- [63] V. D. Romanenko, V. L. Rudzevich, E. B. Rusanov, A. N. Chernega, A. Senio, J.-M. Sotiropoulos, G. Pfister-Guillouzo, M. Sanchez, *J. Chem. Soc. Chem. Commun.* **1995**, 1383–1385.
- [64] J. E. Borger, A. W. Ehlers, M. Lutz, J. C. Sloopweg, K. Lammertsma, *Angew. Chem. Int. Ed.* **2014**, *53*, 12836–12839.
- [65] S. Heintl, S. Reisinger, C. Schwarzmaier, M. Bodensteiner, M. Scheer, *Angew. Chem. Int. Ed.* **2014**, *53*, 7639–7642.
- [66] M. Baudler, C. Adamek, S. Opiela, H. Budzikiewicz, D. Ouzounis, *Angew. Chem. Int. Ed. Engl.* **1988**, *27*, 1059–1061.
- [67] M. B. Power, A. R. Barron, *Angew. Chem. Int. Ed. Engl.* **1991**, *30*, 1353–1354.
- [68] I. Krossing, I. Raabe, *Angew. Chem. Int. Ed.* **2001**, *40*, 4406–4409.
- [69] A. R. Fox, R. J. Wright, E. Rivard, P. P. Power, *Angew. Chem. Int. Ed.* **2005**, *44*, 7729–7733.
- [70] J.-P. Bezombes, P. B. Hitchcock, M. F. Lappert, J. E. Nycz, *Dalton Trans.* **2004**, 499.
- [71] J. J. Weigand, M. Holthausen, R. Fröhlich, *Angew. Chem. Int. Ed.* **2009**, *48*, 295–298.
- [72] D. Holschumacher, T. Bannenberg, K. Ibrom, C. G. Daniliuc, P. G. Jones, M. Tamm, *Dalton Trans.* **2010**, *39*, 10590–10592.
- [73] E. Niecke, R. Rüger, *Angew. Chem. Int. Ed. Engl.* **1982**, *21*, 62–62.
- [74] P. Jutzi, R. Kroos, A. Müller, M. Penk, *Angew. Chem. Int. Ed. Engl.* **1989**, *28*, 600–601.
- [75] H. G. Viehe, R. Merényi, J. F. M. Oth, J. R. Senders, P. Valange, *Angew. Chem. Int. Ed. Engl.* **1964**, *3*, 755–756.
- [76] K. E. Wilzbach, J. S. Ritscher, L. Kaplan, *J. Am. Chem. Soc.* **1967**, *89*, 1031–1032.

- [77] M. Baudler, M. Michels, M. Pieroth, J. Hahn, *Angew. Chem. Int. Ed. Engl.* **1986**, *25*, 471–473.
- [78] P. Jutzi, R. Kroos, A. Müller, H. Bögge, M. Penk, *Chem. Ber.* **1991**, *124*, 75–81.
- [79] T. R. Galeev, A. I. Boldyrev, *Phys. Chem. Chem. Phys.* **2011**, *13*, 20549–20556.
- [80] *Gaussian 09, Revision C.01*, M. J. Frisch, G. W. Trucks, H. B. Schlegel, G. E. Scuseria, M. A. Robb, J. R. Cheeseman, G. Scalmani, V. Barone, B. Mennucci, G. A. Petersson, H. Nakatsuji, M. Caricato, X. Li, H. P. Hratchian, A. F. Izmaylov, J. Bloino, G. Zheng, J. L. Sonnenberg, M. Hada, M. Ehara, K. Toyota, R. Fukuda, J. Hasegawa, M. Ishida, T. Nakajima, Y. Honda, O. Kitao, H. Nakai, T. Vreven, J. A. Montgomery Jr., J. E. Peralta, F. Ogliaro, M. Bearpark, J. J. Heyd, E. Brothers, K. N. Kudin, V. N. Staroverov, T. Keith, R. Kobayashi, J. Normand, K. Raghavachari, A. Rendell, J. C. Burant, S. S. Iyengar, J. Tomasi, M. Cossi, N. Rega, J. M. Millam, M. Klene, J. E. Knox, J. B. Cross, V. Bakken, C. Adamo, J. Jaramillo, R. Gomperts, R. E. Stratmann, O. Yazyev, A. J. Austin, R. Cammi, C. Pomelli, J. W. Ochterski, R. L. Martin, K. Morokuma, V. G. Zakrzewski, G. A. Voth, P. Salvador, J. J. Dannenberg, S. Dapprich, A. D. Daniels, O. Farkas, J. B. Foresman, J. V. Ortiz, J. Cioslowski, D. J. Fox, Gaussian, Inc., Wallingford CT, **2010**.
- [81] E. D. Glendening, J. K. Badenhoop, A. E. Reed, J. E. Carpenter, J. A. Bohmann, C. M. Morales, C. R. Landis, F. Weinhold, *NBO 6.0*, Theoretical Chemistry Institute, University of Wisconsin, Madison, **2013**.
- [82] J. P. Perdew, K. Burke, M. Ernzerhof, *Phys. Rev. Lett.* **1996**, *77*, 3865–3868.
- [83] J. P. Perdew, K. Burke, M. Ernzerhof, *Phys. Rev. Lett.* **1997**, *78*, 1396–1396.
- [84] C. Adamo, V. Barone, *J. Chem. Phys.* **1999**, *110*, 6158–6170.
- [85] R. Ditchfield, W. J. Hehre, J. A. Pople, *J. Chem. Phys.* **1971**, *54*, 724–728.
- [86] W. J. Hehre, R. Ditchfield, J. A. Pople, *J. Chem. Phys.* **1972**, *56*, 2257–2261.
- [87] P. C. Hariharan, J. A. Pople, *Theor. Chim. Acta* **1973**, *28*, 213–222.
- [88] P. C. Hariharan, J. A. Pople, *Mol. Phys.* **1974**, *27*, 209–214.
- [89] M. S. Gordon, *Chem. Phys. Lett.* **1980**, *76*, 163–168.
- [90] M. M. Francl, W. J. Pietro, W. J. Hehre, J. S. Binkley, M. S. Gordon, D. J. DeFrees, J. A. Pople, *J. Chem. Phys.* **1982**, *77*, 3654–3665.
- [91] R. C. Binning Jr., L. A. Curtiss, *J. Comput. Chem.* **1990**, *11*, 1206–1216.

- [92] J.-P. Blaudeau, M. P. McGrath, L. A. Curtiss, L. Radom, *J. Chem. Phys.* **1997**, *107*, 5016–5021.
- [93] V. A. Rassolov, J. A. Pople, M. A. Ratner, T. L. Windus, *J. Chem. Phys.* **1998**, *109*, 1223–1229.
- [94] V. A. Rassolov, M. A. Ratner, J. A. Pople, P. C. Redfern, L. A. Curtiss, *J. Comput. Chem.* **2001**, *22*, 976–984.
- [95] T. H. Dunning Jr., *J. Chem. Phys.* **1989**, *90*, 1007–1023.
- [96] R. A. Kendall, T. H. Dunning Jr., R. J. Harrison, *J. Chem. Phys.* **1992**, *96*, 6796–6806.
- [97] D. E. Woon, T. H. Dunning Jr., *J. Chem. Phys.* **1993**, *98*, 1358–1371.
- [98] K. A. Peterson, D. E. Woon, T. H. Dunning Jr., *J. Chem. Phys.* **1994**, *100*, 7410–7415.
- [99] T. Hashimoto, K. Hirao, H. Tatewaki, *Chem. Phys. Lett.* **1995**, *243*, 190–192.
- [100] A. K. Wilson, T. van Mourik, T. H. Dunning Jr., *J. Mol. Struct. Theochem* **1996**, *388*, 339–349.
- [101] J. P. Merrick, D. Moran, L. Radom, *J. Phys. Chem. A* **2007**, *111*, 11683–11700.
- [102] F. London, *J. Phys. Radium* **1937**, *8*, 397–409.
- [103] R. McWeeny, *Phys. Rev.* **1962**, *126*, 1028–1034.
- [104] R. Ditchfield, *Mol. Phys.* **1974**, *27*, 789–807.
- [105] K. Wolinski, J. F. Hinton, P. Pulay, *J. Am. Chem. Soc.* **1990**, *112*, 8251–8260.
- [106] J. R. Cheeseman, G. W. Trucks, T. A. Keith, M. J. Frisch, *J. Chem. Phys.* **1996**, *104*, 5497–5509.
- [107] C. J. Jameson, A. De Dios, A. Keith Jameson, *Chem. Phys. Lett.* **1990**, *167*, 575–582.
- [108] C. van Wüllen, *Phys. Chem. Chem. Phys.* **2000**, *2*, 2137–2144.
- [109] M. Yoshifuji, in *Synthetic Methods of Organometallic and Inorganic Chemistry, Vol. 3* (Ed.: H.H. Karsch), Thieme, Stuttgart, New York, **1996**, pp. 118–125.
- [110] A. H. Cowley, N. C. Norman, M. Pakulski, G. Becker, M. Layh, E. Kirchner, M. Schmidt, *Inorg. Synth.* **1990**, *27*, 235–240.
- [111] C. J. F. Du, H. Hart, K. K. D. Ng, *J. Org. Chem.* **1986**, *51*, 3162–3165.
- [112] B. Schiemenz, P. P. Power, *Organometallics* **1996**, *15*, 958–964.

- [113] Z. Zhu, M. Brynda, R. J. Wright, R. C. Fischer, W. A. Merrill, E. Rivard, R. Wolf, J. C. Fettinger, M. M. Olmstead, P. P. Power, *J. Am. Chem. Soc.* **2007**, *129*, 10847–10857.
- [114] W. A. Merrill, E. Rivard, J. S. DeRopp, X. Wang, B. D. Ellis, J. C. Fettinger, B. Wrackmeyer, P. P. Power, *Inorg. Chem.* **2010**, *49*, 8481–8486.
- [115] J. Bresien, *Darstellung Neuer Niedervalenter Phosphorverbindungen*, MSc Thesis, University of Rostock, **2013**.
- [116] E. Niecke, R. Rüger, *Angew. Chem. Int. Ed. Engl.* **1983**, *22*, 155–156.
- [117] A. A. Sandoval, H. C. Moser, *Inorg. Chem.* **1963**, *2*, 27–29.
- [118] G. Fritz, J. Härer, *Z. Anorg. Allg. Chem.* **1981**, *481*, 185–200.
- [119] G. Fritz, K. Stoll, *Z. Anorg. Allg. Chem.* **1986**, *538*, 78–112.
- [120] P. Pykkö, M. Atsumi, *Chem. Eur. J.* **2009**, *15*, 12770–12779.
- [121] E. Niecke, R. Rüger, B. Krebs, *Angew. Chem. Int. Ed. Engl.* **1982**, *21*, 544–545.
- [122] P. Jutzi, T. Wippermann, *J. Organomet. Chem.* **1985**, *287*, C5–C7.
- [123] P. Jutzi, U. Meyer, *J. Organomet. Chem.* **1987**, *333*, C18–C20.
- [124] M. Donath, E. Conrad, P. Jerabek, G. Frenking, R. Fröhlich, N. Burford, J. J. Weigand, *Angew. Chem. Int. Ed.* **2012**, *51*, 2964–2967.
- [125] M. H. Holthausen, S. K. Surmiak, P. Jerabek, G. Frenking, J. J. Weigand, *Angew. Chem. Int. Ed.* **2013**, *52*, 11078–11082.
- [126] I. Krossing, A. Reisinger, *Coord. Chem. Rev.* **2006**, *250*, 2721–2744.
- [127] I. Krossing, I. Raabe, *Angew. Chem. Int. Ed.* **2004**, *43*, 2066–2090.
- [128] S. Alvarez, *Dalton Trans.* **2013**, *42*, 8617–8636.
- [129] R. E. Bachman, D. F. Andretta, *Inorg. Chem.* **1998**, *37*, 5657–5663.
- [130] E. L. Muetterties, C. W. Alegranti, *J. Am. Chem. Soc.* **1972**, *94*, 6386–6391.
- [131] R. J. Davidson, J. J. Weigand, N. Burford, T. S. Cameron, A. Decken, U. Werner-Zwanziger, *Chem. Commun.* **2007**, 4671–4673.
- [132] M. F. Guest, I. H. Hillier, V. R. Saunders, *J. Chem. Soc. Faraday Trans. 2* **1972**, *68*, 2070–2074.
- [133] A. H. Cowley, M. Pakulski, N. C. Norman, *Polyhedron* **1987**, *6*, 915–919.

6 Selected Publications

The following chapter contains the original publications wherein the previously presented research was reported. My own contribution to each manuscript is outlined in the following:

All experimental work as well as the computational studies described in chapter 6.1 (*Chem. Eur. J.* **2014**, *20*, 12607–12615) were carried out by me. Additionally, I ran the NMR simulations and refined some of the crystal structures. A few of the experiments had already been done in the course of the work for my MSc thesis, which was supervised by Christian Hering-Junghans; however, the majority of the data was gathered during my PhD period. I wrote the manuscript as well as the supporting information. My own contribution amounts to approx. 85 %.

I carried out a large part of the experimental and computational work described in chapter 6.2 (*Angew. Chem. Int. Ed.* **2015**, *54*, 6926–6930). Additionally, I performed the NMR simulations and refined the crystal structures. Kirill Faust synthesised the title compound in the course of his BSc studies under my supervision. I wrote the manuscript as well as the supporting information. My own contribution amounts to approx. 80 %.

All experimental work as well as the computational studies described in chapters 6.3 (*Dalton Trans.* **2016**, *45*, 498–501) and 6.4 (*Chem. Eur. J.* **2015**, *21*, 18543–18546) were carried out by me. I performed the NMR simulations and refined the crystal structures. Additionally, I wrote the manuscripts as well as the supporting information. My own contribution amounts to approx. 90 %.

About two thirds of the experimental work in chapter 6.5 (*Dalton Trans.* **2016**, *45*, 1998–2007) were carried out by me. Part of the characterisation of the bicyclic tetraphosphanes was performed by Julia Rothe in the course of her BSc studies, which were supervised by Christian Hering-Junghans. The GaCl₃ adducts were first synthesised by me during my MSc studies, however missing analytical data for all compounds were collected during my PhD period. The reduction of [CIP(μ -PMes*)]₂ was first done by Kirill Faust under my supervision and later re-investigated by me. I performed all NMR investigations and computational studies, including the gathering of kinetic and thermodynamic data, and I was involved in the refinement of the crystal structures. Additionally, I wrote the manuscript as well as the supporting information. My own contribution amounts to approx. 70%.

6.1 Dimers and Trimers of Diphosphenes: A Wealth of Cyclophosphanes

Jonas Bresien, Christian Hering, Axel Schulz, and Alexander Villinger

Chem. Eur. J. **2014**, *20*, 12607–12615.

DOI: 10.1002/chem.201403631

Reprinted with permission from John Wiley & Sons, Inc. (Licence No. 3796571110200)

Copyright 2014 John Wiley & Sons, Inc. All rights reserved.

Phosphorus Chemistry

Dimers and Trimers of Diphosphenes: A Wealth of *Cyclo*-Phosphanes

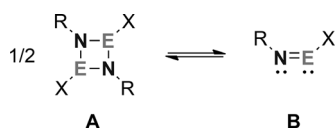
Jonas Bresien,^[a] Christian Hering,^[a] Axel Schulz,^{*,[a, b]} and Alexander Villinger^[a]

Abstract: Various new P-based ring systems were synthesised by transferring established reaction routes from NP chemistry to the analogous PP compounds. Due to the different electronic situations of phosphorus and nitrogen with respect to s and p character of the lone pair, different reactivity of the phosphorus compounds was observed, especially with regard to the specificity of the reactions and the sta-

bility of the products. Whereas Mes^{*}N=PCl (Mes^{*}=2,4,6-*tert*-butylphenyl) is stable in the solid state and in solution, the formal phosphorus congener Mes^{*}P=PCl is highly reactive and could not be observed. Instead, several formal dimers and trimers of Mes^{*}P=PCl could be isolated, which constitute an intriguing variety of three- and four-membered ring systems.

Introduction

The synthesis of compounds containing E–E multiple bonds (E = group 15 element) is a well-established area of main group chemistry.^[1] In particular, we have always had great interest in NE chemistry, for example, the synthesis of *cyclo*-dipnictadiazanes [XE(μ-NR)]₂ (A, X = (pseudo)halogen).^[2–10] These four-membered ring systems are closely related to the highly reactive haloiminopnictanes RN=EX (B), since they can be regarded as formal dimers of the latter (Scheme 1). The stability

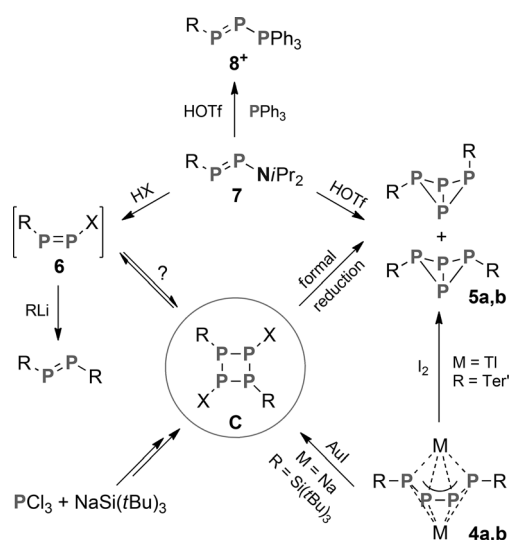


Scheme 1. Formal equilibrium between *cyclo*-dipnictadiazanes (A) and (pseudo)halogen-substituted iminophosphanes (B) depending on the size of the substituent R.

of the monomeric iminopnictanes in comparison with the corresponding dimeric *cyclo*-dipnictadiazanes depends on the size of the sterically demanding substituent R.^[11,12] For example, the supermesityl substituent (Mes^{*}=2,4,6-*tri-tert*-butylphenyl) favours the formation of the monomeric iminophosphane Mes^{*}NPCl (1), which is stable in the solid state and in solution.^[13,14] However, less sterically demanding substituents, such

as the terphenyl group (Ter = 2,6-dimesitylphenyl), promote the formation of dimeric *cyclo*-dipnictadiazanes, for example, [CIP(μ-NTer)]₂ (2).^[5,15]

These earlier findings prompted us to expand the concepts of NE chemistry to the analogous phosphorus compounds. Even though four-membered ring systems based on P are well investigated,^[16] especially with organic or amino substituents at P, little is known about *cyclo*-tetraphosphanes of the type [XP(μ-PR)]₂ (C in Scheme 2). Only two examples of this class of compounds are described in the literature. The chloro-substituted *cyclo*-tetraphosphane [CIP(μ-PSi*t*Bu₃)]₂ (3a) was identified by ³¹P NMR spectroscopy as an intermediate of the reaction of PCl₃ with NaSi*t*Bu₃, but was neither isolated nor further characterised.^[17] In contrast, the iodo-substituted analogue [IP(μ-



Scheme 2. Reactivity of P compounds related to *cyclo*-tetraphosphanes C (4a: R = Si*t*Bu₃; 4b: R = Ter'; 5a: R = Ter'; 5b: R = Mes^{*}; 6: R = Mes^{*}, X = Cl; 7: R = Mes^{*}; 8⁺: R = Mes^{*}).

[a] J. Bresien, Dipl.-Chem. C. Hering, Prof. Dr. A. Schulz, Dr. A. Villinger
Universität Rostock, Institut für Chemie
Albert-Einstein-Strasse 3a, 18059 Rostock (Germany)
E-mail: axel.schulz@uni-rostock.de

[b] Prof. Dr. A. Schulz
Leibniz-Institut für Katalyse e.V. an der Universität Rostock
Albert-Einstein-Straße 29a, 18059 Rostock (Germany)

Supporting information for this article is available on the WWW under
<http://dx.doi.org/10.1002/chem.201403631>.

PSitBu₃]₂ (**3b**), which was obtained by reaction of the tetraphosphenediide Na₂[tBu₃SiPPPSitBu₃] (**4a**) with Aul, was fully characterized, including single crystal structure elucidation.^[18] Upon treatment with iodine, the similar tetraphosphenediide TI₂[Ter'PPPTer'] (**4b**, Ter' = 2,6-(2,6-diisopropylphenyl)phenyl) gave the bicyclotetraphosphane Ter'₂P₄Ter' (**5a**), which can be regarded as the formal reduction product of [XP(μ-PTer')]₂.^[19]

Concerning halogen-substituted diphosphenes, the formal monomers of the discussed *cyclo*-tetraphosphanes, the only reported example is Mes*PPI (**6**), which was proposed to be the labile intermediate of the reaction of Mes*PPN(*i*Pr)₂ (**7**) with various organolithium compounds (RLi) in the presence of HCl, leading to differently substituted diphosphenes of the type Mes*PPR.^[20] However, no analytical information proving the formation of **6** was given in the publication, and thus its existence is uncertain. A closely related compound is the diphenyl-substituted phosphonium salt [Mes*PP(PPh₃)OTf] (**8OTf**), which was synthesized by treating **7** with HOTf in the presence of PPh₃.^[21] The cation was dubbed a “donor-stabilized phosphanetriylphosphonium cation” in the original publication (or as we would call it, a donor-stabilized diphosphadiazonium cation). In our opinion, though, this name does not reflect the actual bonding situation, since experimental and theoretical data give proof for a diphosphene with an adjacent phosphonium centre. The solid-state structure reveals an angled CPPP backbone and a central P–P bond length of 2.035(1) Å that corresponds to a typical double bond ($\Sigma r_{\text{cov}}(\text{P}=\text{P}) = 2.04 \text{ \AA}$).^[22] Furthermore, NBO analysis showed that the positive charge is mostly localized at the P atom of the PPh₃ moiety (Supporting Information). Lack of the stabilizing PPh₃ resulted in the formation of the bicyclotetraphosphane Mes*P₄Mes* (**5b**), which was previously described by Fluck and co-workers.^[23] We took these findings as a starting point for our own investigations, which we report herein.

Results and Discussion

Oftentimes, P-based ring systems and related polyphosphorus compounds are derived from white phosphorus (P₄).^[24] We decided to investigate a different approach, that is, the synthesis of ring systems starting from P₁ building blocks. In analogy to the synthesis of **1**,^[14] we treated Mes*PH₂ (**9**) with an excess of PCl₃ (to avoid multiple substitution) in the presence of NEt₃. After 12 h, the ³¹P NMR spectrum of the reaction mixture (Figure 1) indicated intermediate formation of Mes*P=PP(Mes*)PCl₂ (**10**), which slowly isomerised to the desired compound [CIP(μ-PMes*)]₂ (**11**, Scheme 3) after 20 h.

Both compounds **10** and **11** were identified by calculation of the ³¹P NMR data and subsequent simulation of the spectra (see Supporting Information). Compound **10** is characterised by an ABCD spin system that comprises four threefold doublets (Figure 1). Two of the signals exhibit large downfield shifts ($\delta_{\text{exptl}} = 587.0, 463.2 \text{ ppm}$; $\delta_{\text{calcd}} = 605.1, 468.5 \text{ ppm}$) with a large negative coupling constant ($^1J_{\text{exptl}} = -578 \text{ Hz}$; $^1J_{\text{calcd}} = -507 \text{ Hz}$), which is typical for diphosphenes.^[25–28] The PCl₂ group displays a chemical shift of 209.5 ppm ($\delta_{\text{calcd}} = 163.9 \text{ ppm}$), which is in

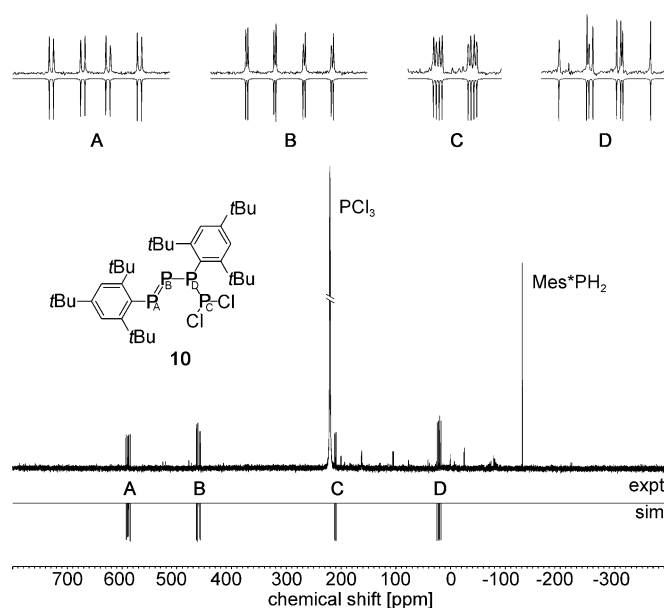
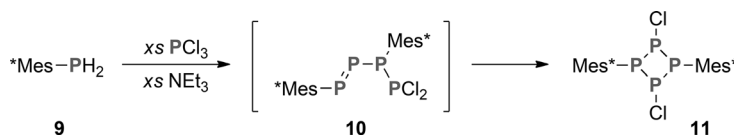


Figure 1. ³¹P NMR spectrum of intermediate **10** from the reaction of **9** with PCl₃ and NEt₃ after 12 h of reaction time. The simulated NMR spectrum is depicted at the bottom.



Scheme 3. Reaction of Mes*PH₂ (**9**) with an excess of PCl₃ and NEt₃ leads to intermediate **10**, which isomerises to [CIP(μ-PMes*)]₂ (**11**).

the expected range of dichloro-substituted phosphanes.^[29–32] The central PMes* moiety is shifted to 21.7 ppm ($\delta_{\text{calcd}} = 7.4 \text{ ppm}$). Compound **11** displays an A₂X₂ spin system (Figure S1, Supporting Information) with chemical shifts of –8.1 ppm ($\delta_{\text{calcd}} = -1.6 \text{ ppm}$) and 131.1 ppm ($\delta_{\text{calcd}} = 119.9 \text{ ppm}$) and a coupling constant of –217 Hz ($^1J_{\text{calcd}} = -166 \text{ Hz}$). These values compare nicely with the NMR shifts and coupling constants previously reported for **3a** (–14.8 ppm, 120.5 ppm; –244 Hz) and **3b** (–34.9 ppm, 149.0 ppm; –227 Hz).^[17,18]

All attempts to crystallize and subsequently isolate **10** failed. Instead, the constitutionally isomeric *cyclo*-tetraphosphane **11** (Figure 2) was isolated in moderate yield from saturated solutions. Moreover, it was possible to crystallize and identify two side products of the reaction, namely, the *cyclo*-tetraphosphanes **12** (see Figure 5 below) and **13** (see Figure 6 below) with exocyclic chlorophosphanyl groups. Interestingly, all compounds display a formal composition that can be described as (Mes*P₂Cl)_n (n = 2, 3), that is, they are formal dimers and trimers of **6**, respectively.

Compound **11** crystallised from saturated fluorobenzene solution as colourless block-shaped crystals in triclinic space group P $\bar{1}$, monoclinic space group P2₁/c or as fluorobenzene solvate **11**·PhF in monoclinic space group P2₁/n. The molecular structure of **11** is similar in each case, although the fold angle

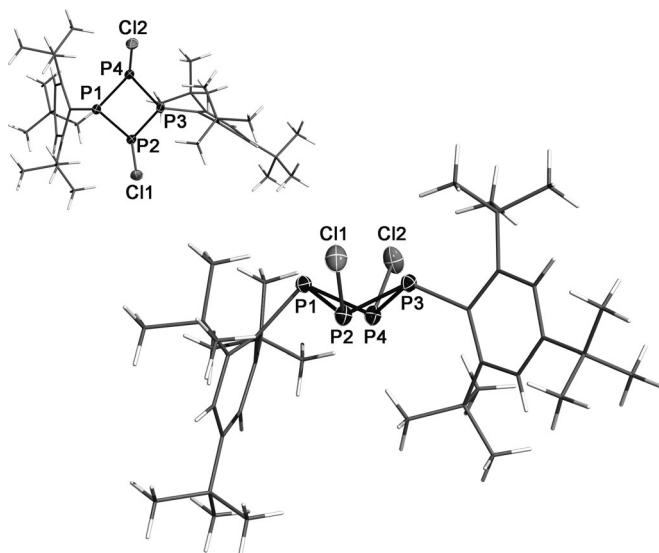


Figure 2. Molecular structure of **11** in the crystal ($P2_1/c$). Thermal ellipsoids drawn at 50% probability and -100°C . Mes* substituents rendered as wire-frame for clarity. Selected bond lengths [Å] and angles [$^\circ$]: P1–P2 2.2731(5), P1–P4 2.2596(5), P1–Cl1 1.869(1), P2–P3 2.1905(5), P2–Cl1 2.0967(5), P3–P4 2.2026(5), P3–C19 1.844(1), P4–Cl2 2.1061(6); C1–P1–P2 99.23(4), C1–P1–P4 101.96(4), P1–P2–P3 80.54(2), P1–P2–Cl1 106.45(2), P3–P2–Cl1 97.97(2), P2–P3–P4 84.65(2), P2–P3–C19 108.97(5), P4–P3–C19 122.05(5), P3–P4–P1 80.58(2), P3–P4–Cl2 97.32(2), P1–P4–Cl2 104.47(2); P1–P2–P4–P3 119.45(3), C11–P2–P4–Cl2 $-1.06(5)$, C1–P1–P3–C19 $-17.9(1)$.

of the four-membered ring system, which adopts a slight butterfly conformation, varies significantly depending on the crystal structure.

The fold angles ϕ_1 and ϕ_2 (Figure 3) describe the puckering of the ring system; values close to 180° represent a nearly flat ring, whereas smaller values indicate a more pronounced puckering of the ring system.^[33] In symmetrically substituted rings, both angles adopt the same value, whereas in asymmetrically substituted rings, the values can differ significantly. In case of **11**, though, the fold angles ϕ_1 and ϕ_2 are very similar ($\Delta\phi \leq 2^\circ$). Therefore, the average values for each crystal structure are discussed. The experimentally determined fold angles vary from 120° ($P2_1/c$) through 139° ($P\bar{1}$), to 143° ($P2_1/n$). The calculated gas-phase structure displays a fold angle of 133° , which is roughly in the middle of the experimental range. Hence, the deviations of the fold angles are presumably due to packing effects in the solid state. These values compare well with those of other P_4 ring systems, in which fold angles span a wide range from 173 to 110° .^[34,35] This demonstrates the high flexibility of the four-membered ring system due to a flat energy potential for that kind of deformation.

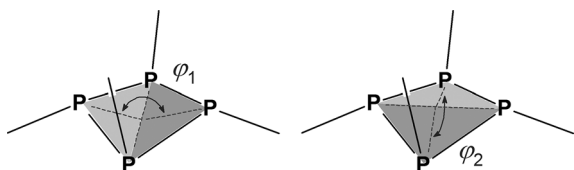


Figure 3. Fold angles ϕ_1 and ϕ_2 .

All substituents at the P_4 ring system are arranged in equatorial positions. One of the Mes* substituents is twisted around the P–C bond axis (angle between least-squares planes of the phenyl rings: 61.0°) to minimize steric repulsion between the *ortho-tert-butyl* groups and the chlorine atoms. Consequently, the chlorine atoms are slightly bent towards P3, and the P1–P2–Cl1 and P1–P4–Cl2 angles (av 103°) are significantly larger than the P3–P2–Cl1 and P3–P4–Cl2 angles (av 98°). This effect is especially pronounced in the structures with small fold angles, due to the increased steric strain between the *ortho-tert-butyl* and Cl substituents. The P–P bond lengths between P1 and P2 or P4 are slightly longer than the sum of the covalent radii (av 2.26 Å; cf. $\Sigma r_{\text{cov}}(\text{PP}) = 2.22$ Å),^[22] whereas the P2–P3 and P3–P4 bond lengths are shortened (av 2.20 Å). The P–Cl bond lengths (av 2.10 Å) correspond to typical single bonds (cf. $\Sigma r_{\text{cov}}(\text{PCL}) = 2.10$ Å).^[22] Detailed structural data are summarized in Table 1.

Table 1. Selected bond lengths [Å] and angles and dihedral angles of **11** [$^\circ$] in the solid state and calculated values [PBE0/6-31G(d,p)].

	$P2_1/c$	$P2_1/n$	$P\bar{1}$	Calcd
P1–P2	2.2731(5)	2.2542(7)	2.2606(5)	2.274
P1–P4	2.2596(5)	2.2533(7)	2.2548(5)	2.272
P2–P3	2.1905(5)	2.1927(7)	2.2184(5)	2.204
P3–P4	2.2026(5)	2.2178(7)	2.1766(5)	2.217
Cl1–P2	2.0967(5)	2.0878(7)	2.1086(5)	2.118
Cl2–P4	2.1061(6)	2.1070(8)	2.0999(5)	2.118
P1–P2–Cl1	106.45(2)	101.87(3)	100.89(2)	104.4
P3–P2–Cl1	97.97(2)	98.23(3)	98.24(2)	100.0
P1–P4–Cl2	104.47(2)	99.76(3)	104.40(2)	104.6
P3–P4–Cl2	97.32(2)	97.63(3)	98.55(2)	98.7
P1–P2–P4–P3 (ϕ_1)	119.45(3)	143.21(4)	138.82(3)	133.3
P2–P1–P3–P4 (ϕ_2)	120.72(3)	143.47(4)	139.47(3)	133.6

Clearly, the conformation of **11** in the solid state does not account for the observed A_2X_2 pattern in the ^{31}P NMR spectrum. However, a slight broadening of the triplet signal, which was assigned to the Mes*-substituted P atoms, hints at a possible underlying dynamic effect, that is, the rotation of the Mes* substituents is fast compared to the NMR timescale. Thus, a variable-temperature NMR experiment was carried out and revealed a distinct broadening of the signal in question at -20°C . Upon cooling to -80°C , the signal divided into two broad resonances, indicating two inequivalent Mes*-substituted P atoms in accordance with the solid-state structure ($\delta_{\text{exptl}} = 9.3, -34.7$ ppm; $\delta_{\text{calcd}} = 2.6, -67.5$ ppm). However, it was impossible to reach the coalescence temperature of the Cl-substituted P atoms; thus, the observed effects in the NMR spectrum cannot be unambiguously assigned to rotation of the Mes* substituent, and other dynamic effects may well contribute to the signal broadening (Figure S1, Supporting Information).

Calculations at the PBE0/6-31G(d,p) level of theory identified two possible rotamers of **11** (Figure 4). The C_2 -symmetric conformer **11B** is about 24.3 kJ mol $^{-1}$ higher in energy than C_1 -symmetric **11A**. The rotational barrier of about 58 kJ mol $^{-1}$ is reasonably small and confirms free rotation of the Mes* substituents at ambient temperature.

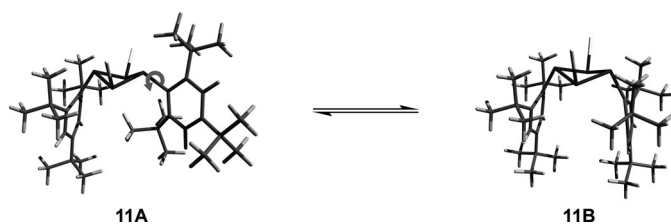


Figure 4. The calculated rotamers **11 A** and **11 B** are minimum structures of **11**. The Gibbs energy of **B** is 24.3 kJ mol⁻¹ higher than that of **A**, and the rotational barrier is estimated to be 58 kJ mol⁻¹ (gas phase).

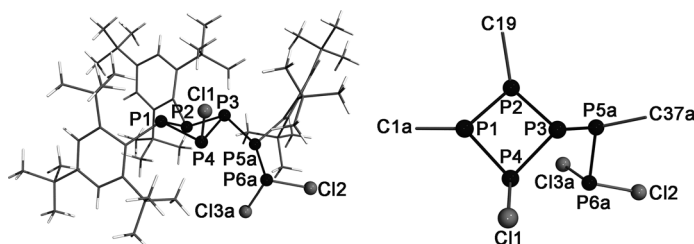


Figure 5. Left: Molecular structure of **12** in the crystal. Right: Central motif, only the *ipso*-C atoms of the Mes* groups are displayed.

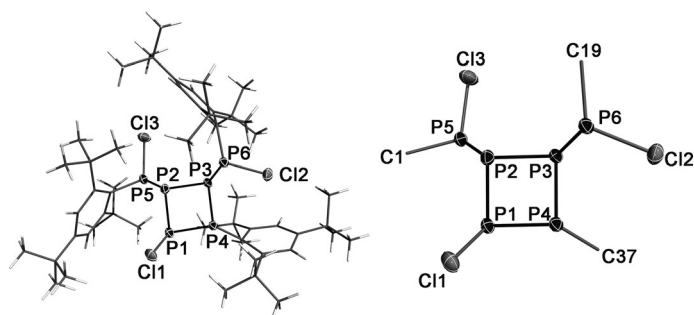


Figure 6. Molecular structure of **13** in the crystal. Thermal ellipsoids drawn at 50% probability and -100 °C. Left: Mes* substituents rendered as wireframe. Right: Central motif, only the *ipso*-C atoms of the Mes* groups are displayed. Selected bond lengths [Å] and angles [°]: P1–P2 2.225(1), P1–P4 2.239(1), P2–P3 2.239(1), P2–P5 2.229(1), P3–P4 2.220(1), P3–P6 2.237(1), P1–C11 2.093(1), P4–C37 1.848(3), P5–Cl3 2.094(1), P5–C1 1.849(3), P6–Cl2 2.104(1), P6–C19 1.855(3); P2–P1–P4 80.79(4), P1–P2–P3 87.36(5), P2–P3–P4 80.89(4), P3–P4–P1 87.50(4); P4–P1–P2–P3 35.30(4), P1–P2–P3–P4 -35.62(4), P5–P2–P3–P6 141.34(5), P2–P3–P4–P1 35.37(4), P3–P4–P1–P2 -35.64(4).

Side product **12** (Figure 5) only gave small crystals; accordingly, the quality of the X-ray diffraction data is not sufficient to discuss detailed bond lengths and angles. However, it can be stated that all P–P, P–Cl and P–C bond length are within the ranges of typical single bonds. The P₄ ring adopts a butterfly conformation, with all substituents arranged in equatorial positions.

Because only small amounts of **12** could be obtained, the signal-to-noise ratio in all ³¹P NMR spectra was too low for unambiguous assignment of the NMR signals. Thus, experimental proof is lacking that **12** does actually persist in solution; possibly, this species is only stable in the solid phase and undergoes rearrangement or dissociation upon dissolution. Owing to the very low yields of **12**, further studies seemed infeasible.

Compound **13** (Figure 6) crystallized from saturated CH₂Cl₂ solution in the space group *P*1̄ with two independent molecules of **13** and two molecules of dichloromethane in the asymmetric unit. This explains the large unit-cell volume of 6251.7(6) Å³. Again, all P–P, P–C and P–Cl bond lengths are within the ranges of typical single bonds. The P₄ ring adopts a butterfly conformation with a fold angle of about 128°. The endocyclic bond angles range between 80.79(4) and 87.50(4)° and all substituents are arranged in equatorial positions. These structural parameters are typical for *cyclo*-tetraphosphanes.^[28,36,37]

Due to the larger size of the crystals, it was possible to separate some of them from a large part of the adhering impurities and thus allow a ³¹P NMR spectrum to be recorded. By means of calculated NMR data (Table 2) and subsequent simulation of the spectrum, all signals arising from **13** could be unambiguously identified (Figure 7), and thus the persistence of **13** in solution was proved.

We emphasize that compounds **12** and **13** were only two side products of the reaction amongst other, possibly similar species that could not be isolated. Due to their functional similarities, general low solubility and low yields, further purification of these compounds was not possible within a reasonable amount of time.

In summary, the identification of compounds **10**–**13** helped to understand the pathway of the reaction of Mes*PH₂ (**9**) with PCl₃ and NEt₃. Formation of the intermediate diphosphene **10** proved that a species with a P–P double bond was generated by base-induced HCl elimination. It is not unlikely that the chlorodiphosphene **6** was actually formed in situ, but underwent further reaction with **9** and PCl₃ to give **10**. After a while, decreasing intensity of the NMR signals of **10** in favour of those of **11** indicated a slow rearrangement reaction, the specificity of which was found to improve upon use of a polar solvent. Compound **12** can be regarded as the formal [2+2] cyclo-

Table 2. Experimentally determined ³¹P NMR shifts and coupling constants of **13**. Calculated values [PBE0/6-31G(d,p)] are given in parentheses.

X	δ [ppm]	J [Hz]				
		P _A -X	P _B -X	P _C -X	P _D -X	P _E -X
P _A	+147.2	-	-	-	-	-
	(+144.9)	-	-	-	-	-
P _B	+96.0	-24	-	-	-	-
	(+67.5)	(-26)	-	-	-	-
P _C	+72.9	+193	-0.5	-	-	-
	(+52.2)	(+151)	(-14)	-	-	-
P _D	-17.4	-210	+303	-19	-	-
	(-51.9)	(-170)	(+191)	(-30)	-	-
P _E	-24.9	-16	-205	+221	-120	-
	(-48.7)	(-5)	(-144)	(+103)	(-73)	-
P _F	-44.8	-185	+225	-174	+80	-140
	(-54.5)	(-152)	(+183)	(-114)	(+60)	(-97)

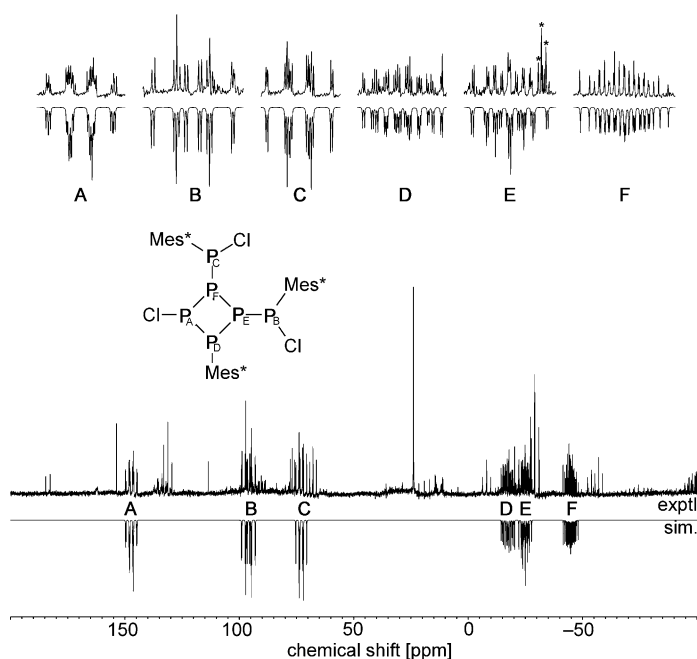
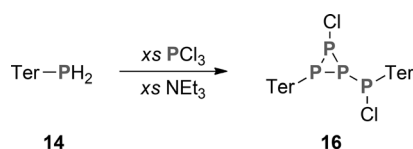


Figure 7. ^{31}P NMR spectrum of impure **13**. All signals of **13** could be identified by NMR spectrum simulation (bottom), thus proving the presence of this species in solution. Starred lines within the enlarged signals arise from impurities.

addition product of **10** and **6**, which hints at possible intermediate formation of **6**. Lastly, compound **13** is most likely the product of a rearrangement reaction, possibly starting from **12**, although the exact reaction pathway remains unclear.

In a next series of experiments, we slightly decreased the steric hindrance by utilizing the terphenyl substituent (average cone angle $\theta_{\text{av}} = 196^\circ$ at 1.85 Å) instead of Mes* ($\theta_{\text{av}} = 224^\circ$ at 1.85 Å).^[38] Upon treatment of TerPH₂ (**14**) with an excess of PCl₃ and NEt₃ under the same reaction conditions, a surprisingly different reaction outcome was observed (Scheme 4). Accord-



Scheme 4. Treatment of TerPH₂ (**14**) with an excess of PCl₃ and NEt₃ leads to the formation of *cyclo*-triphosphane **16**.

ing to the ^{31}P NMR spectrum of the reaction mixture after complete consumption of **14**, only very small amounts of the expected *cyclo*-tetraphosphane [ClP(μ -PTer)]₂ (**15**) had formed. Instead, an intriguing *cyclo*-triphosphane with an exocyclic chlorophosphanyl substituent (**16**, Figure 8) was obtained in moderate yield. Moreover, no intermediate diphosphene species comparable to **10** could be observed during the reaction. Instead, an H/Cl exchange at the P atom of **14** was detected, leading to the presence of TerPH₂, TerPHCl and TerPCl₂ in the reaction mixture. The presence of these species apparently gave rise to reaction channels different to those observed for Mes*PH₂ (see above).

Compound **16** crystallized from diethyl ether/benzene in monoclinic space group $P2_1/n$ as an Et₂O/C₆H₆ solvate. The three-membered ring system adopts the shape of an almost equilateral triangle in which the P₃–P₄ bond is slightly shorter (2.1787(9) Å) than the other P–P bonds (av 2.23 Å; cf. $\Sigma r_{\text{cov}}(\text{PP}) = 2.22$ Å).^[22] The inner angles of the P₃ ring vary from 58.55(3) to 60.97(3) $^\circ$; thus, all angles are close to the ideal value of 60 $^\circ$, which is typical for *cyclo*-triphosphanes.^[39–44] The P–C and P–Cl distances are all within the range of typical single bonds. The two Ter substituents are at an angle of 65.4 $^\circ$ to one another (angle between the least-squares planes of the P-bound aryl groups), and thus the central P₄Cl₂ scaffold is effectively shielded by the *ortho*-mesityl groups. To the best of our knowledge, **16** is the first structurally characterized *cyclo*-triphosphane with a chloro substituent at the P₃ ring system. Other similar species were only characterized by NMR spectroscopy so far.^[31,32,45–48]

In the ^{31}P NMR spectrum, **16** is characterized by an ABCD pattern (Figure 9). The signals A and B, which can be assigned to P1 and P4, respectively, are split into pseudo-doublets of doublets due to the unresolved coupling between the two nuclei ($^2J_{\text{A,B}} = -1.2$ Hz). The other two signals display a threefold doublet splitting, as expected. Detailed NMR data can be found in Table 3.

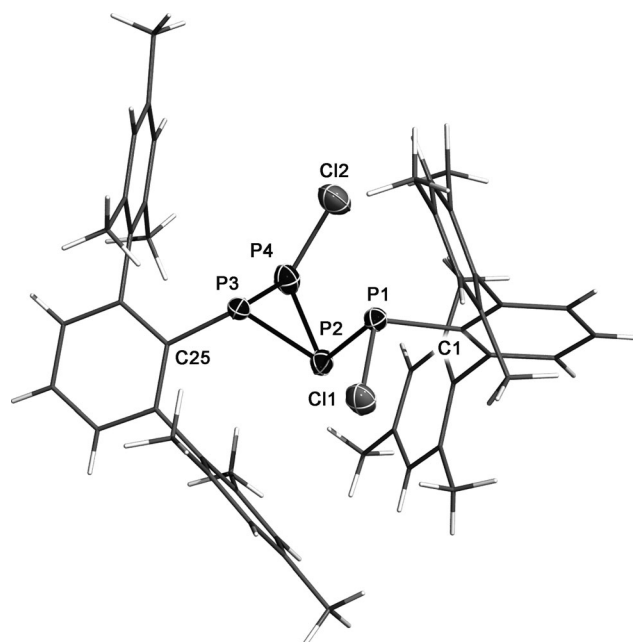


Figure 8. Molecular structure of **16** in the crystal. Thermal ellipsoids drawn at 50% probability and -100°C . Ter substituents are shown as wireframe for clarity. Selected bond lengths [Å] and angles [$^\circ$]: P1–C1 1.852(2), P1–Cl1 2.0954(9), P1–P2 2.2329(9), P2–P3 2.2222(9), P2–P4 2.233(1), P3–P4 2.1787(9), P3–C25 1.846(2), P4–Cl2 2.077(1); C1–P1–P2 109.10(8), Cl1–P1–P2 92.80(4), P1–P2–P3 86.48(3), P1–P2–P4 102.17(4), P3–P2–P4 58.55(3), P2–P3–P4 60.97(3), P2–P3–C25 109.03(8), P4–P2–C25 101.39(8), P3–P4–P2 60.48(3), Cl2–P4–P2 110.43(4), Cl2–P4–P3 102.91(4); P1–P2–P3–P4 106.57(4), P1–P2–P4–P3 78.15(4).

Intriguingly, **16** is a constitutional isomer of *cyclo*-tetrphosphane **15**, which was the expected reaction product in the first place. Hence, we were interested in the relative stabilities of these isomers. DFT calculations revealed that **15** is slightly lower in energy than **16** ($\Delta G_{298} = 2.2 \text{ kJ mol}^{-1}$). Accordingly, we reasoned that it might be possible to isomerise **16** to **15** at elevated temperatures. Therefore, a sample of **16** was dissolved in THF and kept at 75°C . After 1 d, the ^{31}P NMR spectrum did indeed indicate incipient formation of **15**. Continual observation of the slow isomerisation over a longer period of time indicated that the consumption of **16** corresponds to a first-order reaction (for further information, see Supporting Information). Two configurational isomers of **15** were formed: one features a *cis* arrangement of the Cl substituents (*cis*-**15**) with respect to the four-membered ring system, and the other a *trans* arrangement (*trans*-**15**; Figure 10). This was also observed in the case of the analogous NP system $[\text{CIP}(\mu\text{-N}^i\text{Ter})]_2$.^[15]

Compound *cis*-**15** is characterised by an A_2X_2 pattern in the ^{31}P NMR spectrum ($\delta_{\text{exptl}} = 100.3, 12.6 \text{ ppm}$; $^1J_{\text{exptl}} = -200 \text{ Hz}$),

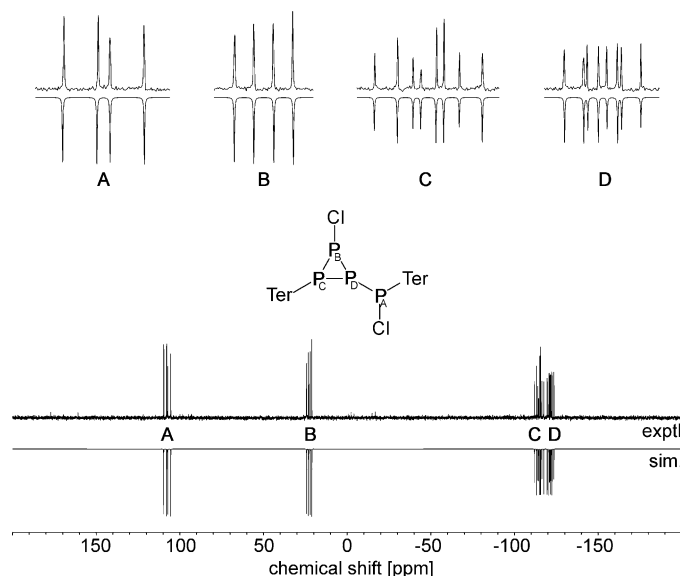


Figure 9. Experimental (up) and simulated (down) ^{31}P NMR spectrum of **16**.

Table 3. Experimentally determined ^{31}P NMR shifts and coupling constants of **16**. Calculated values [PBE0/6-31G(d,p)] are given in parentheses.

X	δ [ppm]	J [Hz]		
		P_A-X	P_B-X	P_C-X
P_A	+107.6 (+92.2)	–	–	–
P_B	+22.7 (+20.6)	–1.2 (–15)	–	–
P_C	–114.8 (–136.4)	+298 (+210)	–249 (–215)	–
P_D	–121.5 (–119.8)	–214 (–160)	–121 (–96)	–148 (–117)

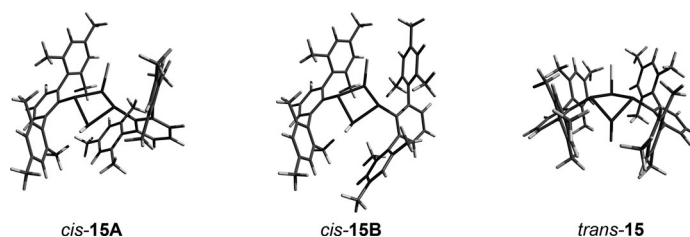


Figure 10. Isomers of **15** identified by DFT calculations. In the case of *cis*-**15**, two energetically similar rotamers (*cis*-**15A**, *cis*-**15B**) were found to be minimum structures.

which compares well with that of Mes^* -substituted compound **11**. The downfield part was assigned to the Cl-substituted P nuclei, and the upfield part to the Ter-substituted P nuclei. As in the case of **11**, two possible rotamers of *cis*-**15** with very similar absolute Gibbs energies ($\Delta G_{298} = 1.6 \text{ kJ mol}^{-1}$) and a low rotational barrier ($\Delta G_{298}^\ddagger = 12.1 \text{ kJ mol}^{-1}$) between them were identified by DFT calculations. The calculated ^{31}P NMR shifts of the symmetric isomer **15B** were found to be in relatively good agreement with the experimental values ($\delta_{\text{calcd}} = 88.8, -11.1 \text{ ppm}$; $^1J_{\text{calcd}} = -168 \text{ Hz}$), although the deviations are somewhat larger than usual, which is most likely due to dynamic effects in the experimental spectrum.

Compound *trans*-**15** is characterised by an ABX_2 pattern. The Cl-substituted P atoms resonate at 119.8 and 82.2 ppm ($\delta_{\text{calcd}} = 117.9, 81.5 \text{ ppm}$), and the Ter-substituted P atoms at -3.2 ppm ($\delta_{\text{calcd}} = -29.4 \text{ ppm}$). Apart from the discussed isomers of **15**, the bicyclic tetrphosphane TerP_4Ter (**5c**; $\delta(^{31}\text{P}) = -171.4, -323.9 \text{ ppm}$) as well as the primary phosphanes TerPHCl (24.1 ppm) and TerPCl_2 (161.1 ppm)^[19,49,50] were identified as side products (<20 mol%) of the isomerisation reaction (Figure 11).

Unfortunately, isolation of the different products was impossible, most likely due to the *cis*–*trans* isomerism of **15**, which led to rather low partial concentrations of the individual species. Moreover, the long reaction time of about one month rendered the reaction infeasible for synthetic use, which is why no further attempts to increase the scale of the reaction and thus to isolate one of the species were made.

Conclusion

The simple reaction of Mes^*PH_2 (**9**) with an excess of PCl_3 and NEt_3 led to the formation of new *cyclo*-tetrphosphanes, among which the main product $[\text{CIP}(\mu\text{-PMes}^*)]_2$ (**11**) is a rare example of a fully characterized all-P equivalent of the well-studied 2,4-dihalo-*cyclo*-2,4-dipnicta-1,3-diazanes. However, in comparison, the lack of electronically stabilizing nitrogen atoms leads to rather unspecific reaction pathways, which makes isolation and purification of the products a challenge.

In case of TerPH_2 (**14**), rapid H/Cl exchange at phosphorus led to the formation of the new *cyclo*-triphosphane $\text{TerP}_3(\text{Cl})\text{P}(\text{Cl})\text{Ter}$ (**16**), which isomerised to $[\text{CIP}(\mu\text{-PTer})]_2$ at 75°C over a period of approximately four weeks.

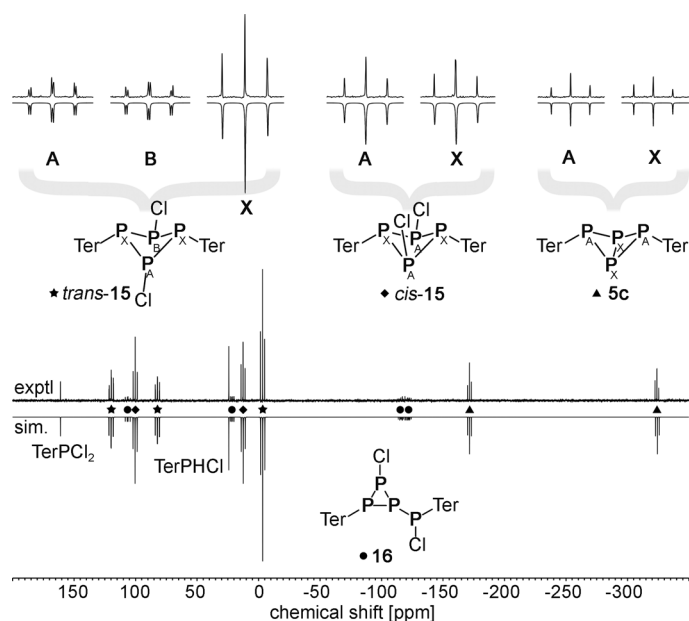


Figure 11. Experimental (up) and simulated (down) ^{31}P NMR spectrum of the isomerisation reaction after 27 d. The starting material **16** (circle) is almost consumed. Main products are *cis*-**15** (diamond) and *trans*-**15** (star).

Experimental Section

Methods

All manipulations were carried out under oxygen- and moisture-free conditions under argon by using standard Schlenk or drybox techniques. Solvents were obtained from commercial sources, purified, dried and freshly distilled prior to use. Starting materials and reactants were commercially obtained and purified or synthesised. For further information, see the Supporting Information.

NMR spectra were obtained on a Bruker AVANCE 300 spectrometer and were referenced internally to the deuterated solvent (^{13}C : CD_2Cl_2 , $\delta_{\text{ref}} = 54.0$ ppm), to protic impurities in the deuterated solvent (^1H : CD_2Cl_2 , $\delta_{\text{ref}} = 5.31$ ppm) or externally (^{31}P : 85% H_3PO_4 , $\delta_{\text{ref}} = 0$ ppm). Absolute signs of ^{31}P - ^{31}P coupling constants were derived from theoretical calculations (see below). IR spectra were recorded on a Nicolet 380 FTIR spectrometer with a Smart Orbit ATR unit at ambient temperature. Raman spectra were recorded on a LabRAM HR 800 Horiba Jobin YVON Raman spectrometer equipped with an Olympus BX41 microscope with variable lenses. The samples were excited by an IR laser (785 nm, 100 mW) or a red laser (633 nm, 17 mW). All measurements were carried out at ambient temperature. Elemental analyses were obtained by using a Thermoquest Flash EA 1112 CHNS analyzer. Melting points (uncorrected) were determined with a Stanford Research Systems EZ Melt at a heating rate of $20^\circ\text{C min}^{-1}$.

X-ray-quality crystals were selected in Fomblin YR-1800 perfluoroether (AlfaAesar) at ambient temperature. The samples were cooled to 173(2) K during measurement. The data were collected on a Bruker Apex Kappa II CCD diffractometer by using graphite-monochromated $\text{Mo}_{\text{K}\alpha}$ radiation ($\lambda = 0.71073$ Å). The structures were solved by direct methods (SHELXS-97)^[51] and refined by full-matrix least-squares procedures (SHELXL-97).^[52] Semi-empirical absorption corrections were applied (SADABS).^[53] All non-hydrogen atoms were refined anisotropically; hydrogen atoms were included

in the refinement at calculated positions by using a riding model. Disordered groups or molecules were split into parts. The occupancy of each part was refined freely. Heavily disordered solvent molecules were removed from the model by using Platon/SQUEEZE,^[54] but were included in the empirical formulae (**13**: CH_2Cl_2 , $16 \cdot 0.5\text{Et}_2\text{O} \cdot 0.5\text{C}_6\text{H}_6$). Detailed crystallographic data of all compounds is given in the Supporting Information.

All computations were carried out with the Gaussian 09 program package^[55] and the standalone version of NBO 5.9.^[56–59] The hybrid DFT functional PBE0^[60–62] and a 6-31G(d,p) basis set^[63–72] [notation PBE0/6-31G(d,p)] were used for all calculations. The structures were fully optimized and confirmed as minima by frequency analyses. Calculated frequencies were scaled by 0.9512, which was found to be a suitable value for this method and basis set.^[73] Chemical shifts and coupling constants were derived by the GIAO method.^[74–78] The theoretical data were used for subsequent simulation and fitting of the parameters to the experimental spectra (Supporting Information).

Synthesis

[CIP(μ -PMes*)]₂ (11): PCl_3 (2.88 g, 20.9 mmol) was added to a solution of Mes^*PH_2 (557 mg, 2.0 mmol) and NEt_3 (1.82 g, 18.0 mmol) in 20 mL of Et_2O at -80°C . The reaction mixture was warmed to ambient temperature and stirred for 24 h. All volatile components are removed in vacuo and the residue was extracted with 20 mL of *n*-hexane. The suspension was filtered over a Celite-packed frit to give a clear filtrate. The solvent was evaporated and the remaining solid dried in vacuo. Recrystallisation from PhF at room temperature gave **11** as slightly yellow, block-shaped crystals in 30% yield (206 mg, 0.3 mmol). M.p. 154°C ; elemental analysis (%) calcd (found): C 63.06 (64.06), H 8.53 (8.28); $^{31}\text{P}\{^1\text{H}\}$ NMR (CD_2Cl_2 , 121.5 MHz): $\delta = -8.1$ (t, $^1J(^{31}\text{P}, ^{31}\text{P}) = 218$ Hz, PMes*), 131.3 (t, $^1J(^{31}\text{P}, ^{31}\text{P}) = 218$ Hz, PCl); ^1H NMR (CD_2Cl_2 , 300.1 MHz): $\delta = 1.29$ (s, 9H, *p*-tBu), 1.40 (s, 18H, *o*-tBu), 7.28 ppm (m, 2H, *m*-H); $^{13}\text{C}\{^1\text{H}\}$ NMR (CD_2Cl_2 , 75.5 MHz): $\delta = 31.5$ (s, *p*-CMe₃), 34.1 (m, *o*-CMe₃), 35.2 (s, *p*-CMe₃), 39.6 (s, *o*-CMe₃), 115.8 (d, $^1J(^{13}\text{C}, ^{31}\text{P}) = 20.9$ Hz, *ipso*-C), 123.9 (s, *m*-C), 130.6 (d, $^2J(^{13}\text{C}, ^{31}\text{P}) = 7.7$ Hz, *o*-C), 151.2 ppm (s, *p*-C); IR (ATR, 32 scans): $\tilde{\nu} = 2954$ (s), 2902 (m), 2864 (m), 2743 (w), 2713 (w), 1592 (m), 1581 (m), 1521 (w), 1493 (m), 1474 (s), 1461 (s), 1441 (m), 1391 (s), 1361 (s), 1278 (w), 1235 (m), 1212 (s), 1178 (m), 1152 (m), 1122 (m), 1064 (m), 1020 (m), 947 (w), 932 (w), 920 (m), 893 (m), 875 (s), 830 (w), 804 (m), 753 (s), 740 (s), 714 (w), 684 (m), 650 (m), 646 (m), 637 (m), 597 (m), 581 (m), 574 (m), 546 (w), 539 cm^{-1} (w); Raman (633 nm, 30 s, 4 scans): $\tilde{\nu} = 3086$ (1), 3067 (2), 2969 (4), 2962 (4), 2922 (4), 2902 (5), 2864 (2), 2781 (1), 2709 (1), 1590 (5), 1579 (3), 1458 (2), 1444 (2), 1384 (2), 1359 (1), 1281 (4), 1239 (2), 1204 (3), 1172 (4), 1151 (2), 1122 (5), 1008 (10), 931 (2), 920 (3), 891 (1), 876 (1), 819 (6), 803 (3), 772 (1), 748 (2), 642 (1), 596 (3), 580 (3), 564 (6), 516 (3), 488 (4), 461 (6), 445 (8), 435 (8), 400 (4), 385 (2), 360 (1), 322 (2), 298 (2), 254 (4), 232 (4), 172 (3), 163 cm^{-1} (4); MS (Cl positive, isobutene, $I > 10\%$): m/z (%): 685 (47) $[\text{M}+\text{H}]^+$, 649 (100) $[\text{M}-\text{Cl}]^+$, 627 (19) $[\text{M}-\text{tBu}]^+$, 615 (14), 557 (14) $[\text{M}-\text{tBu}-\text{Cl}_2]^+$, 343 (30) $[\text{MesPPCl}+\text{H}]^+$, 307 (23), 275 (12).

TerP₃(Cl)P(Cl)Ter (16): PCl_3 (2.66 g, 19.4 mmol) was added to a solution of TerPH_2 (693 mg, 2.0 mmol) and NEt_3 (1.84 g, 18.2 mmol) in 20 mL of Et_2O at -80°C . The reaction mixture was warmed to ambient temperature and stirred for 18 h. All volatile components were removed in vacuo and the residue extracted with 20 mL of benzene. The suspension was filtered over a Celite-packed frit. The filtrate was concentrated. Addition of 0.5 mL of Et_2O and storage overnight yielded **16** $\cdot 0.5\text{C}_6\text{H}_6 \cdot 0.5\text{Et}_2\text{O}$ as slightly yellow, block-shaped crystals in 22% yield (190 mg, 0.21 mmol). M.p. 219°C ; ele-

mental analysis (%) calcd (found): C 70.90 (70.57), H 6.51 (6.20); $^{31}\text{P}\{^1\text{H}\}$ NMR (CD_2Cl_2 , 121.5 MHz): $\delta = 107.6$ (m, 1P, P(Cl)Ter), 22.7 (m, 1P, PCl), -114.8 (m, 1P, PTer), -121.5 ppm (m, 1P, P_{ring}), see Table 3; ^1H NMR (CD_2Cl_2 , 300.1 MHz): $\delta = 1.15$ (t, $^3J(^1\text{H},^1\text{H}) = 7.0$ Hz, 1.5H, Et_2O), 1.88 (s, 6H, *o*-Me), 1.90 (s, 6H, *o*-Me), 1.93 (s, 6H, *o*-Me), 1.95 (s, 6H, *o*-Me), 2.31 (s, 6H, *p*-Me), 2.32 (s, 6H, *p*-Me), 3.43 (q, $^3J(^1\text{H},^1\text{H}) = 7.0$ Hz, 1H, Et_2O), 6.85–7.00 (12H, arom. H), 7.33 (m, 1H, *p*-H), 7.35 (s, 3H, C_6H_6), 7.47 ppm (m, 1H, *p*-H); $^{13}\text{C}\{^1\text{H}\}$ NMR (CD_2Cl_2 , 75.5 MHz): $\delta = 21.2$ – 21.8 (me), 22.0 (s, Me), 128.8 (s, CH), 128.9 (s, CH), 129.0 (s, CH), 129.5 (d, $J(^{13}\text{C},^{31}\text{P}) = 3.2$ Hz, CH), 129.7 (s, CH), 130.0 (s, CH), 130.8 (s, CH), 132.2 (s, CH), 136.1 (d, $J(^{13}\text{C},^{31}\text{P}) = 4.6$ Hz), 137.7–138.4, 147.4 (d, $J(^{13}\text{C},^{31}\text{P}) = 18.8$ Hz, *ipso*-C), 147.8 ppm (d, $J(^{13}\text{C},^{31}\text{P}) = 11.4$ Hz, *ipso*-C); IR (ATR, 32 scans): $\tilde{\nu} = 3088$ (w), 3033 (w), 2969 (w), 2941 (w), 2913 (m), 2853 (w), 2729 (w), 1610 (m), 1559 (w), 1478 (m), 1444 (s), 1375 (m), 1299 (w), 1283 (w), 1261 (w), 1243 (w), 1180 (w), 1161 (w), 1110 (w), 1088 (w), 1031 (m), 1014 (m), 974 (w), 934 (w), 885 (w), 847 (s), 805 (s), 775 (w), 748 (s), 739 (m), 719 (m), 676 (s), 589 (w), 575 (w), 557 (w), 548 (w), 530 cm^{-1} (w); Raman (633 nm, 20 s, 4 scans): $\#\# = 3120$ (1), 3060 (3), 3039 (3), 3012 (3), 2945 (2), 2914 (7), 2852 (2), 2727 (1), 1609 (5), 1573 (3), 1563 (3), 1478 (2), 1435 (2), 1379 (4), 1298 (10), 1279 (3), 1260 (2), 1239 (1), 1222 (1), 1176 (3), 1160 (2), 1105 (1), 1084 (1), 1033 (8), 997 (2), 988 (6), 941 (2), 848 (1), 801 (1), 735 (5), 716 (1), 572 (10), 557 (4), 527 (5), 520 (4), 506 (2), 487 (3), 454 (4), 439 (5), 429 (7), 405 (5), 386 (2), 366 (5), 344 (3), 319 (1), 293 (1), 276 (1), 253 (2), 237 (5), 215 (5), 177 cm^{-1} (1); MS (CI positive, isobutene, $I > 10\%$): m/z (%): 821 (100) $[\text{M}+\text{H}]^+$, 785 (56) $[\text{M}-\text{Cl}]^+$, 751 (95) $[\text{M}+\text{H}-\text{Cl}_2]^+$, 441 (35) $[\text{M}-\text{TerPCl}]$, 379 (11), 375 (14), 343 (23).

Isomerisation of $\text{TerP}_3(\text{Cl})\text{P}(\text{Cl})\text{Ter}$ (16): $\text{TerP}_3(\text{Cl})\text{P}(\text{Cl})\text{Ter}$ (20 mg, 24 μmol) was dissolved in 0.5 mL of THF. The solution was degassed and the atmosphere in the reaction vessel evacuated. The solution was kept at 75°C over a period of 30 d. $^{31}\text{P}\{^1\text{H}\}$ NMR (C_6D_6 , 121.5 MHz): *cis*-15: $\delta = 12.6$ (t, $J(^{31}\text{P},^{31}\text{P}) = -200$ Hz, 2P, PTer), 100.3 ppm (t, $J(^{31}\text{P},^{31}\text{P}) = -200$ Hz, 2P, PCl); *trans*-15: $\delta = -3.2$ (dd, $J(^{31}\text{P},^{31}\text{P}) = -211$ Hz, $J(^{31}\text{P},^{31}\text{P}) = -212$ Hz, 2P, PTer), 82.2 (td, $J(^{31}\text{P},^{31}\text{P}) = -211$ Hz, $J(^{31}\text{P},^{31}\text{P}) = -18$ Hz, 1P, PCl), 119.8 ppm (td, $J(^{31}\text{P},^{31}\text{P}) = -212$ Hz, $J(^{31}\text{P},^{31}\text{P}) = -18$ Hz, 1P, PCl); *exo,exo*- TerP_4Ter : $\delta = -323.9$ (t, $J(^{31}\text{P},^{31}\text{P}) = -182$ Hz, 2P, $\text{P}_{\text{bridgehead}}$), -171.4 (t, $J(^{31}\text{P},^{31}\text{P}) = -182$ Hz, 2P, PTer); TerPHCl , $\delta = 24.1$ (s); TerPCl_2 , $\delta = 161.1$ ppm (s).

Acknowledgements

Dr. Dirk Michalik and Dr. Wolfgang Baumann are gratefully acknowledged for their aid with NMR spectroscopic investigations. Moreover, J.B. wishes to thank Matthias Linke for technical support for the compute cluster and the Fonds der Chemischen Industrie for financial support.

Keywords: cyclophosphanes • isomerization • phosphanes • phosphorus • P–P coupling

- [1] P. P. Power, *Chem. Rev.* **1999**, *99*, 3463–3504.
- [2] L. Stahl, *Coord. Chem. Rev.* **2000**, *210*, 203–250.
- [3] M. S. Balakrishna, D. J. Eisler, T. Chivers, *Chem. Soc. Rev.* **2007**, *36*, 650–664.
- [4] G. He, O. Shynkaruk, M. W. Lui, E. Rivard, *Chem. Rev.* **2014**, *##DOI* 10.1021/cr400547x.
- [5] D. Michalik, A. Schulz, A. Villinger, N. Weding, *Angew. Chem.* **2008**, *120*, 6565–6568; *Angew. Chem. Int. Ed.* **2008**, *47*, 6465–6468.

- [6] R. Kuzora, A. Schulz, A. Villinger, R. Wustrack, *Dalton Trans.* **2009**, 9304–9311.
- [7] M. Kuprat, R. Kuzora, M. Lehmann, A. Schulz, A. Villinger, R. Wustrack, *J. Organomet. Chem.* **2010**, *695*, 1006–1011.
- [8] T. Beveries, R. Kuzora, U. Rosenthal, A. Schulz, A. Villinger, *Angew. Chem.* **2011**, *123*, 9136–9140; *Angew. Chem. Int. Ed.* **2011**, *50*, 8974–8978.
- [9] M. Kuprat, M. Lehmann, A. Schulz, A. Villinger, *Inorg. Chem.* **2011**, *50*, 5784–5792.
- [10] M. Lehmann, A. Schulz, A. Villinger, *Angew. Chem.* **2012**, *124*, 8211–8215; *Angew. Chem. Int. Ed.* **2012**, *51*, 8087–8091.
- [11] N. Burford, T. S. Cameron, C. L. B. Macdonald, K. N. Robertson, R. Schurko, D. Walsh, R. McDonald, R. E. Wasylshen, *Inorg. Chem.* **2005**, *44*, 8058–8064.
- [12] M. Lehmann, A. Schulz, A. Villinger, *Struct. Chem.* **2010**, *21*, 35–43.
- [13] E. Niecke, M. Nieger, F. Reichert, *Angew. Chem.* **1988**, *100*, 1781–1782; *Angew. Chem. Int. Ed. Engl.* **1988**, *27*, 1715–1716.
- [14] N. Burford, J. A. C. Clyburne, P. Losier, T. M. Parks, in *Synthetic Methods of Organometallic and Inorganic Chemistry, Volume 3* (Ed.: H. H. Karsch), Thieme, Stuttgart, New York, **1996**, pp. 21–28.
- [15] F. Reiß, A. Schulz, A. Villinger, N. Weding, *Dalton Trans.* **2010**, *39*, 9962–9972.
- [16] M. Baudler, K. Glinka, *Chem. Rev.* **1993**, *93*, 1623–1667.
- [17] N. Wiberg, A. Wörner, H.-W. Lerner, K. Karaghiosoff, *Z. Naturforsch. B* **2002**, *57*, 1027–1035.
- [18] A. Lorbach, A. Nadj, S. Tüllmann, F. Dornhaus, F. Schödel, I. Sängler, G. Margraf, J. W. Bats, M. Bolte, M. C. Holthausen, M. Wagner, H.-W. Lerner, *Inorg. Chem.* **2009**, *48*, 1005–1017.
- [19] A. R. Fox, R. J. Wright, E. Rivard, P. P. Power, *Angew. Chem.* **2005**, *117*, 7907–7911; *Angew. Chem. Int. Ed.* **2005**, *44*, 7729–7733.
- [20] L. N. Markovski, V. D. Romanenko, A. V. Ruban, *Phosphorus Sulfur Relat. Elem.* **1987**, *30*, 447–450.
- [21] V. D. Romanenko, V. L. Rudzevich, E. B. Rusanov, A. N. Chernega, A. Senio, J.-M. Sotiropoulos, G. Pfister-Guillouzo, M. Sanchez, *J. Chem. Soc. Chem. Commun.* **1995**, 1383–1385.
- [22] P. Pyykkö, M. Atsumi, *Chem. Eur. J.* **2009**, *15*, 12770–12779.
- [23] R. Riedel, H.-D. Hausen, E. Fluck, *Angew. Chem.* **1985**, *97*, 1050–1050; *Angew. Chem. Int. Ed. Engl.* **1985**, *24*, 1056–1057.
- [24] M. Scheer, G. Balázs, A. Seitz, *Chem. Rev.* **2010**, *110*, 4236–4256.
- [25] A. H. Cowley, J. E. Kilduff, T. H. Newman, M. Pakulski, *J. Am. Chem. Soc.* **1982**, *104*, 5820–5821.
- [26] E. Niecke, R. Rüger, *Angew. Chem.* **1983**, *95*, 154–155; *Angew. Chem. Int. Ed. Engl.* **1983**, *22*, 155–156.
- [27] P. Jutz, U. Meyer, B. Krebs, M. Dartmann, *Angew. Chem.* **1986**, *98*, 894–895; *Angew. Chem. Int. Ed. Engl.* **1986**, *25*, 919–921.
- [28] R. C. Smith, E. Urnezus, K. Lam, A. L. Rheingold, J. D. Protasiewicz, *Inorg. Chem.* **2002**, *41*, 5296–5299.
- [29] A. A. Sandoval, H. C. Moser, *Inorg. Chem.* **1963**, *2*, 27–29.
- [30] G. Fritz, J. Härer, *Z. Anorg. Allg. Chem.* **1981**, *481*, 185–200.
- [31] M. Baudler, B. Makowka, *Z. Anorg. Allg. Chem.* **1985**, *528*, 7–21.
- [32] G. Fritz, K. Stoll, *Z. Anorg. Allg. Chem.* **1986**, *538*, 78–112.
- [33] W. W. Schoeller, T. Busch, *Chem. Ber.* **1991**, *124*, 1369–1371.
- [34] F. Knoch, R. Appel, V. Barth, *Z. Kristallogr.* **1996**, *211*, 343–344.
- [35] M. Schmitz, S. Leininger, U. Bergsträßer, M. Regitz, *Heteroat. Chem.* **1998**, *9*, 453–460.
- [36] H. Westermann, M. Nieger, *J. Cryst. Spec. Res.* **1991**, *21*, 523–528.
- [37] R. Riegel, A. Pfizner, G. Heckmann, H. Binder, E. Fluck, *Z. Anorg. Allg. Chem.* **1995**, *621*, 1365–1372.
- [38] A. Schulz, *Z. Anorg. Allg. Chem.* **2014**; DOI: 10.1002/zaac.201400243.
- [39] N. Wiberg, A. Wörner, *Eur. J. Inorg. Chem.* **1998**, 833–841.
- [40] A. Baldy, J. Estienne, *Acta Cryst. Sect. C* **1988**, *44*, 747–749.
- [41] C. Frenzel, E. Hey-Hawkins, *Phosphorus Sulfur Silicon Relat. Elem.* **1998**, *143*, 1–17.
- [42] N. Burford, C. A. Dyker, M. Lumsden, A. Decken, *Angew. Chem.* **2005**, *117*, 6352–6355; *Angew. Chem. Int. Ed.* **2005**, *44*, 6196–6199.
- [43] J. D. Masuda, W. W. Schoeller, B. Donnadieu, G. Bertrand, *Angew. Chem.* **2007**, *119*, 7182–7185; *Angew. Chem. Int. Ed.* **2007**, *46*, 7052–7055.
- [44] N. Tokitoh, A. Tsurusaki, T. Sasamori, *Phosphorus Sulfur Silicon Relat. Elem.* **2009**, *184*, 979–986.
- [45] G. Fritz, J. Härer, *Z. Anorg. Allg. Chem.* **1983**, *500*, 14–22.
- [46] G. Fritz, T. Vaahs, M. Jarmer, *Z. Anorg. Allg. Chem.* **1990**, *589*, 12–22.
- [47] P. Jutz, T. Wippermann, *J. Organomet. Chem.* **1985**, *287*, C5–C7.

- [48] M. Scheer, S. Gremler, Z. Anorg. Allg. Chem. **1993**, 619, 471–475.
- [49] S. Shah, G. P. A. Yap, J. D. Protasiewicz, *J. Organomet. Chem.* **2000**, 608, 12–20.
- [50] E. Urnėžius, J. D. Protasiewicz, *Main Group Chem.* **1996**, 1, 369–372.
- [51] G. M. Sheldrick, *SHELXS-2013: Program for the Solution of Crystal Structures*, University of Göttingen, Germany, **2013**.
- [52] G. M. Sheldrick, *SHELXL-2013: Program for the Refinement of Crystal Structures*, University of Göttingen, Germany, **2013**.
- [53] G. M. Sheldrick, University of Göttingen, Germany, **2004**.
- [54] A. L. Spek, *J. Appl. Cryst.* **2003**, 36, 7–13.
- [55] Gaussian 09, Revision C.01, M. J. Frisch, G. W. Trucks, H. B. Schlegel, G. E. Scuseria, M. A. Robb, J. R. Cheeseman, G. Scalmani, V. Barone, B. Menucci, G. A. Petersson, H. Nakatsuji, M. Caricato, X. Li, H. P. Hratchian, A. F. Izmaylov, J. Bloino, G. Zheng, J. L. Sonnenberg, M. Hada, M. Ehara, K. Toyota, R. Fukuda, J. Hasegawa, M. Ishida, T. Nakajima, Y. Honda, O. Kitao, H. Nakai, T. Vreven, J. A. Montgomery, Jr., J. E. Peralta, F. Ogliaro, M. Bearpark, J. J. Heyd, E. Brothers, K. N. Kudin, V. N. Staroverov, T. Keith, R. Kobayashi, J. Normand, K. Raghavachari, A. Rendell, J. C. Burant, S. S. Iyengar, J. Tomasi, M. Cossi, N. Rega, J. M. Millam, M. Klene, J. E. Knox, J. B. Cross, V. Bakken, C. Adamo, J. Jaramillo, R. Gomperts, R. E. Stratmann, O. Yazyev, A. J. Austin, R. Cammi, C. Pomelli, J. W. Ochterski, R. L. Martin, K. Morokuma, V. G. Zakrzewski, G. A. Voth, P. Salvador, J. J. Dannenberg, S. Dapprich, A. D. Daniels, O. Farkas, J. B. Foresman, J. V. Ortiz, J. Cioslowski, D. J. Fox, Gaussian, Inc., Wallingford CT, **2010**.
- [56] E. D. Glendening, J. K. Badenhop, A. E. Reed, J. E. Carpenter, J. A. Bohmann, C. M. Morales, F. Weinhold, *NBO 5.9*, Theoretical Chemistry Institute, University of Wisconsin, Madison, **2011**.
- [57] J. E. Carpenter, F. Weinhold, *J. Mol. Struct.* **1988**, 169, 41–62.
- [58] F. Weinhold, J. E. Carpenter, *The Structure of Small Molecules and Ions*, Plenum, New York, **1988**.
- [59] F. Weinhold, C. Landis, *Valency and Bonding: A Natural Bond Orbital Donor–Acceptor Perspective*, Cambridge University Press, Cambridge, **2005**.
- [60] J. P. Perdew, K. Burke, M. Ernzerhof, *Phys. Rev. Lett.* **1996**, 77, 3865–3868.
- [61] J. P. Perdew, K. Burke, M. Ernzerhof, *Phys. Rev. Lett.* **1997**, 78, 1396–1396.
- [62] C. Adamo, V. Barone, *J. Chem. Phys.* **1999**, 110, 6158–6170.
- [63] R. Ditchfield, W. J. Hehre, J. A. Pople, *J. Chem. Phys.* **1971**, 54, 724–728.
- [64] W. J. Hehre, R. Ditchfield, J. A. Pople, *J. Chem. Phys.* **1972**, 56, 2257–2261.
- [65] P. C. Hariharan, J. A. Pople, *Theor. Chim. Acta* **1973**, 28, 213–222.
- [66] P. C. Hariharan, J. A. Pople, *Mol. Phys.* **1974**, 27, 209–214.
- [67] M. S. Gordon, *Chem. Phys. Lett.* **1980**, 76, 163–168.
- [68] M. M. Francl, W. J. Pietro, W. J. Hehre, J. S. Binkley, M. S. Gordon, D. J. DeFrees, J. A. Pople, *J. Chem. Phys.* **1982**, 77, 3654–3665.
- [69] R. C. Binning Jr., L. A. Curtiss, *J. Comput. Chem.* **1990**, 11, 1206–1216.
- [70] J.-P. Blaudeau, M. P. McGrath, L. A. Curtiss, L. Radom, *J. Chem. Phys.* **1997**, 107, 5016–5021.
- [71] V. A. Rassolov, J. A. Pople, M. A. Ratner, T. L. Windus, *J. Chem. Phys.* **1998**, 109, 1223–1229.
- [72] V. A. Rassolov, M. A. Ratner, J. A. Pople, P. C. Redfern, L. A. Curtiss, *J. Comput. Chem.* **2001**, 22, 976–984.
- [73] J. P. Merrick, D. Moran, L. Radom, *J. Phys. Chem. A* **2007**, 111, 11683–11700.
- [74] F. London, *J. Phys. Radium* **1937**, 8, 397–409.
- [75] R. McWeeny, *Phys. Rev.* **1962**, 126, 1028–1034.
- [76] R. Ditchfield, *Mol. Phys.* **1974**, 27, 789–807.
- [77] K. Wolinski, J. F. Hinton, P. Pulay, *J. Am. Chem. Soc.* **1990**, 112, 8251–8260.
- [78] J. R. Cheeseman, G. W. Trucks, T. A. Keith, M. J. Frisch, *J. Chem. Phys.* **1996**, 104, 5497–5509.

Received: May 21, 2014

Published online on August 21, 2014

6.2 Low-Temperature Isolation of the Bicyclic Phosphino-phosponium Salt [Mes*₂P₄Cl][GaCl₄]

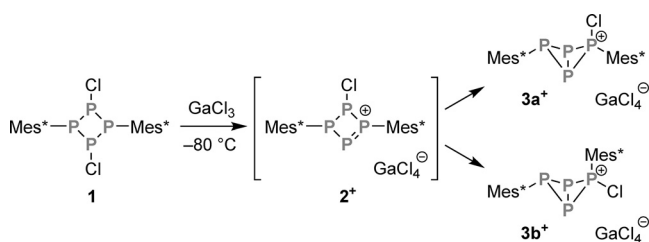
Jonas Bresien, Kirill Faust, Axel Schulz, and Alexander Villinger

Angew. Chem. **2015**, *127*, 7030–7034; *Angew. Chem. Int. Ed.* **2015**, *54*, 6926–6930.

DOI: 10.1002/ange.201500892; 10.1002/anie.201500892

Reprinted with permission from John Wiley & Sons, Inc. (Licence No. 3796580355802)

Copyright 2015 John Wiley & Sons, Inc. All rights reserved.



Scheme 3. Synthesis of $[\text{Mes}^*\text{P}_4(\text{Cl})\text{Mes}^*][\text{GaCl}_4]$ ($3[\text{GaCl}_4]$). The isomeric ratio between 3a^+ and 3b^+ varies from 1:8 (-50°C , 3 h) to 3:4 (-80°C , 12 h) depending on the reaction conditions.

reaction (ca. 40% by mole fraction). Full conversion of **1** to **2**⁺ could be confirmed by a trapping reaction (see below).

The resonances were assigned on the basis of computed NMR data (Supporting Information). The calculated gas-phase structure of **2**⁺ (PBE0/6-31G(d,p)) reveals C_1 symmetry and incorporates a P=P double bond (2.05 Å; Wiberg bond index: 1.49; cf. 2.034(2) Å in $\text{Mes}^*\text{P}=\text{PMes}^*$)^[35] that stabilizes the positive charge. In agreement with the Lewis formula, the highest partial charge is therefore found at one of the Mes^* -substituted P atoms (+0.45 e), which adopts a nearly planar coordination environment ($\Sigma(\angle\text{P})=359.9^\circ$). Even though the minimum structure displays four inequivalent P nuclei, a relatively fast exchange between two enantiomers accounts for both the observed NMR pattern and the signal broadening (Figure 1). As the dynamic equilibrium renders both Mes^* -

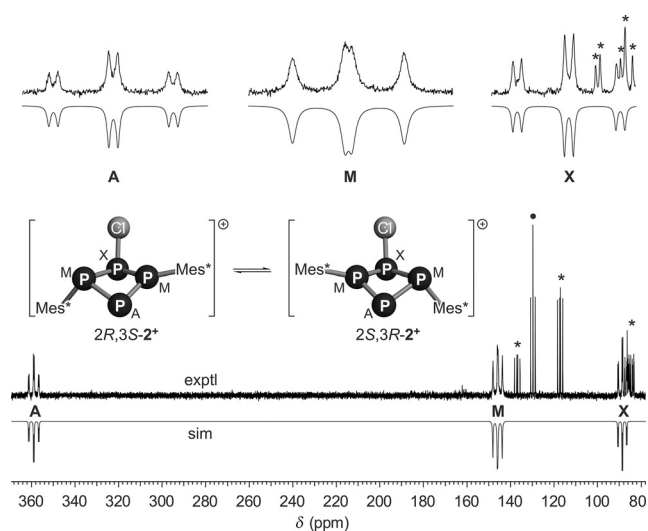


Figure 1. Experimental and simulated in situ ^{31}P NMR spectrum of the reaction of **1** and GaCl_3 (-60°C). The AM_2X pattern is caused by a dynamic equilibrium between two enantiomers of **2**⁺ (calculated structures). Labeled lines/signals are caused by starting material (●) and other intermediates (*).

substituted P atoms equivalent, a single resonance at the center of their individual shifts ($\delta_{\text{calc}}=206.5, 48.6$ ppm; $\delta_{\text{av}}=127.6$ ppm) is expected. Taking this into consideration, the calculated and experimental data show reasonable agreement (Supporting Information, Table S7). Two other intermediates were observed at temperatures below -20°C , which could not

be identified unambiguously (Supporting Information, Figure S1).

The color of the reaction mixture faded slowly to orange/yellow over a period of one day at low temperatures. After full conversion of the starting material, two main products were formed, which were identified as *exo-exo* and *endo-exo* isomers of $[\text{Mes}^*\text{P}_4(\text{Cl})\text{Mes}^*]^+$ (**3a**⁺, **3b**⁺, Scheme 3) on the basis of NMR data (85% yield). Intriguingly, the chlorine atom of the reaction product is connected to one of the Mes^* -substituted P atoms, resulting in the formation of a novel, bicyclic triphosphinophosphonium framework. According to DFT calculations, these constitutional isomers of **2**⁺, which are formed after a formal 1,2-Cl shift, are energetically favored by 46.3 kJ mol⁻¹ (**3a**⁺) or 45.3 kJ mol⁻¹ (**3b**⁺) with respect to intermediate **2**⁺ (ΔG^{298}).

Addition of *n*-pentane facilitated crystallization at -80°C and afforded colorless crystals that were characterized as $\text{CH}_2\text{Cl}_2/\text{C}_6\text{H}_5\text{F}$ solvate of **3a** $[\text{GaCl}_4]$ (40% yield of isolated product). The molecular structure was determined by single-crystal X-ray diffraction (Figure 2). All P–P bond lengths are

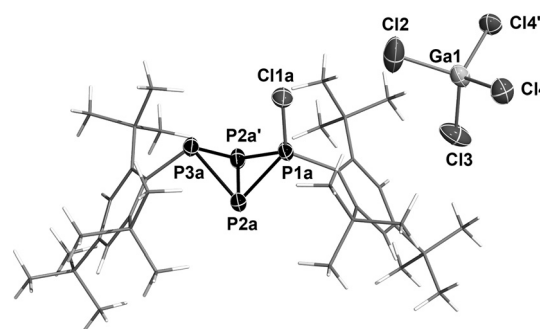


Figure 2. Molecular structure of **3a** $[\text{GaCl}_4]$. Ellipsoids are set at 50% probability (173 K). Selected bond lengths [Å] and angles [$^\circ$]: P1a–P2a 2.150(2), P1a–Cl1a 2.009(2), P2a–P2a' 2.244(2), P2a–P3a 2.244(2); Cl1a–P1a–P2a 117.65(7), Cl1–P1a–Cl1a 118.7(2), P2a'–P1a–P2a 62.91(7), P1a–P2a–P2a' 58.55(3), P3a–P2a–P2a' 59.99(3), P1a–P2a–P3a 83.60(6), P2a'–P3a–P2a 60.02(7); P1a–P2a–P2a'–P3a $-101.68(3)$.^[56]

within the range of typical single bonds (cf. $\Sigma r_{\text{cov}}=2.22$ Å),^[36] although the bonds to P1a (2.150(2) Å) are somewhat shortened owing to bond polarization. Similarly, the P1a–Cl1a bond (2.009(2) Å) is slightly shorter than the sum of covalent radii (2.10 Å).^[36] A distorted tetrahedral coordination environment is found for P1a, which can be compared to tetracoordinate P atoms in cyclic phosphinohalophosphonium ions or bicyclic $\text{TerP}_4\text{Me}\cdot\text{B}(\text{C}_6\text{F}_5)_3$ (Ter = 2,6-dimesitylphenyl).^[18,32] All other P atoms exhibit typical trigonal pyramidal coordination (bond angles 58° – 96°). The fold angle of the butterfly-shaped bicyclic P_4 scaffold amounts to $101.68(3)^\circ$, which compares well to known tetraphosphabicyclo[1.1.0]butane frameworks (88.6° – 108.1°).^[25,26,32,37–41] No close contacts are found between anion and cation. Several attempts to crystallize the *endo-exo* isomer **3b** $[\text{GaCl}_4]$, which is actually formed in excess according to ^{31}P NMR spectra, remained futile.

The solid-state Raman spectrum of **3a** $[\text{GaCl}_4]$ (at -60°C) shows characteristic bands at 340 cm^{-1} (GaCl_4 “breathing”

mode), 485 cm⁻¹ (P₄ deformation), 513 cm⁻¹ (P₄Cl “breathing”), 588 cm⁻¹ (P–C stretching at tricoordinate P), 615 cm⁻¹ (P–Cl stretching), and 633 cm⁻¹ (P–C stretching at tetracoordinate P). Upon warming, the sample started to decompose above 0°C as indicated by decreasing signal intensities (Supporting Information, Figure S2).

To further investigate the electronic structure of **3a**⁺ and **3b**⁺, density functional theory (DFT) calculations were performed.^[42] For both isomers, NBO^[43] analysis revealed that the positive charge is mostly localized at the phosphonium center (P1, +0.76 *e*), but also resides at the tricoordinate Mes* substituted atom (P3, +0.37 *e*). The bridgehead atoms (P2) are only slightly positive (+0.12 *e*), whereas the Cl atom bears a slightly negative charge (−0.16 *e*). Thus, the overall charge of the P₄Cl scaffold amounts to +1.21 *e*, or +1.37 *e* if only the P₄ unit is regarded. Comparison with neutral Mes*P₄Mes* (+0.54 *e*, Supporting Information) or even dicationic [(Ph₃As)P₄(AsPh₃)]²⁺ (+0.12 *e*)^[26] confirms the unique charge distribution within both isomers of **3**⁺.

In the ³¹P NMR spectrum, **3a**⁺ and **3b**⁺ are characterized by AMX₂ patterns (Figure 3). A characteristic high

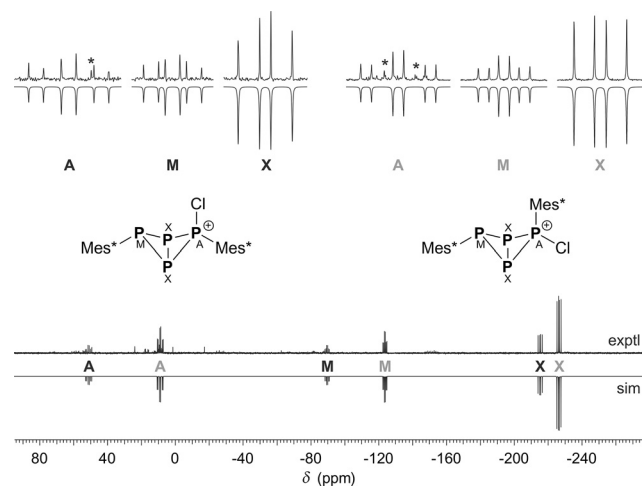


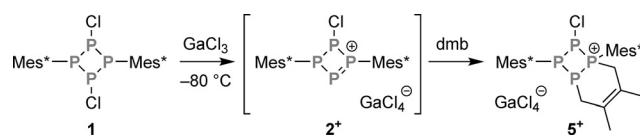
Figure 3. In situ ³¹P NMR spectrum at 0°C displaying the formation of **3a**⁺ and **3b**⁺. Starred lines in the enlarged section are caused by impurities that are due to incipient decomposition at this temperature.

field shift is observed for the bridgehead atoms (P_X: **3a**⁺: −214.5 ppm; **3b**⁺: −226.4 ppm), which compares to known tetraphosphabicyclo[1.1.0]butanes (−220 to −370 ppm),^[25,26,32,37–41,44–46] but is still shifted slightly downfield owing to the positive charge of the P₄ scaffold. The tricoordinate bridging atom (P_M) displays a moderate high-field shift (**3a**⁺: −89.5 ppm; **3b**⁺: −123.6 ppm) within the typical range, whereas the tetracoordinate P atom (P_A) is shifted significantly downfield (**3a**⁺: +51.2 ppm; **3b**⁺: +9.0 ppm), which has not yet been observed for nuclei within bicyclic P₄ frameworks. All of the experimental values are in good agreement with theoretical data (Supporting Information, Tables S8 and S9).

At ambient temperature, solution NMR spectra indicate that **3a**⁺ and **3b**⁺ decompose within hours.^[47] One of the decomposition products was identified as

[Mes*P(H)(Cl)*t*Bu][GaCl₄] (**4**[GaCl₄]; Supporting Information). Remarkably, a *t*Bu group is transferred from a Mes* substituent to the P atom of **4**⁺ in the course of this reaction, which demonstrates the intrinsic lability of **3a**⁺ and **3b**⁺. Displacement of *t*Bu groups from Mes* substituents has previously been observed in the presence of Lewis acids or under thermal conditions.^[6,48–51]

In a next series of experiments, we aimed to further establish the identity of low-temperature intermediate **2**⁺. For that purpose, **1** was treated with GaCl₃ in the presence of dimethylbutadiene (dmb) as trapping reagent.^[52,53] This time, no red color was observed upon addition of GaCl₃. According to ³¹P NMR data, the reaction led to quantitative formation of tetraphosphabicyclo[4.2.0]octenium salt **5**[GaCl₄] (Scheme 4), which can be regarded as [4+2] cycloaddition



Scheme 4. Synthesis of [Mes*P₄(Cl)(C₆H₁₀)Mes*][GaCl₄] (**5**[GaCl₄]).

product of intermediate **2**⁺ and dmb. In this vein, the trapping reaction also proved quantitative conversion of **1** to **2**⁺ at low temperatures.

At ambient temperature, cation **5**⁺ is characterized by four broad signals in the ³¹P NMR spectrum, indicating unresolved dynamic effects. Cooling to −80°C revealed dynamic equilibria between several conformers or rotamers (Supporting Information, Figure S3). Heating to +80°C barely improved the resolution of the NMR spectrum and led to slow decomposition of **5**⁺. In the ¹H NMR spectrum, some of the signals are also significantly broadened, which is most likely due to hindered rotation of some *t*Bu groups.

Crystallization at 5°C yielded colorless crystals of **5**·[GaCl₄]·CH₂Cl₂ (yield of isolated product after workup: 45%; see the Supporting Information). The solid-state structure was determined by single-crystal X-ray diffraction (Figure 4).

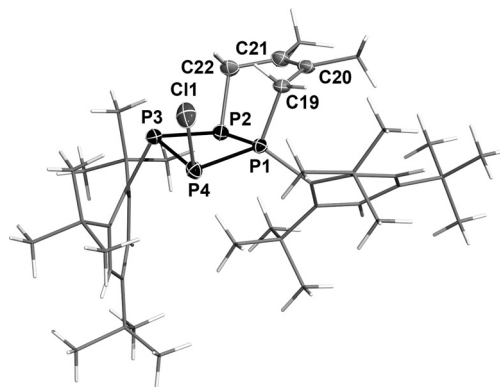


Figure 4. Molecular structure of **5**⁺.^[56] Ellipsoids are set at 50% probability (173 K). Selected bond lengths [Å] and angles [°]: P1–P2 2.195(1), P1–C19 1.846(3), C19–C20 1.514(4), C20–C21 1.334(4), C21–C22 1.500(4), P2–C22 1.871(3), P4–Cl1 2.068(1); P2–P1–P4 91.78(4), C19–P1–P2 102.3(1), C19–P1–P4 116.1(1); P1–P2–P4–P3 159.03(1).

The bicyclic system is folded along the P1–P2 and C19–C22 axes (angles between least squares planes: P3–P4–P1–P2/P1–P2–C22–C19/C22–C19–C20–C21 72.1°/63.2°). The P₄ ring system is rather flat (fold angle: 159°), but well within typical parameters (110°–173°).^[54,55] P1 sits in a distorted tetrahedral environment, and the other P atoms exhibit trigonal pyramidal coordination. The P1–P2 bond (2.195(1) Å) is slightly shorter than the other three P–P bonds (av. 2.25 Å). The structural data of the P₄ ring system correspond to other known cyclotriphosphinophosphonium ions.^[16–18] The Mes* moiety at P1 is highly distorted owing to Pauli repulsion between the *o*-tBu groups and the P₄C₆H₁₀ scaffold; the P atom is bent out of the least-squares plane of the phenyl ring by 52.1°. No close contacts are found between anion and cation. As expected, the positive charge is essentially localized at P1 (+0.92 *e*) according to NBO analysis. The partial charges of the other P atoms are only slightly positive (av. +0.32 *e*). To exclude the possibility that **5**⁺ was formed by a “reverse” reaction of **3a**⁺ or **3b**⁺ with dmb, a solution of both salts was treated with the latter. This did not lead to the formation of **5**⁺; in fact, no reaction was observed after two hours based on ³¹P NMR data.

In conclusion, the synthesis of the first tetraphosphabicyclo[1.1.0]butan-2-ium salt, **3**[GaCl₄], which incorporates a positively charged, bicyclic P₄ scaffold, is achieved by selective chlorine abstraction starting from [CIP(μ-PMes*)]₂ (**1**). **3**[GaCl₄] is temperature-sensitive and only stable at low temperatures. The formation of **3**⁺ was studied by means of low-temperature NMR experiments. This led to the discovery of tetraphosphonium intermediate **2**⁺, which could be identified on the basis of DFT calculations. Moreover, a trapping reaction with dmb could provide chemical evidence for the identity of **2**⁺. Currently, we are investigating the reactivity of **1** with other Lewis acids and under different conditions to diversify the product scope.

Keywords: bicyclic compounds · NMR spectroscopy · phosphorus cations · phosphorus compounds · ring systems

How to cite: *Angew. Chem. Int. Ed.* **2015**, *54*, 6926–6930
Angew. Chem. **2015**, *127*, 7030–7034

- [1] L. Stahl, *Coord. Chem. Rev.* **2000**, *210*, 203–250.
- [2] M. S. Balakrishna, D. J. Eisler, T. Chivers, *Chem. Soc. Rev.* **2007**, *36*, 650–664.
- [3] G. He, O. Shynkaruk, M. W. Lui, E. Rivard, *Chem. Rev.* **2014**, *114*, 7815–7880.
- [4] N. Burford, T. S. Cameron, K. D. Conroy, B. Ellis, M. Lumsden, C. L. B. Macdonald, R. McDonald, A. D. Phillips, P. J. Ragnogna, R. W. Schurko, D. Walsh, R. E. Wasylshen, *J. Am. Chem. Soc.* **2002**, *124*, 14012–14013.
- [5] N. Burford, T. S. Cameron, C. L. B. Macdonald, K. N. Robertson, R. Schurko, D. Walsh, R. McDonald, R. E. Wasylshen, *Inorg. Chem.* **2005**, *44*, 8058–8064.
- [6] A. Schulz, A. Villinger, *Angew. Chem. Int. Ed.* **2008**, *47*, 603–606; *Angew. Chem.* **2008**, *120*, 614–617.
- [7] M. Lehmann, A. Schulz, A. Villinger, *Struct. Chem.* **2011**, *22*, 35–43.
- [8] M. Kuprat, A. Schulz, A. Villinger, *Angew. Chem. Int. Ed.* **2013**, *52*, 7126–7130; *Angew. Chem.* **2013**, *125*, 7266–7270.
- [9] A. Villinger, P. Mayer, A. Schulz, *Chem. Commun.* **2006**, 1236–1238.
- [10] M. Lehmann, A. Schulz, A. Villinger, *Angew. Chem. Int. Ed.* **2011**, *50*, 5221–5224; *Angew. Chem.* **2011**, *123*, 5327–5331.
- [11] G. David, E. Niecke, M. Nieger, V. Von Der Gönna, W. W. Schoeller, *Chem. Ber.* **1993**, *126*, 1513–1517.
- [12] R. J. Davidson, J. J. Weigand, N. Burford, T. S. Cameron, A. Decken, U. Werner-Zwanziger, *Chem. Commun.* **2007**, 4671–4673.
- [13] D. Michalik, A. Schulz, A. Villinger, N. Weding, *Angew. Chem. Int. Ed.* **2008**, *47*, 6465–6468; *Angew. Chem.* **2008**, *120*, 6565–6568.
- [14] A. Schulz, A. Villinger, *Inorg. Chem.* **2009**, *48*, 7359–7367.
- [15] M. Lehmann, A. Schulz, A. Villinger, *Angew. Chem. Int. Ed.* **2012**, *51*, 8087–8091; *Angew. Chem.* **2012**, *124*, 8211–8215.
- [16] N. Burford, C. A. Dyker, M. Lumsden, A. Decken, *Angew. Chem. Int. Ed.* **2005**, *44*, 6196–6199; *Angew. Chem.* **2005**, *117*, 6352–6355.
- [17] C. A. Dyker, N. Burford, G. Menard, M. D. Lumsden, A. Decken, *Inorg. Chem.* **2007**, *46*, 4277–4285.
- [18] J. J. Weigand, N. Burford, R. J. Davidson, T. S. Cameron, P. Seelheim, *J. Am. Chem. Soc.* **2009**, *131*, 17943–17953.
- [19] Y. Carpenter, N. Burford, M. D. Lumsden, R. McDonald, *Inorg. Chem.* **2011**, *50*, 3342–3353.
- [20] S. J. Geier, M. A. Dureen, E. Y. Ouyang, D. W. Stephan, *Chem. Eur. J.* **2010**, *16*, 988–993.
- [21] K. O. Feldmann, J. J. Weigand, *Angew. Chem. Int. Ed.* **2012**, *51*, 7545–7549; *Angew. Chem.* **2012**, *124*, 7663–7667.
- [22] I. Krossing, I. Raabe, *Angew. Chem. Int. Ed.* **2001**, *40*, 4406–4409; *Angew. Chem.* **2001**, *113*, 4544–4547.
- [23] T. Köchner, T. A. Engesser, H. Scherer, D. A. Plattner, A. Steffani, I. Krossing, *Angew. Chem. Int. Ed.* **2012**, *51*, 6529–6531; *Angew. Chem.* **2012**, *124*, 6635–6637.
- [24] M. H. Holthausen, J. J. Weigand, *J. Am. Chem. Soc.* **2009**, *131*, 14210–14211.
- [25] M. H. Holthausen, S. K. Surmiak, P. Jerabek, G. Frenking, J. J. Weigand, *Angew. Chem. Int. Ed.* **2013**, *52*, 11078–11082; *Angew. Chem.* **2013**, *125*, 11284–11288.
- [26] M. Donath, E. Conrad, P. Jerabek, G. Frenking, R. Fröhlich, N. Burford, J. J. Weigand, *Angew. Chem. Int. Ed.* **2012**, *51*, 2964–2967; *Angew. Chem.* **2012**, *124*, 3018–3021.
- [27] J. Bresien, C. Hering, A. Schulz, A. Villinger, *Chem. Eur. J.* **2014**, *20*, 12607–12615.
- [28] N. Wiberg, A. Wörner, H.-W. Lerner, K. Karaghiosoff, *Z. Naturforsch. B* **2002**, *57*, 1027–1035.
- [29] A. Lorbach, A. Nadj, S. Tüllmann, F. Dornhaus, F. Schödel, I. Sängler, G. Margraf, J. W. Bats, M. Bolte, M. C. Holthausen, M. Wagner, H.-W. Lerner, *Inorg. Chem.* **2009**, *48*, 1005–1017.
- [30] J. D. Masuda, W. W. Schoeller, B. Donnadiou, G. Bertrand, *Angew. Chem. Int. Ed.* **2007**, *46*, 7052–7055; *Angew. Chem.* **2007**, *119*, 7182–7185.
- [31] M. Scheer, G. Balázs, A. Seitz, *Chem. Rev.* **2010**, *110*, 4236–4256.
- [32] J. E. Borger, A. W. Ehlers, M. Lutz, J. C. Slootweg, K. Lammermsma, *Angew. Chem. Int. Ed.* **2014**, *53*, 12836–12839; *Angew. Chem.* **2014**, *126*, 13050–13053.
- [33] S. Heinl, S. Reisinger, C. Schwarzmaier, M. Bodensteiner, M. Scheer, *Angew. Chem. Int. Ed.* **2014**, *53*, 7639–7642; *Angew. Chem.* **2014**, *126*, 7769–7773.
- [34] M. Baudler, K. Glinka, *Chem. Rev.* **1993**, *93*, 1623–1667.
- [35] M. Yoshifuji, I. Shima, N. Inamoto, K. Hirotsu, T. Higuchi, *J. Am. Chem. Soc.* **1981**, *103*, 4587–4589.
- [36] P. Pyykkö, M. Atsumi, *Chem. Eur. J.* **2009**, *15*, 12770–12779.
- [37] E. Niecke, R. Rüger, B. Krebs, *Angew. Chem. Int. Ed. Engl.* **1982**, *21*, 544–545; *Angew. Chem.* **1982**, *94*, 553–554.
- [38] R. Riedel, H.-D. Hausen, E. Fluck, *Angew. Chem. Int. Ed. Engl.* **1985**, *24*, 1056–1057; *Angew. Chem.* **1985**, *97*, 1050–1050.

- [39] M. B. Power, A. R. Barron, *Angew. Chem. Int. Ed. Engl.* **1991**, *30*, 1353–1354; *Angew. Chem.* **1991**, *103*, 1403–1404.
- [40] J. Bezombes, P. B. Hitchcock, M. F. Lappert, J. E. Nycz, *Dalton Trans.* **2004**, 499–501.
- [41] A. R. Fox, R. J. Wright, E. Rivard, P. P. Power, *Angew. Chem. Int. Ed.* **2005**, *44*, 7729–7733; *Angew. Chem.* **2005**, *117*, 7907–7911.
- [42] The Supporting Information includes details about syntheses and characterization of all compounds as well as computational details.
- [43] E. D. Glendening, J. K. Badenhop, A. E. Reed, J. E. Carpenter, J. A. Bohmann, C. M. Morales, F. Weinhold, *NBO 5.9*, Theoretical Chemistry Institute, University of Wisconsin, Madison, **2011**.
- [44] P. Jutzi, T. Wippermann, *J. Organomet. Chem.* **1985**, *287*, C5–C7.
- [45] P. Jutzi, U. Meyer, *J. Organomet. Chem.* **1987**, *333*, C18–C20.
- [46] V. D. Romanenko, V. L. Rudzevich, E. B. Rusanov, A. N. Chernega, A. Senio, J.-M. Sotiropoulos, G. Pfister-Guillouzo, M. Sanchez, *J. Chem. Soc. Chem. Commun.* **1995**, 1383–1385.
- [47] In the presence of trace amounts of H₂O, the formation of Mes*P(H₂)OGaCl₃ (**6**) is observed; see the Supporting Information.
- [48] Y. Okamoto, H. Shimizu, *J. Am. Chem. Soc.* **1968**, *90*, 6145–6148.
- [49] C. M. D. Komen, F. Bickelhaupt, *Synth. Commun.* **1996**, *26*, 1693–1697.
- [50] F. Rivière, S. Ito, M. Yoshifuji, *Tetrahedron Lett.* **2002**, *43*, 119–121.
- [51] C. G. E. Fleming, A. M. Z. Slawin, K. S. A. Arachchige, R. Randall, M. Bühl, P. Kilian, *Dalton Trans.* **2013**, *42*, 1437–1450.
- [52] D. Tofan, C. C. Cummins, *Angew. Chem. Int. Ed.* **2010**, *49*, 7516–7518; *Angew. Chem.* **2010**, *122*, 7678–7680.
- [53] C. Hering, A. Schulz, A. Villinger, *Chem. Sci.* **2014**, *5*, 1064–1073.
- [54] M. Schmitz, S. Leininger, U. Bergsträßer, M. Regitz, *Heteroat. Chem.* **1998**, *9*, 453–460.
- [55] F. Knoch, R. Appel, V. Barth, *Z. Kristallogr.* **1996**, *211*, 343–344.
- [56] CCDC 1053909 (**3a**[GaCl₄]), CCDC 1053910 (**4**[GaCl₄]), CCDC 1053911 (**5**[GaCl₄]), and CCDC 1053912 (**6**) contain the supplementary crystallographic data for this paper. These data can be obtained free of charge from The Cambridge Crystallographic Data Centre via www.ccdc.cam.ac.uk/data_request/cif.

Received: January 30, 2015

Revised: March 11, 2015

Published online: April 17, 2015

6.3 Low-Temperature Isolation of a Dinuclear Silver Complex of the Cyclotetraphosphane [ClP(μ -PMes*)]₂

Jonas Bresien, Axel Schulz, and Alexander Villinger

Dalton Trans. **2016**, *45*, 498–501.

DOI: 10.1039/c5dt03928b

This Open Access article is licensed under a Creative Commons Attribution 3.0 Unported Licence.



Cite this: *Dalton Trans.*, 2016, **45**, 498

Received 7th October 2015,
Accepted 2nd December 2015

DOI: 10.1039/c5dt03928b

www.rsc.org/dalton

Low temperature isolation of a dinuclear silver complex of the cyclotetraphosphane [CIP(μ -PMes*)]₂[†]

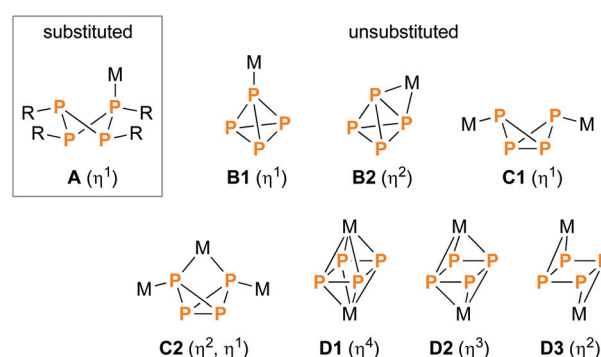
Jonas Bresien,^a Axel Schulz^{*a,b} and Alexander Villingner^a

The reaction of the cyclotetraphosphane [CIP(μ -PMes*)]₂ (**1**, Mes* = 2,4,6-tri-*tert*-butylphenyl) with Ag[Al(OR^F)₄] (R^F = CH(CF₃)₂) resulted in a labile, dinuclear silver complex of **1**, which eliminates AgCl above –30 °C. Its properties were investigated by spectroscopic methods, single crystal X-ray diffraction and DFT calculations.

such as Cp*FeP₅ (Cp* = pentamethylcyclopentadiene)^{32,33} to chain-like poly-cations^{34,35} or spherical macromolecules.^{36–39}

Introduction

Ring systems composed of Group 15 elements (pnictogens) are an intriguing aspect of main group chemistry.¹ Especially, those comprising a binary N₂E₂ (E = P, As, Sb, Bi) scaffold represent versatile reagents in pnictogen chemistry.² Metal complexes of such ring systems were investigated to quite some extent,^{3–5} including studies about their potential application in catalysis⁶ and even anti-tumour studies.⁷ Interestingly, despite the indisputable importance of phosphorus compounds as ligands in catalysis,⁸ the coordination chemistry of homologous P₄ ring systems (cyclotetraphosphanes) has received much less attention. Examples include mainly P₄R₄ systems (**A**, Scheme 1; R = organic substituent) which coordinate to transition metal fragments such as metal carbonyls,^{9–13} metal halides¹⁴ or phosphane substituted metal complexes.¹⁵ The coordination chemistry of unsubstituted P_n scaffolds, on the other hand, is more versatile;^{16,17} in particular, there are numerous examples of coordination to P₄, which can adopt either a tetrahedral (**B1**, **B2**),^{18–22} bicyclic (**C1**, **C2**)^{23–26} or rectangular/square planar structure (**D1–D3**)^{27–31} in the complex (Scheme 1). Likewise, the coordination chemistry of the *cyclo*-P₅[–] moiety was well investigated; it found application in a variety of syntheses ranging from “simple” molecules



Scheme 1 Common coordination patterns of various P₄ scaffolds.

Results and discussion

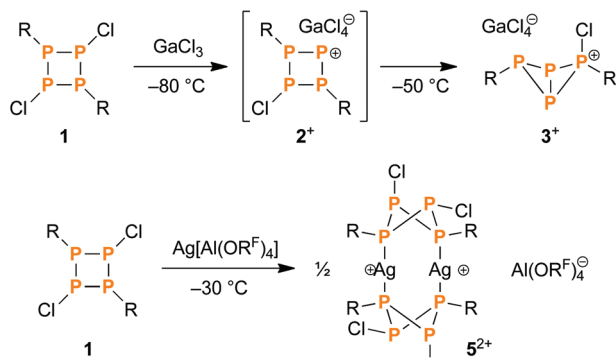
Pursuing our interest in the chemistry of the recently reported cyclotetraphosphane [CIP(μ -PMes*)]₂ (**1**),⁴⁰ we explored its reactivity towards silver salts of the weakly coordinating anions [Al(OR^F)₄][–] (R^F = CH(CF₃)₂) and [B(C₆F₅)₄][–].^{41,42} Taking advantage of the bulky, weakly coordinating anion and naked Ag⁺ ion – in terms of both stabilization and halide abstraction abilities – we hoped to find access to the dark red cyclotetraphosphonium ion [CIP(μ -PMes*)₂P]⁺ (**2**⁺), which had previously been observed as an intermediate during the reaction of **1** and the Lewis acid GaCl₃ (Scheme 2, top).⁴³ However, when mixing Ag[Al(OR^F)₄] (**4**) and **1** in a 1 : 1 ratio in CH₂Cl₂ at low temperatures, no precipitation of AgCl was observed. Instead, crystallization at –80 °C afforded colourless crystals that were identified as CH₂Cl₂ solvate of a dimeric silver complex of **1** (5[Al(OR^F)₄]₂, Scheme 2, bottom; yield of isolated substance: 28%).

^aInstitut für Chemie, Universität Rostock, Albert-Einstein-Straße 3a, D-18059 Rostock, Germany. E-mail: axel.schulz@uni-rostock.de

^bLeibniz-Institut für Katalyse e.V. an der Universität Rostock, Albert-Einstein-Straße 29a, D-18059 Rostock, Germany

[†]Electronic supplementary information (ESI) available: Experimental and computational details, crystallographic and spectroscopic data. CCDC 1417701. For ESI and crystallographic data in CIF or other electronic format see DOI: 10.1039/c5dt03928b





Scheme 2 Top: the reaction of cyclophosphane **1** with GaCl_3 led to the formation of the intermediate 2^+ . Bottom: the reaction of **1** and **4** at low temperatures yielded the dinuclear silver complex 5^{2+} ($R = \text{Mes}^*$).

Molecular structure

Most interestingly, both chlorine atoms remained at the P_4 scaffold; nonetheless two rather long $\text{Ag}\cdots\text{Cl}$ contacts were observed, which are shorter than the sum of van der Waals radii ($\text{Ag1}-\text{Cl2A}$ 3.496(1) Å, $\text{Ag1}-\text{Cl2A}'$ 3.641(2) Å; cf. $\sum r_{\text{vdW}} = 4.35$ Å)⁴⁴ as revealed by single crystal X-ray diffraction (Fig. 1). The $\text{P}-\text{Ag}$ bond lengths ($\text{P1A}-\text{Ag1}$ 2.394(2) Å, $\text{P3A}-\text{Ag1}'$ 2.391(2) Å) compare well to the sum of the covalent radii (2.39 Å),⁴⁵ whereas the $\text{Ag}-\text{Ag}$ distance (3.0511(7) Å) lies between the sum of the covalent (2.56 Å)⁴⁵ and van der Waals radii (5.06 Å).⁴⁴ The silver atoms are almost linearly coordinated ($177.52(5)^\circ$) and lie in a perfect plane with the Mes^* substituted P atoms. Strikingly, the configuration at P2 is inverted in comparison with the starting material, where both chlorine atoms are arranged in an equatorial position with respect to the P_4 ring system. The dinuclear silver complex is nicely shielded by all

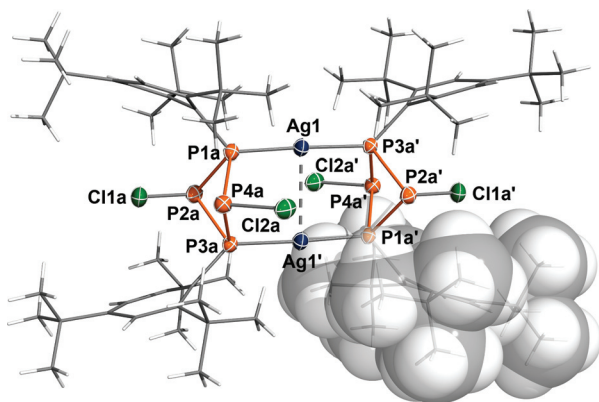


Fig. 1 Molecular structure of 5^{2+} . Ellipsoids are set at 50% probability (173 K). The cation is situated on a crystallographic inversion centre and thus displays C_i symmetry. Selected bond lengths [Å] and angles [$^\circ$]: $\text{P1a}-\text{Ag1}$ 2.394(2), $\text{P1a}-\text{P2a}$ 2.235(2), $\text{P1a}-\text{P4a}$ 2.242(2), $\text{P2a}-\text{Cl1a}$ 2.059(2), $\text{P2a}-\text{P3a}$ 2.232(2), $\text{P3a}-\text{Ag1}'$ 2.391(2), $\text{P3a}-\text{P4a}$ 2.252(2), $\text{P4a}-\text{Cl2a}$ 2.069(2), $\text{Ag1}-\text{Ag1}'$ 3.0511(7), $\text{P3a}'-\text{Ag1}-\text{P1a}$ 177.52(5), $\text{P1a}-\text{Ag1}-\text{Ag1}'$ 90.68(4), $\text{P3a}'-\text{Ag1}-\text{Ag1}'$ 87.24(4).

four Mes^* substituents: the Ag atoms and the equatorial Cl atoms (Cl2A , $\text{Cl2A}'$) are protected by the *ortho*-*t*Bu groups, while the axial Cl atoms (Cl1A , $\text{Cl1A}'$) are sandwiched between the phenyl rings (Fig. S1, ESI[†]). A similar coordination pattern was previously observed in $[(\text{Cy}_4\text{P}_4)_2\text{Sb}_2\text{Cl}_2]^{2+}$ ($\text{Cy} = \text{cyclohexyl}$), where a planar Sb_2Cl_2 scaffold is coordinated by two Cy_4P_4 rings.⁴⁶ To the best of our knowledge, it is the only other example of a dinuclear metal complex capped by two P_4 ring systems.

Spectroscopic characterization

The low temperature ^{31}P NMR spectrum (-60 °C) of $5[\text{Al}(\text{OR}^{\text{F}})_4]_2$ showed a complex AA'BB'MM'M'M''XX' spin system (Fig. 2). The A and B part were assigned to the inequivalent Cl substituted P atoms (axially substituted: 126.9 ppm, equatorially substituted: 122.1 ppm), the M part to the Mes^* substituted P atoms (16.8 ppm) and the X part to the Ag nuclei. The $^1J(^{31}\text{P}-^{31}\text{P})$ coupling constants amount to -205 ($^1J_{\text{AM}}$) and -248 Hz ($^1J_{\text{BM}}$); the $^1J(^{31}\text{P}-^{107}\text{Ag})$ coupling is -468 Hz ($^1J_{\text{MX}}$), which compares to reported (unsigned) coupling constants of other two-coordinate complexes such as $[(\text{Ph}_3\text{P})_2\text{Ag}]^+$ (552 Hz) or $[(p\text{-Tol}_3\text{P})_2\text{Ag}]^+$ (496 Hz).^{47,48} Due to the complex multiplet structure and generally low solubility of $5[\text{Al}(\text{OR}^{\text{F}})_4]_2$, the signal to noise ratio of the NMR spectrum was rather poor, which is why only the large 1J coupling constants could be determined unambiguously, while all smaller coupling constants have higher uncertainties. Nonetheless, the experimental data agree well with calculated NMR shifts and coupling constants (Table S3[†]).

In the solid state Raman spectrum (at -60 °C), characteristic bands of the $[\text{P}_4\text{Ag}]_2$ fragment are observed at 464 cm^{-1} ($\text{P}-\text{P}$ stretching within the P_4 scaffold), 493 cm^{-1} ($\text{P}-\text{Cl}$ stretching) and 514 cm^{-1} ($\text{P}-\text{C}$ stretching). Further intense signals in the Raman spectrum can be attributed to the Mes^* moieties (e.g. 563 , 603 cm^{-1} : *t*Bu deformation; 739 cm^{-1} : phenyl ring deformation; 1007 , 1018 cm^{-1} : Me deformation; 1130 cm^{-1} : combination of ring and CH deformation; 1582 cm^{-1} : ring stretching; 2900 – 3000 cm^{-1} : CH stretching of Me groups) and the $[\text{Al}(\text{OR}^{\text{F}})_4]^-$ anion (e.g. 563 cm^{-1} : CF deformation;

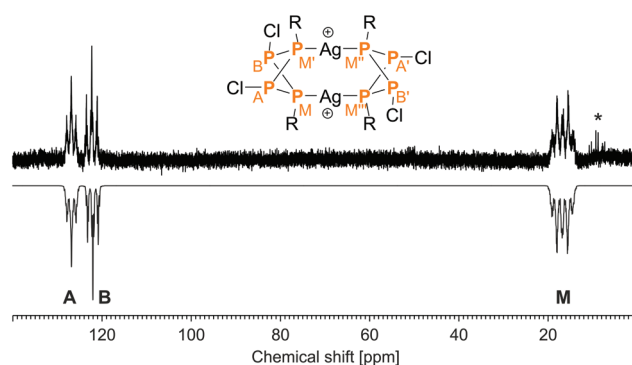


Fig. 2 Experimental (up) and simulated (down) ^{31}P NMR spectrum of 5^{2+} . Starred lines are due to slow elimination of AgCl even at low temperatures.



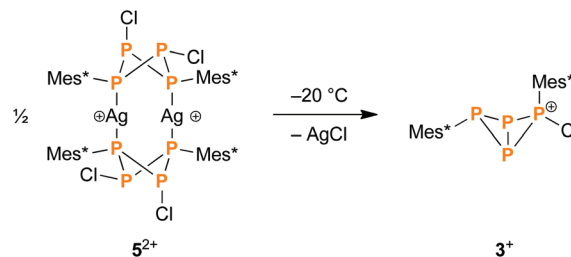
746 cm^{-1} : symmetrical AlO_4 stretching; 818 cm^{-1} : combination of deformation at O and CF_3 ; 1364, 1386 cm^{-1} : CH deformation; 2873 cm^{-1} : CH stretching). The assignments of the signals were made on the basis of computed vibrational data.

Computational study

To further investigate the bonding situation in 5^{2+} , density functional theory (DFT) calculations were performed.[†] According to NBO analysis,⁴⁹ there is no significant bonding interaction between the two Ag atoms, as already indicated by the nearly linear coordination of the Ag centres. Furthermore, both Wiberg bond index (0.31) and natural bond index (0.56) indicate a low covalent character of the Ag–P bonds; accordingly, the natural Lewis representation comprises two distinguished Ag^+ cations and two neutral cyclophosphane moieties. Second order perturbation analysis reveals two stabilizing interactions per Ag^+ cation between the empty s-orbital and the lone pairs (LPs) of the flanking P atoms (346.2 kJ mol^{-1} each), which is consistent with a classical dative bond from P to Ag (Fig. 3). The natural partial charge of each Ag centre is +0.59e, while each of the four coordinating P atoms bears a charge of +0.17e. Hence, the formal charge transfer amounts to $-0.41e$ per Ag^+ ion.

Intramolecular elimination of AgCl

When the reaction mixture of the cyclophosphane **1** and the silver salt **4** was allowed to warm to temperatures above $-30\text{ }^\circ\text{C}$, precipitation of a white solid was observed, indicating elimination of AgCl. *In situ* ^{31}P NMR spectroscopy revealed that the intermediately formed silver complex 5^{2+} decomposed above that temperature (Fig. S3[†]), yielding the bicyclic cation $[\text{Mes}^*\text{P}_4(\text{Cl})\text{Mes}^+]^+$ (**3**⁺, Scheme 3), which had previously been obtained by reacting **1** with GaCl_3 (Scheme 2, top).⁴³ The same reaction outcome was observed when warming a solution of pure $5[\text{Al}(\text{OR}^F)_4]_2$. In this respect, $5[\text{Al}(\text{OR}^F)_4]_2$ can be viewed as an isolable intermediate, which demonstrates that the eventual AgCl elimination does not occur *via* direct attack of a silver



Scheme 3 Above $-30\text{ }^\circ\text{C}$, the silver complex 5^{2+} eliminates AgCl, which leads to the formation of the bicyclic phosphino-phosphonium cation **3**⁺.

ion, but rather *via* complexation and a subsequent intramolecular elimination reaction.

Interestingly, when treating **1** with $\text{Ag}[\text{B}(\text{C}_6\text{F}_5)_4]$ (**6**) under the same reaction conditions, precipitation of AgCl was observed even at $-80\text{ }^\circ\text{C}$, leading once more to the formation of **3**⁺, as indicated by ^{31}P NMR spectroscopy. However, an intermediate similar to the cyclotetraphosphenium cation **2**⁺ could not be observed in any of these reactions.

Conclusions

In conclusion, we present a thermally labile dinuclear silver complex capped by two P_4 ring systems, which eliminates AgCl at temperatures above $-30\text{ }^\circ\text{C}$. Thus it can be considered an intermediate of the chloride abstraction from $[\text{ClP}(\mu\text{-PMes}^*)]_2$, demonstrating that the reaction occurs *via* an intramolecular rather than an intermolecular process.

Acknowledgements

We would like to thank Dr Dirk Michalik for low temperature NMR measurements as well as the Fonds der Chemischen Industrie (scholarship for JB) and Deutsche Forschungsgemeinschaft (SCHU 1170/11-1) for funding.

Notes and references

- 1 L. Stahl, *Coord. Chem. Rev.*, 2000, **210**, 203–250.
- 2 G. He, O. Shynkaruk, M. W. Lui and E. Rivard, *Chem. Rev.*, 2014, **114**, 7815–7880.
- 3 M. S. Balakrishna, V. S. Reddy, S. S. Krishnamurthy, J. F. Nixon and J. C. T. R. B. St. Laurent, *Coord. Chem. Rev.*, 1994, **129**, 1–90.
- 4 G. G. Briand, T. Chivers and M. Krahn, *Coord. Chem. Rev.*, 2002, **233–234**, 237–254.
- 5 M. S. Balakrishna, D. J. Eisler and T. Chivers, *Chem. Soc. Rev.*, 2007, **36**, 650–664.
- 6 D. W. Stephan, *Angew. Chem., Int. Ed.*, 2000, **39**, 314–329.
- 7 D. Suresh, M. S. Balakrishna, K. Rathinasamy, D. Panda and S. M. Mobin, *Dalton Trans.*, 2008, 2812–2814.

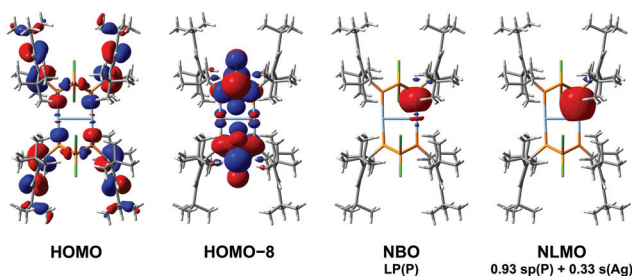


Fig. 3 Left: molecular orbitals (MOs) of 5^{2+} . The HOMO shows contributions to the LPs at the coordinating P atoms, the HOMO–8 encompasses the LPs at Cl and the other P atoms as well as bonding within the P_4 ring systems. Right: natural bond orbital (NBO) representation of a LP at phosphorus and the corresponding natural localized molecular orbital (NLMO), which consists mainly of a formal sp hybrid orbital at P (86%) and an s orbital at Ag (11%), thus illustrating the bonding between these two centres.



- 8 *Phosphorus(III) Ligands in Homogeneous Catalysis: Design and Synthesis*, ed. P. C. J. Kamer and P. W. N. M. Van Leeuwen, John Wiley & Sons, 2012.
- 9 H. G. Ang, J. S. Shannon and B. O. West, *Chem. Commun.*, 1965, 10–11.
- 10 G. W. A. Fowles and D. K. Jenkins, *Chem. Commun.*, 1965, 61–62.
- 11 M. A. Bush, V. R. Cook and P. Woodward, *Chem. Commun.*, 1967, 630–631.
- 12 N. H. Tran Huy, Y. Inubushi, L. Ricard and F. Mathey, *Organometallics*, 1997, **16**, 2506–2508.
- 13 N. H. Tran Huy, Y. Lu and F. Mathey, *Organometallics*, 2011, **30**, 1734–1737.
- 14 C. S. Cundy, M. Green, F. G. A. Stone and A. Taunton-Rigby, *J. Chem. Soc. A*, 1968, 1776–1778.
- 15 I. G. Phillips, R. G. Ball and R. G. Cavell, *Inorg. Chem.*, 1992, **31**, 1633–1641.
- 16 M. Scheer, G. Balázs and A. Seitz, *Chem. Rev.*, 2010, **110**, 4236–4256.
- 17 B. M. Cossairt, N. A. Piro and C. C. Cummins, *Chem. Rev.*, 2010, **110**, 4164–4177.
- 18 O. J. Scherer, *Comments Inorg. Chem.*, 1987, **6**, 1–22.
- 19 I. Krossing, *J. Am. Chem. Soc.*, 2001, **123**, 4603–4604.
- 20 V. Mirabello, M. Caporali, V. Gallo, L. Gonsalvi, D. Gudat, W. Frey, A. Ienco, M. Latronico, P. Mastrorilli and M. Peruzzini, *Chem. – Eur. J.*, 2012, **18**, 11238–11250.
- 21 S. Heintl, E. V. Peresyphkina, A. Y. Timoshkin, P. Mastrorilli, V. Gallo and M. Scheer, *Angew. Chem., Int. Ed.*, 2013, **52**, 10887–10891.
- 22 F. Spitzer, M. Sierka, M. Latronico, P. Mastrorilli, A. V. Virovets and M. Scheer, *Angew. Chem., Int. Ed.*, 2015, **54**, 4392–4396.
- 23 S. Heintl and M. Scheer, *Chem. Sci.*, 2014, **5**, 3221–3225.
- 24 C. Schwarzmaier, A. Y. Timoshkin, G. Balázs and M. Scheer, *Angew. Chem., Int. Ed.*, 2014, **53**, 9077–9081.
- 25 S. Pelties, D. Herrmann, B. de Bruin, F. Hartl and R. Wolf, *Chem. Commun.*, 2014, 7014–7016.
- 26 C. Schwarzmaier, S. Heintl, G. Balázs and M. Scheer, *Angew. Chem., Int. Ed.*, 2015, **54**, 13116–13121.
- 27 W. W. Seidel, O. T. Summerscales, B. O. Patrick and M. D. Fryzuk, *Angew. Chem., Int. Ed.*, 2009, **48**, 115–117.
- 28 A. S. P. Frey, F. G. N. Cloke, P. B. Hitchcock and J. C. Green, *New J. Chem.*, 2011, **35**, 2022.
- 29 A. Velian and C. C. Cummins, *Chem. Sci.*, 2012, **3**, 1003.
- 30 C. Camp, L. Maron, R. G. Bergman and J. Arnold, *J. Am. Chem. Soc.*, 2014, **136**, 17652–17661.
- 31 S. Yao, N. Lindenmaier, Y. Xiong, S. Inoue, T. Szilvási, M. Adelhardt, J. Sutter, K. Meyer and M. Driess, *Angew. Chem., Int. Ed.*, 2015, **54**, 1250–1254.
- 32 O. J. Scherer and T. Brück, *Angew. Chem., Int. Ed. Engl.*, 1987, **26**, 59–59.
- 33 M. Baudler, S. Akpapoglou, D. Ouzounis, F. Wasgestian, B. Meinigke, H. Budzikiewicz and H. Münster, *Angew. Chem., Int. Ed. Engl.*, 1988, **27**, 280–281.
- 34 S. Welsch, L. J. Gregoriades, M. Sierka, M. Zabel, A. V. Virovets and M. Scheer, *Angew. Chem., Int. Ed.*, 2007, **46**, 9323–9326.
- 35 C. Heindl, S. Heintl, D. Lüdeker, G. Brunklaus, W. Kremer and M. Scheer, *Inorg. Chim. Acta*, 2014, **422**, 218–223.
- 36 M. Scheer, J. Bai, B. P. Johnson, R. Merkle, A. V. Virovets and C. E. Anson, *Eur. J. Inorg. Chem.*, 2005, **5**, 4023–4026.
- 37 M. Scheer, A. Schindler, R. Merkle, B. P. Johnson, M. Linseis, R. F. Winter, C. E. Anson and A. V. Virovets, *J. Am. Chem. Soc.*, 2007, **129**, 13386–13387.
- 38 C. Schwarzmaier, A. Schindler, C. Heindl, S. Scheuermayer, E. V. Peresyphkina, A. V. Virovets, M. Neumeier, R. Gschwind and M. Scheer, *Angew. Chem., Int. Ed.*, 2013, **52**, 10896–10899.
- 39 F. Dielmann, C. Heindl, F. Hastreiter, E. V. Peresyphkina, A. V. Virovets, R. M. Gschwind and M. Scheer, *Angew. Chem., Int. Ed.*, 2014, **53**, 13605–13608.
- 40 J. Bresien, C. Hering, A. Schulz and A. Villinger, *Chem. – Eur. J.*, 2014, **20**, 12607–12615.
- 41 I. Krossing and A. Reisinger, *Coord. Chem. Rev.*, 2006, **250**, 2721–2744.
- 42 I. Krossing and I. Raabe, *Angew. Chem., Int. Ed.*, 2004, **43**, 2066–2090.
- 43 J. Bresien, K. Faust, A. Schulz and A. Villinger, *Angew. Chem., Int. Ed.*, 2015, **54**, 6926–6930.
- 44 S. Alvarez, *Dalton Trans.*, 2013, **42**, 8617–8636.
- 45 P. Pyykkö and M. Atsumi, *Chem. – Eur. J.*, 2009, **15**, 12770–12779.
- 46 E. Conrad, N. Burford, U. Werner-Zwanziger, R. McDonald and M. J. Ferguson, *Chem. Commun.*, 2010, **46**, 2465–2467.
- 47 R. E. Bachman and D. F. Andretta, *Inorg. Chem.*, 1998, **37**, 5657–5663.
- 48 E. L. Muetterties and C. W. Alegranti, *J. Am. Chem. Soc.*, 1972, **94**, 6386–6391.
- 49 E. D. Glendening, J. K. Badenhop, A. E. Reed, J. E. Carpenter, J. A. Bohmann, C. M. Morales, C. R. Landis and F. Weinhold, *NBO 6.0*, Theoretical Chemistry Institute, University of Wisconsin, Madison, 2013.



6.4 A Tricyclic Hexaphosphane

Jonas Bresien, Axel Schulz, and Alexander Villinger

Chem. Eur. J. **2015**, *21*, 18543–18546.

DOI: 10.1002/chem.201503808

Reprinted with permission from John Wiley & Sons, Inc. (Licence No. 3796580460778)

Copyright 2015 John Wiley & Sons, Inc. All rights reserved.

Phosphorus Chemistry

A Tricyclic Hexaphosphane

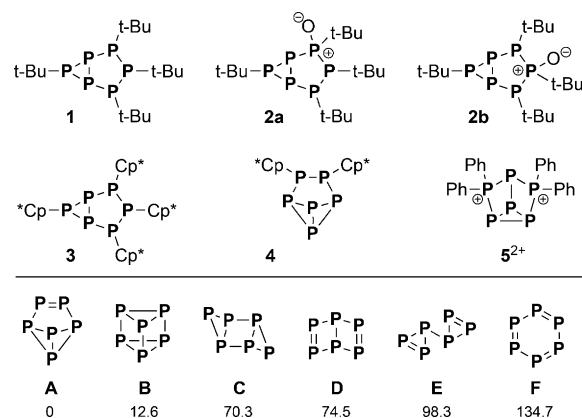
Jonas Bresien,^[a] Axel Schulz,^{*[a, b]} and Alexander Villinger^[a]

Dedicated to Prof. Dr. F. Ekkehardt Hahn on the occasion of his 60th birthday

Abstract: The reaction of the functionalized *cyclo*-tetraphosphane [ClP(μ -PMes^{*})₂] (Mes^{*} = 2,4,6-tri-*tert*-butylphenyl) with different Lewis bases led to the formation of an unprecedented tricyclic hexaphosphane, Mes^{*}P₆Mes^{*}. The formation of this compound was investigated by spectroscopic and theoretical methods, revealing an unusual ring expansion reaction. The title compound was fully characterized by experimental and computational methods.

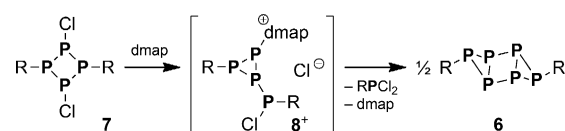
Phosphorus has fascinated chemists since its discovery by Hennig Brand in 1669.^[1] Especially since the development of modern day chemistry, various modifications of phosphorus have been identified,^[2,3] and countless polyphosphorus systems with (organic) substituents have been reported that incorporate a plethora of different structural motifs.^[2–5] The most prominent ones are possibly monocyclic ring systems with three to six phosphorus atoms, bicyclic tetra- or pentaphosphanes, derivatives of the heptaphosphatriide anion, as well as higher aggregates which resemble strands of violet phosphorus. Moreover, with the development of computational methods, a broad range of hypothetical P clusters was studied to identify possible minima on the potential energy surface.^[6–13]

However, examples of polycyclic hexaphosphanes are still rare. Baudler and co-workers reported on (tBu)₄P₆ (**1**, Scheme 1) and the related oxide (tBu)₄P₆O (**2**), which were derived from tBuPCl₂ and PCl₃ by reduction with Mg and subsequent oxidation by exposure to air.^[14,15] As reported by the group of Jutzi, thermolysis of (Cp^{*}P)₃ yielded the structurally related bicyclic hexaphosphane Cp^{*}₄P₆ (**3**, Cp^{*} = pentamethylcyclopentadienyl) as well as the tricyclic hexaphosphane Cp^{*}₂P₆ (**4**), which incorporates a benzvalene type P₆ scaffold (**A**).^[16,17] Weigand and co-workers reported on the cationic compound [Ph₄P₆]²⁺ (**5**), which can formally be derived from the prismane type structure (**B**) of P₆.^[18] Additionally, a salt containing a bicyclic hexastibine scaffold similar to **1** and **3** was reported recently.^[19]



Scheme 1. Top: Experimental examples of polycyclic hexaphosphanes. Bottom: Computed minimum structures on the potential energy surface of neutral P₆ (relative energies given in kJ mol⁻¹).^[13]

Theoretical investigations revealed that the benzvalene type structure (**A**) of neutral P₆ is the most favorable isomer in the gas phase.^[6–9,13] Nonetheless, other structures (**B–F**) were identified as local minima (Scheme 1),^[13] which present desirable new structural motives in phosphorus chemistry. To date, no tricyclic hexaphosphanes that incorporate a P₆ scaffold of type **C** have been reported.^[20] Therefore, we wish to present herein our results concerning the synthesis of the tricyclic hexaphosphane Mes^{*}P₆Mes^{*} (**6**, Mes^{*} = 2,4,6-tri-*tert*-butylphenyl), which was derived from a P₄ precursor by an unusual ring expansion reaction (Scheme 2).



Scheme 2. Synthesis of the tricyclic hexaphosphane **6** (R = Mes^{*}).

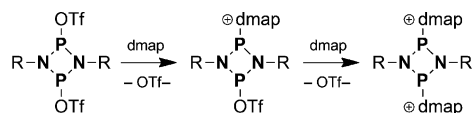
Recently, we reported on the synthesis of the cyclophosphane [ClP(μ -PMes^{*})₂] (**7**),^[21] which allows for selective functionalization of the P₄ ring system due to the chlorine substituents. Cyclophosphane **7** was synthesized from Mes^{*}PH₂ and PCl₃ in the presence of NEt₃; thus, it can be regarded as a P₄ building block that was derived from P₁ units, as opposed to the commonly applied strategy to functionalize white phosphorus (P₄) directly using Lewis acids, (transition) metals, or singlet carbenes.^[22–25] After investigating the reactivity of **7** to-

[a] J. Bresien, Prof. Dr. A. Schulz, Dr. A. Villinger
Institut für Chemie, Universität Rostock
Albert-Einstein-Straße 3a, 18059 Rostock (Germany)
E-mail: axel.schulz@uni-rostock.de

[b] Prof. Dr. A. Schulz
Leibniz-Institut für Katalyse an der Universität Rostock e.V.
Albert-Einstein-Straße 29a, 18059 Rostock (Germany)

Supporting information for this article is available on the WWW under <http://dx.doi.org/10.1002/chem.201503808>.

wards Lewis acids,^[26] we aimed at nucleophilic substitution of the Cl atoms at the P₄ scaffold. Since 4-(*N,N*-dimethylamino)pyridine (dmap) had previously been proven to be a good nucleophile and can effectively stabilize positive charges,^[27–29] the reaction of **7** with dmap was investigated. In analogy to the reaction of [TfOP(μ-NDmp)]₂ (Dmp = 2,6-dimethylphenyl) with dmap (Scheme 3),^[28] the formation of a base-stabilized cyclo-



Scheme 3. Reaction of a cyclodiphosphadiazane with dmap (R = Dmp).^[28]

phosphenium cation could be expected. In fact, in situ ³¹P NMR spectroscopy revealed the formation of a P₄ species as indicated by an ABMX spin system (−99.3, −91.2, +9.7, and +79.3 ppm); however, the chemical shifts were indicative of a species containing a three- rather than a four-membered ring system (Figure 1).^[21,30] Comprehensive DFT studies helped

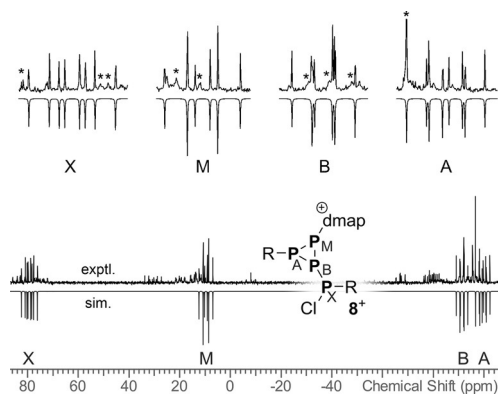


Figure 1. In situ ³¹P NMR spectrum of the reaction mixture after 5 h. The main signals were attributed to the intermediate **8**⁺ (* denotes other species in solution).

us assign the NMR signals to the intermediate [Mes*P₃(dmap)P(Cl)Mes*]Cl (**8Cl**, Scheme 2). The calculated NMR data agrees well with the experimental spectrum (Table S3, Supporting Information). With respect to the starting material, the formation of **8**⁺ can be understood in terms of a formal 1,2-Cl shift and rearrangement of one P–P bond.

Other signals in the in situ NMR spectrum were likely caused by different (configurational or rotational) isomers of **8**⁺. However, due to low intensity of the resonances, these could not be assigned unambiguously.

All attempts to crystallize the intermediate **8Cl** failed. Instead, colorless crystals of the novel tricyclic hexaphosphane **6** were obtained (yield: 58%). According to ³¹P NMR spectroscopy, compound **6** and Mes*PCl₂ were in fact the only products after a total reaction time of about two days. Based on NMR integrals, the ratio of Mes*PCl₂ and **6** was found to be 2:1; thus,

the formation of **6** can be rationalized in terms of formal Mes*PCl₂ extrusion and subsequent dimerization of the three-membered ring system. Comparable three-membered intermediates have been discussed previously in P₄ activation routes.^[2,3,31]

The molecular structure of the tricyclic hexaphosphane **6** was determined by single-crystal X-ray diffraction (Figure 2).^[32]

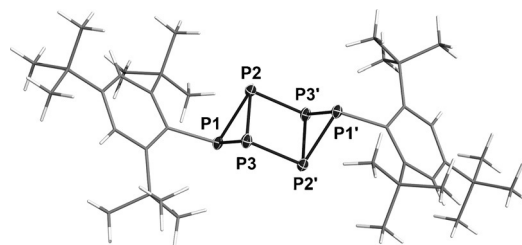


Figure 2. Molecular structure of **6**. Ellipsoids are set at 50% probability (123 K). Selected bond lengths [Å] and angles [°]: P1–C1 1.876(1), P1–P2 2.2189(5), P1–P3 2.2151(5), P2–P3 2.2373(5), P2–P3' 2.2368(5); P3–P1–P2 60.61(2), P1–P2–P3 59.61(2), P1–P3–P2 59.78(2), P1–P2–P3' 92.87(2), P2'–P3–P2 90.01(2); P1–P2–P3–P2' 93.33(2).

The molecule is located on a crystallographic inversion center, hence the central P₄ ring system is perfectly planar. All bond angles within the four-membered ring system are close to 90°, the bond angles within the three-membered rings are close to 60°. The six-membered ring molecule adopts a chair conformation with two transannular P–P bonds. The P1–P2 and P1–P3 bonds are slightly shorter (average 2.217 Å) than the P2–P3 and P2–P3' bonds (average 2.237 Å). Therefore, the central P₄ scaffold adopts an almost square geometry, while the three-membered rings correspond to isosceles triangles. All P–P bond lengths correspond to typical single bonds (Σr_{cov} = 2.22 Å).^[33] The angle between the least-squares planes of the three- and four-membered ring systems is 93.3°, which compares to those of other polycyclic phosphanes, such as bicyclic tetraphosphanes (≈ 100°)^[22,34–36] or the aforementioned bicyclic hexaphosphanes **1** and **3** (89.8° and 99.2°, respectively).^[14,17]

In the solid-state Raman spectrum, the P₆ scaffold can be identified by three characteristic bands at 414, 442, and 537 cm^{−1}, which were assigned on the basis of computed vibrational data (Table 1, for more details see Figure S5 in the Supporting Information)

In the ³¹P NMR spectrum, the tricyclic hexaphosphane **6** is characterized by an AA'BB'B''B''' spin system (−107.7 and −96.1 ppm; Figure 3). Due to dynamic rotation of the *t*Bu groups in solution, all four P atoms of the central P₄ scaffold become equivalent, resulting in apparent C_{2h} symmetry. The chemical shifts are similar to the NMR shifts of the P₃ unit of the structurally related compounds **1** and **3**,^[14,17] but also comparable to either cyclotriphosphanes^[21,30] or the bridging P atoms in bicyclic tetraphosphanes.^[22,34–36] The experimental NMR data are in good agreement with calculated NMR shifts and coupling constants (Table 2).

Table 1. Characteristic Raman vibrations of 6 .		
Vibration mode (● = P)	Main contribution	Frequency [cm ⁻¹]
	in-phase P ₃ ring mode	537
	out-of-phase P ₄ ring mode	442
	out-of-phase P ₃ ring mode	414

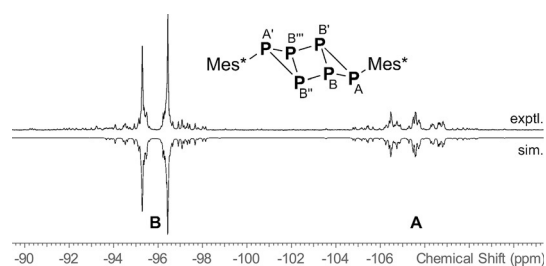


Figure 3. Experimental (top) and simulated (bottom) ³¹P NMR spectrum of **6**.

Table 2. ³¹ P NMR data of 6 . Calculated values [PBE0/6-31G(d,p), GIAO method] are given in brackets.		
	δ [ppm]	J [Hz]
P _A	-107.7 (-126.2)	J _{AA'} = -45 (-56)
P _B	-96.1 (-88.8)	J _{AB} = J _{AB'} = -191 (-158) J _{AB''} = J _{AB'''} = +54 (+35) J _{BB'} = -111 (-78) J _{BB''} = -146 (-90) J _{BB'''} = -30 (-45)

To investigate the bonding situation within the P₆ scaffold, DFT calculations were performed.^[37] As expected, natural bond orbital (NBO)^[38] analysis revealed eight P–P single bonds, of which six are considerably bent out of the line of nuclear centers due to the small bonding angles within the three-membered rings. This effect is also reflected in the symmetry and shape of the Kohn–Sham orbitals and can be nicely visualized by the electron localization function (ELF, Figure 4), where the local maxima are located beside the bond axes. Hence, the bonding within the P₃ units is comparable to that of tetrahedral P₄.^[39] To evaluate the stability of compound **6**, the corresponding *cis*-tricyclic, which can formally be derived from the prismane-type structure (**B**) of P₆, as well as the benzvalene type isomer (**A**) were calculated (Figure 5). These were found to be 40.2 or 72.6 kJ mol⁻¹ higher in energy (Δ*G*₂₉₈) than the experimental structure, respectively. However, in case of the smaller Cp* compound (**4**) or *t*Bu substituents (**9**), the benzvalene type isomers (**A**) were found to be the most stable ones, in accordance with the findings for neutral P₆ and experimen-

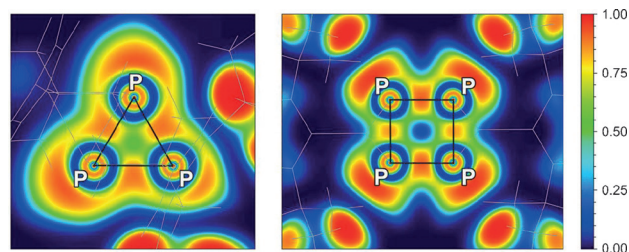


Figure 4. Depiction of the electron localization function, showing the P–P bonding system and the lone pairs at the P atoms; left: three-membered ring plane; right: four-membered ring plane.

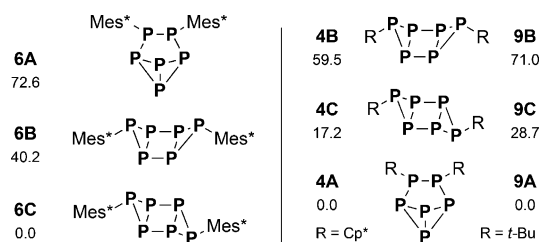


Figure 5. Relative stabilities of R₂P₆ isomers (Δ*G*₂₉₈ in kJ mol⁻¹).

tal evidence.^[16] Thus, the unusual tricyclic structure of type **C** is stabilized by the bulky Mes* moiety.

The tricyclic hexaphosphane **6** is poorly soluble in common organic solvents. It decomposes at 212 °C under inert conditions. Intriguingly, it was found to be stable in air. Even upon adding water to solution of **6** in CD₂Cl₂, 60% of the substance (by mole fraction) remained intact over a period of ten days at ambient temperature. This prompted us to develop an alternate synthetic protocol: starting from Mes*PH₂ and PCl₃, the precursor **7** was generated in situ by base-assisted HCl elimination. After removal of the hydrochloride, the crude product was treated with dmap without further purification. This led to precipitation of the tricyclic hexaphosphane, which was subsequently washed with water and acetone to remove all polar and nonpolar impurities. In this vein, compound **6** could be synthesized in 47% yield (based on Mes*PH₂), which is a significant improvement over the synthesis from pure **7** (combined yield based on Mes*PH₂: 26%).

When treating the cyclophosphane **7** with other Lewis bases, such as PPh₃ or tetramethylethylenediamine (TMEDA), practically no reaction was observed. Slow consumption of the starting material could only be detected after prolonged stirring, and a mixture of different products was observed in the ³¹P NMR spectrum. In the case of PPh₃, trace amounts of **6** were identified in the NMR spectrum after nine days. On the other hand, the reaction of **7** with tetramethylimidazolyliene led to degradation of the P₄ ring system; the main products were identified as the *endo-exo* isomer of the bicyclic phosphane Mes*P₄Mes*, the diphosphane Mes*PPMes*, and the primary phosphane Mes*PCL₂ (5:1:7 ratio).^[40] Accordingly, the unusual reactivity of the cyclophosphane **7** towards dmap cannot be generalized to other Lewis basic systems.

In conclusion, the first [3.1.0.0^{2,4}]-tricyclic hexaphosphane, Mes*P₆Mes* (6), could be prepared starting from a P₄ precursor molecule by formal ring expansion. Due to its symmetry, compound 6 displayed an unusual AA'BB'B''B''' spin system in the ³¹P NMR spectrum. The P₆ scaffold could be well discerned in the solid-state Raman spectrum due to three characteristic bands. Furthermore, DFT calculations showed that the structural motif is stabilized by the bulky Mes* substituents; in case of smaller moieties, such as Cp* or tBu, a benzvalene type structure of the P₆ scaffold is preferred. This demonstrates the advantages of bulky substituents for the stabilization of unusual bonding patterns.

Experimental Section

All manipulations were carried out under an inert atmosphere of argon. A mixture of [(ClIP(μ-PMes*))₂] (350 mg, 0.51 mmol) and 4-(*N,N*-dimethylamino)pyridine (dmap, 69 mg, 0.56 mmol) was dissolved in CH₂Cl₂ (3 mL) and stirred at ambient temperature for 2.5 days. Subsequently, the solution was slowly cooled to 5 °C, whereupon crystallization of colorless crystals was observed. The yellowish supernatant was removed by syringe and the crystals were washed with cold CH₂Cl₂ (0.5 mL) to remove adhering impurities. Drying in vacuo yielded a colorless product (100 mg, 0.15 mmol, 58%); m.p. 212 °C (decomposition); elemental analysis calcd (%): C 63.90, H 8.64; found: C 63.75, H 8.82; ³¹P{¹H} NMR (CD₂Cl₂, 121.5 MHz): δ = -107.7 (m, ¹J_{AB} = -191.3 Hz, ²J_{AB'} = +54.3 Hz, ³J_{AA'} = -44.8 Hz, 2 P, (Mes*P)₂P₄), -96.1 (m, ¹J_{AB} = -191.3 Hz, ¹J_{BB'} = -110.5 Hz, ¹J_{BB''} = -146.1 Hz, ²J_{BB'''}} = -29.7 Hz, ²J_{AB'} = +54.3 Hz, 4 P, (Mes*P)₂P₄); MS (CI positive, *iso*-butane): *m/z* (%): 677 [M]⁺. Further experimental details can be found in the Supporting Information.}}}}}

Acknowledgements

Financial support from the Fonds der Chemischen Industrie (scholarship for J.B.) and the Deutsche Forschungsgemeinschaft (SCHU 1170/11-1) is gratefully acknowledged.

Keywords: Lewis base · 4-(*N,N*-dimethylamino)pyridine · NMR spectroscopy · phosphorus compounds · polycyclic phosphanes · structure elucidation

- [1] A. Oppenheim, in *Allgemeine Deutsche Biographie, Dritter Band*, Duncker & Humblot, Leipzig (Germany), 1876, p. 236.
- [2] M. Scheer, G. Balázs, A. Seitz, *Chem. Rev.* 2010, 110, 4236–4256.
- [3] N. A. Giffin, J. D. Masuda, *Coord. Chem. Rev.* 2011, 255, 1342–1359.
- [4] M. Baudler, K. Glinka, *Chem. Rev.* 1993, 93, 1623–1667.
- [5] G. He, O. Shynkaruk, M. W. Lui, E. Rivard, *Chem. Rev.* 2014, 114, 7815–7880.
- [6] R. O. Jones, D. Hohl, *J. Chem. Phys.* 1990, 92, 6710–6721.
- [7] R. Janoschek, *Chem. Ber.* 1992, 125, 2687–2689.
- [8] M. Häser, U. Schneider, R. Ahlrichs, *J. Am. Chem. Soc.* 1992, 114, 9551–9559.
- [9] D. S. Warren, B. M. Gimarc, *J. Am. Chem. Soc.* 1992, 114, 5378–5385.
- [10] M. Häser, *J. Am. Chem. Soc.* 1994, 116, 6925–6926.

- [11] M. Häser, O. Treutler, *J. Chem. Phys.* 1995, 102, 3703–3711.
- [12] L. Guo, H.-S. Wu, Z.-H. Jin, *J. Mol. Struct.* 2004, 677, 59–66.
- [13] T. R. Galeev, A. I. Boldyrev, *Phys. Chem. Chem. Phys.* 2011, 13, 20549–20556.
- [14] M. Baudler, Y. Aktalay, K.-F. Tebbe, T. Heinlein, *Angew. Chem. Int. Ed. Engl.* 1981, 20, 967–969; *Angew. Chem.* 1981, 93, 1020–1022.
- [15] M. Baudler, M. Michels, M. Pieroth, J. Hahn, *Angew. Chem. Int. Ed. Engl.* 1986, 25, 471–473; *Angew. Chem.* 1986, 98, 465–467.
- [16] P. Jutzi, R. Kroos, A. Müller, M. Penk, *Angew. Chem. Int. Ed. Engl.* 1989, 28, 600–601; *Angew. Chem.* 1989, 101, 628–629.
- [17] P. Jutzi, R. Kroos, A. Müller, H. Bögge, M. Penk, *Chem. Ber.* 1991, 124, 75–81.
- [18] J. J. Weigand, M. Holthausen, R. Fröhlich, *Angew. Chem. Int. Ed.* 2009, 48, 295–298; *Angew. Chem.* 2009, 121, 301–304.
- [19] S. S. Chitnis, N. Burford, J. J. Weigand, R. McDonald, *Angew. Chem. Int. Ed.* 2015, 54, 7828–7832; *Angew. Chem.* 2015, 127, 7939–7943.
- [20] A tricyclic structure of type C was proposed for the salt [H₃NCy][HS₂P₆], but no analytical evidence could prove this connectivity. See: M. Becke-Goehring, H. Hoffmann, *Z. Anorg. Allg. Chem.* 1969, 369, 73–82.
- [21] J. Bresien, C. Hering, A. Schulz, A. Villinger, *Chem. Eur. J.* 2014, 20, 12607–12615.
- [22] R. Riedel, H.-D. Hausen, E. Fluck, *Angew. Chem. Int. Ed. Engl.* 1985, 24, 1056–1057; *Angew. Chem.* 1985, 97, 1050–1050.
- [23] J. D. Masuda, W. W. Schoeller, B. Donnadiou, G. Bertrand, *Angew. Chem. Int. Ed.* 2007, 46, 7052–7055; *Angew. Chem.* 2007, 119, 7182–7185.
- [24] J. E. Borger, A. W. Ehlers, M. Lutz, J. C. Sloatweg, K. Lammertsma, *Angew. Chem. Int. Ed.* 2014, 53, 12836–12839; *Angew. Chem.* 2014, 126, 13050–13053.
- [25] S. Heinl, S. Reisinger, C. Schwarzmaier, M. Bodensteiner, M. Scheer, *Angew. Chem. Int. Ed.* 2014, 53, 7639–7642; *Angew. Chem.* 2014, 126, 7769–7773.
- [26] J. Bresien, K. Faust, A. Schulz, A. Villinger, *Angew. Chem. Int. Ed.* 2015, 54, 6926–6930; *Angew. Chem.* 2015, 127, 7030–7034.
- [27] E. Rivard, K. Huynh, A. J. Lough, I. Manners, *J. Am. Chem. Soc.* 2004, 126, 2286–2287.
- [28] R. J. Davidson, J. J. Weigand, N. Burford, T. S. Cameron, A. Decken, U. Werner-Zwanziger, *Chem. Commun.* 2007, 4671–4673.
- [29] C. Hering-Junghans, M. Thomas, A. Villinger, A. Schulz, *Chem. Eur. J.* 2015, 21, 6713–6717.
- [30] M. Baudler, B. Makowka, *Z. Anorg. Allg. Chem.* 1985, 528, 7–21.
- [31] A. Lorbach, A. Nadj, S. Tüllmann, F. Dornhaus, F. Schödel, I. Sängler, G. Margraf, J. W. Bats, M. Bolte, M. C. Holthausen, *Inorg. Chem.* 2009, 48, 1005–1017.
- [32] CCDC 1417832 (6) contain the supplementary crystallographic data for this paper. These data are provided free of charge by The Cambridge Crystallographic Data Centre.
- [33] P. Pyykkö, M. Atsumi, *Chem. Eur. J.* 2009, 15, 12770–12779.
- [34] E. Niecke, R. Rüger, B. Krebs, *Angew. Chem. Int. Ed. Engl.* 1982, 21, 544–545; *Angew. Chem.* 1982, 94, 553–554.
- [35] P. Jutzi, U. Meyer, *J. Organomet. Chem.* 1987, 333, C18–C20.
- [36] A. R. Fox, R. J. Wright, E. Rivard, P. P. Power, *Angew. Chem. Int. Ed.* 2005, 44, 7729–7733; *Angew. Chem.* 2005, 117, 7907–7911.
- [37] Detailed information on experimental and computational methods is given in the Supporting Information.
- [38] E. D. Glendening, J. K. Badenhoop, A. E. Reed, J. E. Carpenter, J. A. Bohmann, C. M. Morales, C. R. Landis, F. Weinhold, *NBO 6.0*, Theoretical Chemistry Institute, University of Wisconsin, Madison, 2013.
- [39] M. F. Guest, I. H. Hillier, V. R. Saunders, *J. Chem. Soc. Faraday Trans. 2* 1972, 68, 2070–2074.
- [40] J. Bresien, K. Faust, C. Hering-Junghans, J. Rothe, A. Schulz, A. Villinger, *Dalton Trans.* 2016, DOI 10.1039/C5DT02757H.

Received: September 23, 2015

Published online on November 5, 2015

6.5 Synthetic Strategies to Bicyclic Tetraphosphanes using P₁, P₂ and P₄ Building Blocks

Jonas Bresien, Kirill Faust, Christian Hering-Junghans, Julia Rothe, Axel Schulz, and Alexander Villinger

Dalton Trans. **2016**, 45, 1998–2007.

DOI: 10.1039/c5dt02757h

This Open Access article is licensed under a Creative Commons Attribution 3.0 Unported Licence.



Cite this: *Dalton Trans.*, 2016, **45**, 1998

Received 20th July 2015,
Accepted 28th August 2015
DOI: 10.1039/c5dt02757h

www.rsc.org/dalton

Synthetic strategies to bicyclic tetraphosphanes using P₁, P₂ and P₄ building blocks†

Jonas Bresien,^a Kirill Faust,^a Christian Hering-Junghans,^a Julia Rothe,^a Axel Schulz^{*a,b} and Alexander Villinger^a

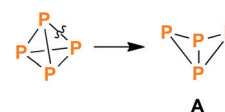
Different reactions of Mes* substituted phosphanes (Mes* = 2,4,6-tri-*tert*-butylphenyl) led to the formation of the bicyclic tetraphosphane Mes*P₄Mes* (**5**) and its unknown Lewis acid adduct **5**·GaCl₃. In this context, the *endo*–*exo* isomer of **5** was fully characterized for the first time. The synthesis was achieved by reactions involving “self-assembly” of the P₄ scaffold from P₁ building blocks (*i.e.* primary phosphanes) or by reactions starting from P₂ or P₄ scaffolds (*i.e.* a diphosphene or cyclic tetraphosphane). Furthermore, interconversion between the *exo*–*exo* and *endo*–*exo* isomer were studied by ³¹P NMR spectroscopy. All compounds were fully characterized by experimental as well as computational methods.

Introduction

Ring systems composed of group 15 elements (pnictogens, Pn) are an intriguing and widely investigated aspect of main group chemistry.^{1–3} Within this field of research, the chemistry of phosphorus based ring systems has become an important branch of inorganic chemistry,^{4,5} especially in view of the fact that various phosphorus ring systems can be obtained by direct activation of white phosphorus.^{6–8} A lot of work has been carried out to improve the selectivity of these activation processes, involving functionalization of P₄ by Lewis acids and bases, (transition) metals, radicals, or singlet carbenes such as N-heterocyclic carbenes (NHCs) or cyclic alkylaminocarbenes (CAACs).^{9–12}

Among a plethora of structural motifs found in phosphorus ring systems, the simple tetraphosphabicyclo[1.1.0]butane scaffold (**A**, Scheme 1) is of special interest. Firstly, it can formally be derived from tetrahedral P₄ by “simple” cleavage of one PP bond. Secondly, and more importantly, tetraphosphabicyclo[1.1.0]butanes were indeed obtained by P₄ activation, thus representing worthwhile target molecules in phosphorus chemistry.

The first tetraphosphabicyclo[1.1.0]butane, (Me₃Si)₂N–P₄–N(SiMe₃)₂ (**1a**, **1b**, Scheme 2), was synthesized by the group of



Scheme 1 Breaking one of the PP bonds in tetrahedral P₄ formally yields the tetraphosphabicyclo[1.1.0]butane scaffold (**A**).

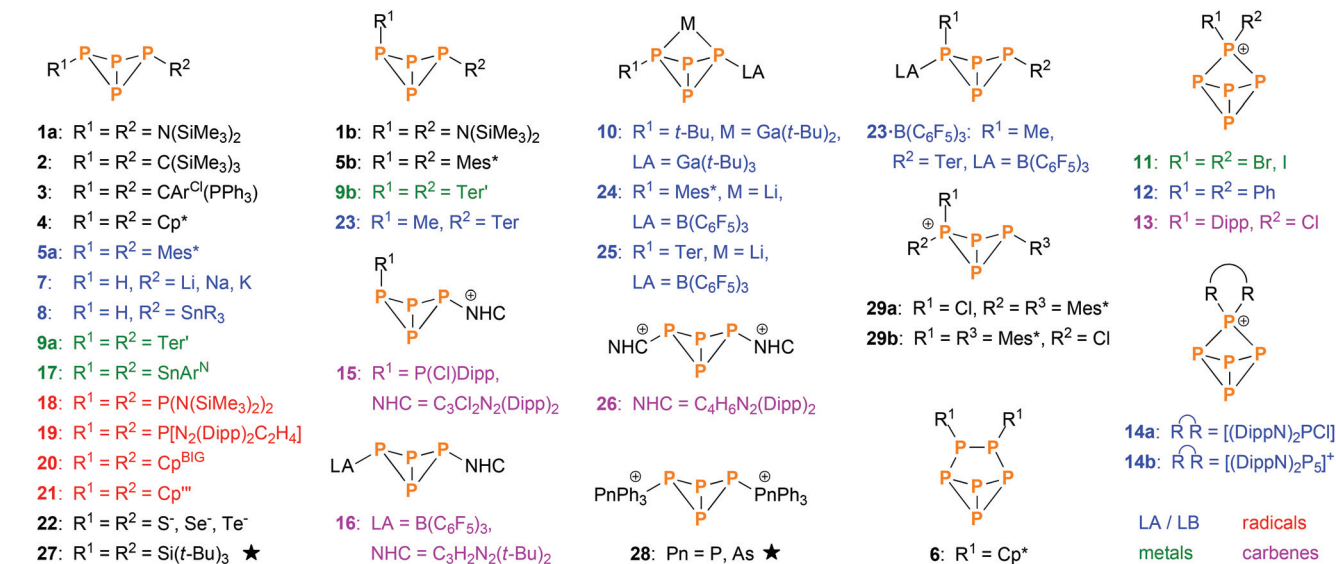
Niecke in 1982.¹³ It was derived from P₂ building blocks utilizing PP coupling reactions. In the following years, some more examples emerged that were derived from P₂ or P₃ units, as reported by Cowley (**2**),¹⁴ Schmidpeter (**3**),¹⁵ Jutzi (**4–6**),^{16–19} Weber (**5a**),²⁰ and Romanenko (**5a**).²¹ However, the majority of bicyclic tetraphosphanes was synthesized by P₄ activation, the first example being *exo*–*exo*–Mes*P₄Mes* (**5a**, Mes* = 2,4,6-tri-*tert*-butylphenyl), which was reported by Fluck and co-workers in 1985.^{22,23} Improvement of P₄ activation methods led to various other bicyclic P₄ species, which can be categorized by the aforementioned types of P₄ activation (Scheme 2); important contributions were made by the groups of Baudler (**7**, **8**),^{24,25} Power (**9–10**),^{26,27} Krossing (**11**),²⁸ Weigand (**12–15**),^{29,30} Tamm (**16**),³¹ Roesky and Stalke (**17**),³² Lappert (**18**),³³ Masuda (**19**),³⁴ Scheer (**20**, **21**),¹⁰ Karaghiosoff (**22**),³⁵ Lammertsma (**23–25**),¹² and Jones (**26**).³⁶ Additionally, various examples of transition metal complexes that incorporate bicyclic P₄ scaffolds were reported.^{11,37–42} In contrast, very few examples of self-assembly reactions exist (*i.e.* the bicyclic P₄ scaffold is built from P₁ building blocks in a single reaction); literature reports include Wiberg's (*t*-Bu)₃Si–P₄–Si(*t*-Bu)₃ (**27**)⁴³ and Weigand's [Ph₃Pn–P₄–PnPh₃]²⁺ (**28**, Pn = P, As).⁴⁴ Just recently, we reported on the cation [Mes*P₄(Cl)Mes*]⁺ (**29**),⁴⁵ which in itself was not derived by a self-assembly reaction, but its cyclic P₄ precursor was.⁴⁶

^aInstitut für Chemie, Universität Rostock, Albert-Einstein-Straße 3a, D-18059 Rostock, Germany. E-mail: axel.schulz@uni-rostock.de

^bLeibniz-Institut für Katalyse e.V. an der Universität Rostock, Albert-Einstein-Straße 29a, D-18059 Rostock, Germany

†Electronic supplementary information (ESI) available: Experimental and computational details, crystallographic and spectroscopic data. CCDC 1413820–1413827. For ESI and crystallographic data in CIF or other electronic format see DOI: 10.1039/c5dt02757h





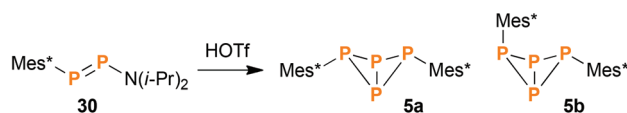
Scheme 2 Overview of known bicyclic tetraphosphane species (not including transition metal complexes). Most were synthesized by direct activation of P_4 using Lewis acids and bases (blue), metals or metal fragments (green), radical species (red) or singlet carbenes (violet). The rest was derived from other precursors, mainly P_2 and P_4 building blocks. Species indicated by a star were derived directly from P_1 building blocks in a self-assembly reaction. $\text{Ar}^{\text{Cl}} = 2,6$ -dichlorophenyl; $\text{Ar}^{\text{N}} = \text{C}_6\text{H}_3-2,6$ -($\text{C}(\text{NDipp})\text{CH}_3$)₂; $\text{Cp} = \text{cyclopentadienyl}$; $\text{Cp}^* = \text{pentamethyl-Cp}$; $\text{Cp}^{\text{'''}} = 2,3,5$ -tri-*tert*-butyl-Cp; $\text{Cp}^{\text{BIG}} = \text{pentakis}(4\text{-}n\text{-butylphenyl})\text{-Cp}$; $\text{Dipp} = 2,6$ -diisopropylphenyl; $\text{SnR}_3 = \text{SnMe}_3, \text{SnPh}_3, \text{Sn}(c\text{-Hex})_3$ or $\text{Sn}(o\text{-Tol})_3$; $\text{Ter} = 2,6$ -dimesitylphenyl; $\text{Ter}^r = 2,6$ -bis(diisopropylphenyl)phenyl; $\text{LA} = \text{Lewis acid}$, $\text{LB} = \text{Lewis Base}$, $\text{NHC} = \text{N-heterocyclic carbene}$.

Interestingly, *exo-exo*-substituted tetraphosphabicyclo-[1.1.0]butanes are considerably more common than their *endo-exo*-substituted counterparts, indicating that the latter are energetically less favoured. We therefore took interest in the synthesis and characterization of rare *endo-exo*-substituted derivatives, which could be synthesized from P_1 , P_2 and P_4 building blocks and were analysed by experimental and computational methods.

Results and discussion

Synthesis and characterization of *endo-exo*- $\text{Mes}^*\text{P}_4\text{Mes}^*$ (**5b**)

During our research in functionalized *cyclo*-tetraphosphanes,⁴⁶ we came across a publication of Romanenko *et al.*,²¹ wherein the authors described the synthesis of *exo-exo*- $\text{Mes}^*\text{P}_4\text{Mes}^*$ (**5a**) and the asymmetrically substituted bicyclic system $\text{Mes}^*\text{P}_4\text{N}(i\text{-Pr})_2$ by reacting the diphosphene $\text{Mes}^*\text{PPN}(i\text{-Pr})_2$ (**30**) with equimolar amounts of HOTf ($\text{Tf} = \text{SO}_2\text{CF}_3$). Intrigued by this curious method to synthesize bicyclic tetraphosphanes, we tried to reproduce the experiment described in the publication. However, fractional crystallization of the product mixture did not yield the reported compound $\text{Mes}^*\text{P}_4\text{N}(i\text{-Pr})_2$, but rather *endo-exo*- $\text{Mes}^*\text{P}_4\text{Mes}^*$ (**5b**, Scheme 3), alongside the known product **5a** and minor amounts of the diphosphene $\text{Mes}^*\text{PPMes}^*$ (**31**).^{47,48} Probably the available NMR and MS data were misinterpreted in the original publication. Compound **5b** was now fully characterized for the first time, including NMR, Raman and IR spectroscopy, mass spectrometry, and single crystal X-ray diffraction.



Scheme 3 Reaction of diphosphene **30** with HOTf, yielding bicyclic phosphanes **5a** and **5b** as main products.

Spectroscopic characterization

Apart from minor impurities, the ^{31}P NMR spectrum of the reaction mixture showed an A_2X_2 ($-273.2, -128.3$ ppm) and an A_2MX spin system ($-220.4, -94.8, -54.7$ ppm) in a ratio of 1 : 4. The former set of signals was assigned to **5a** (17% yield based on ^{31}P NMR integrals), the latter to **5b** (67%); hence, the *endo-exo*-isomer was actually formed in significant excess. The same NMR data were obtained for pure **5a** and **5b** (Fig. 1), which agree well with calculated NMR shifts and coupling constants (ESI^\dagger) as well as previously reported NMR data.^{17,22} Moreover, both isomers could be nicely distinguished in the Raman spectrum due to different excitation energies of the vibrational “breathing” mode of the P_4 scaffold (Table 1). The corresponding Raman bands were easily identified as the most intense signals in both spectra (**5a**: 592 cm^{-1} , **5b**: 568 cm^{-1}). The wavenumbers compare well to the symmetrical A_1 mode of tetrahedral P_4 in the gas phase (600 cm^{-1}).⁴⁹ In case of **5b**, two distinct P–C valence modes were identified at 584 (*exo*) and 591 cm^{-1} (*endo*). In **5a**, the single P–C valence band was superimposed by the “breathing” mode of the bicyclic scaffold and could not be discerned.



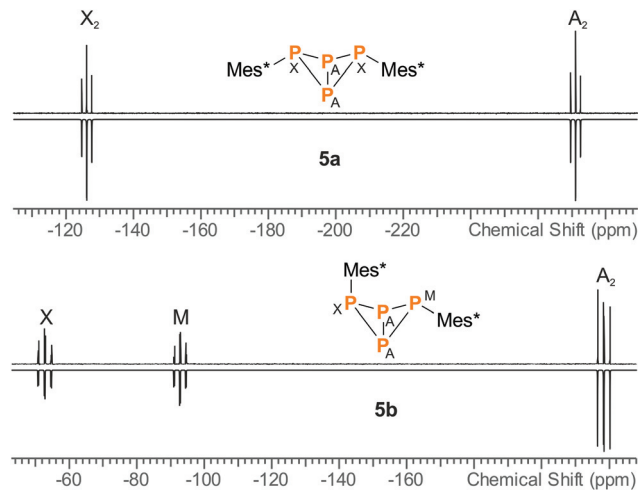


Fig. 1 Experimental (up) and simulated (down) ^{31}P NMR spectra of **5a** and **5b**.

Molecular structure

Crystallization from *n*-hexane yielded single crystals of **5b** in the space group $P\bar{1}$ while crystallization from CH_2Cl_2 afforded crystals in the space group $P2_1/n$ (Fig. 2, right). The P–P and P–C bond lengths are similar in both modifications of **5b**: the P1–P2 and P1–P3 bonds (av. 2.227, 2.233 Å) are close to the sum of the covalent radii ($\sum r_{\text{cov}} = 2.22$ Å),⁵⁰ whereas the P2–P4 and P3–P4 bonds (av. 2.213, 2.210 Å) as well as the transannular bond P2–P3 (av. 2.177 Å) are slightly shorter. This is in contrast to the structure of the previously reported *exo-exo*-isomer **5a** (Fig. 2, left),²² where all four peripheral P–P bonds exhibit similar lengths (av. 2.225 Å); the transannular bond, however,

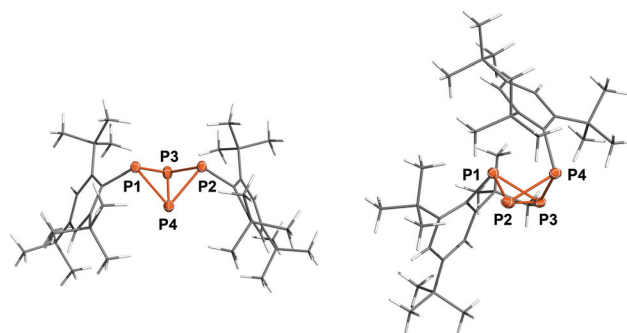


Fig. 2 Molecular structure of **5a** (left) and **5b** (monoclinic, right). Ellipsoids are set at 50% probability (173 K). Selected bond lengths [Å] and angles [°]: **5a** P1–P3 2.2310(7), P1–P4 2.2171(7), P2–P3 2.2294(7), P2–P4 2.2236(7), P3–P4 2.1634(8); P1–P3–P4–P2 $-95.66(3)^\circ$; **5b** P1–P2 2.2244(7), P1–P3 2.2326(8), P2–P4 2.2131(8), P3–P4 2.2101(8), P2–P3 2.1773(8); P1–P2–P3–P4 $107.78(3)^\circ$.

is likewise only 2.1634(8) Å. The bond angles at the P atoms are all close to 60° and thus compare to tetrahedral P_4 . Interestingly, the Mes* substituent in **5b** is bent backwards above the P_4 scaffold, so the *p*-*tert*-butyl group rests on top of the *exo*-Mes* substituent, effectively shielding the top side of the bicyclic ring system. Hence, the fold angle of the butterfly-shaped P_4 scaffold is quite different in all three cases; it varies from $95.66(3)^\circ$ (**5a**) across $105.75(5)^\circ$ (triclinic **5b**) to $107.78(3)^\circ$ (monoclinic **5b**), which can be attributed to Pauli repulsion between the *endo*-substituent and the opposite bridging atom (P1) in case of **5b** as well as packing effects to account for the difference between the two modifications. A similar effect was observed in case of $\text{Ter}'\text{P}_4\text{Ter}'$ (**9a**, **9b**, $\text{Ter}' = 2,6\text{-bis}(\text{diisopropylphenyl})\text{phenyl}$), where the difference between *exo-exo* (92.9°) and *endo-exo*-isomer (108.1°) is even larger.²⁷

Table 1 Main vibrational modes of bicyclic tetraphosphanes in the Raman spectrum. Assignment of the symmetries based on approximate C_{2v} symmetry of the P_4 scaffold

Vibration mode	Description	Frequency [cm^{-1}]
	Symmetrical valence “breathing mode” (A_1 mode, in phase)	5a : 592 5b : 568 5a · GaCl_3 : 597 5b · GaCl_3 : 567
	Peripheral bond stretch (B_1 mode)	5a : 447 5b : 500 5a · GaCl_3 : 497 5b · GaCl_3 : 518
	Transannular bond stretch (A_1 mode, out of phase)	5a : 412 5b : — 5a · GaCl_3 : 436 5b · GaCl_3 : —
	Peripheral bond stretch (B_2 mode)	5a : 412 5b : 412 5a · GaCl_3 : 451 5b · GaCl_3 : 438



Computational study

Comprehensive DFT calculations were carried out to compare the isomers **5a** and **5b**. According to NBO analysis,⁵¹ the bonding situation is similar in both cases. The Wiberg and NLMO bond indices are near unity for all P–P bonds. However, due to the small bond angles, the electron density is not distributed symmetrically around the P–P bond axes, but rather bent outwards, resulting in banana-shaped bonds. This is illustrated by the electron localization function (ELF, Fig. 3 right), where the local maxima between the P atoms are found outside the lines of nuclear centres. Additionally, the symmetry and shape of the natural bond orbitals (NBOs) and molecular orbitals (MOs) support this picture.

Isomerization of **5b** to **5a**

At the PBE0/aug-cc-pVDZ level of theory, the *exo-exo*-isomer **5a** is energetically favoured with respect to **5b** by 10.4 kJ mol⁻¹ (ΔH^{298}) or 8.80 kJ mol⁻¹ (ΔG^{298}), respectively. These findings prompted us to investigate the thermodynamic equilibrium between both isomers: Indeed, when heating a THF solution of **5a** and **5b** (1 : 4 ratio) to 75 °C over a period of 50 days, slow conversion of **5b** to **5a** was observed in the ³¹P NMR spectrum. The forward and backward reaction were modelled as first order kinetics according to eqn (1).



Hence, eqn (2) defines the reaction rate, $[\mathbf{5a}]$ and $[\mathbf{5b}]$ being the partial concentrations of **5a** and **5b**, respectively.

$$\frac{d[\mathbf{5b}]}{dt} = -k_f[\mathbf{5b}] + k_b[\mathbf{5a}] \quad (2)$$

Let $[\mathbf{5a}]_0$ and $[\mathbf{5b}]_0$ denominate the initial concentrations at $t = 0$. Due to the conservation of mass, $[\mathbf{5b}]_0 - [\mathbf{5b}]$ equals

$[\mathbf{5a}] - [\mathbf{5a}]_0$. Furthermore, the reaction rate becomes zero at equilibrium, when the system reaches a steady state with constant concentrations of both isomers. Using these boundary conditions to integrate eqn (2), we obtain

$$[\mathbf{5b}] = c + ([\mathbf{5b}]_0 - c)e^{-(k_f+k_b)t} \quad (3)$$

$$c = \frac{k_b}{k_f + k_b} ([\mathbf{5a}]_0 + [\mathbf{5b}]_0) \quad (4)$$

Least-squares fitting of eqn (3) against the experimentally determined concentrations gave $k_f = 2.77(11) \times 10^{-6} \text{ s}^{-1}$ and $k_b = 0.30(3) \times 10^{-6} \text{ s}^{-1}$. Accordingly, the experimental equilibrium constant is:

$$K = \frac{k_f}{k_b} = 9.3(1.4) \quad (5)$$

Thus, the experimental Gibbs energy (at 75 °C) can be calculated:

$$\Delta_R G = -RT \ln K = -6.4(3) \text{ kJ mol}^{-1} \quad (6)$$

This value compares well to the calculated value of $\Delta_R G^{348} = -8.54 \text{ kJ mol}^{-1}$ for the gas phase reaction.

Intriguingly, an equilibrium between *endo-exo* and *exo-exo*-isomers was also described for Ter'P₄Ter' (**9a**, **9b**); however, the system was found to be highly dynamic and both isomers afforded identical NMR spectra even at low temperature. Crystallization of either one of the isomers depended solely on the solvent used.²⁷

Synthesis of *endo-exo*-Mes*P₄Mes* (**5b**) by carbene promoted degradation of [CIP(μ-PMes*)]₂ (**32**)

Using the synthetic protocol described above, **5a** and **5b** were always obtained in mixture. Separation was difficult and could only be achieved for small amounts of substance by repeated re-crystallization. Designing a reaction that would yield **5b**

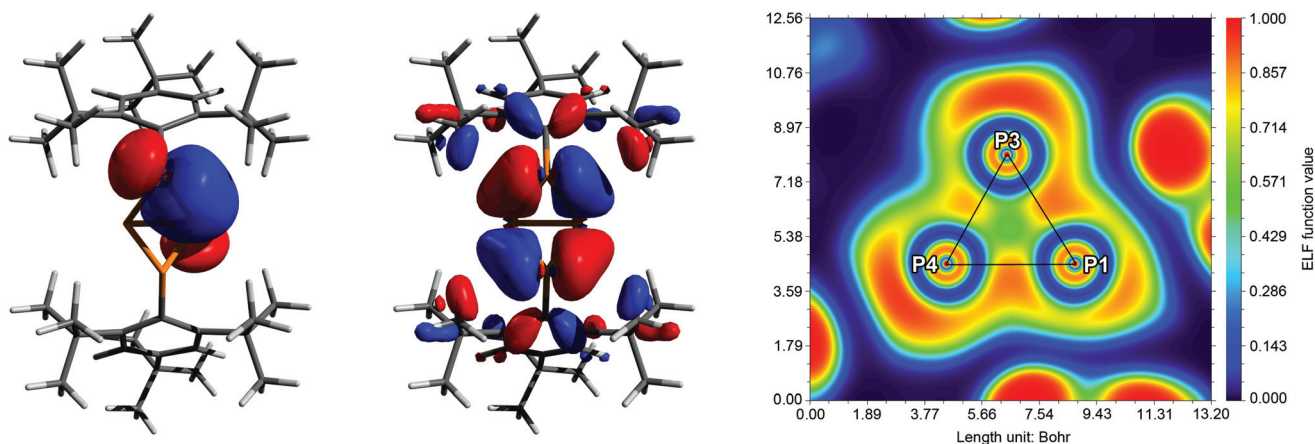
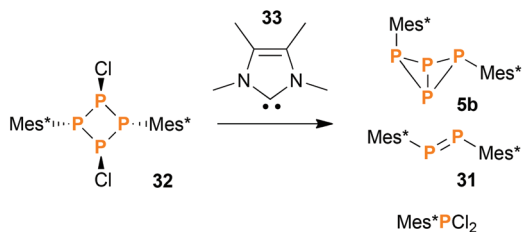


Fig. 3 Exemplary description of the bonding in **5a**. Left: NBO/NLMO depiction of one PP bond, illustrating the “banana” bond character. Middle: HOMO–6 with large coefficients at the central P₄ scaffold. Right: Electron localization function (ELF) depicted in a plane through atoms P1, P3 and P4. The maximum densities between the P atoms are found outside the lines of nuclear centres (black). The maxima at the corners of the triangle show the location of the lone pairs (LPs).



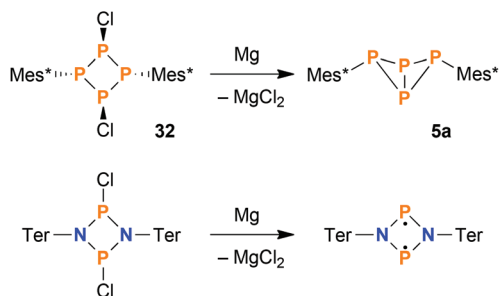


Scheme 4 The carbene promoted degradation of **32** yields a mixture of products, of which some were identified.

exclusively proved to be difficult: obviously, all reactions involving elevated temperatures led to (at least) partial formation of the thermodynamically favoured *exo-exo*-isomer **5a**. Still, we found that the reaction of the *cyclo*-tetraphosphane $[\text{ClP}(\mu\text{-PMes}^*)_2]$ (**32**)⁴⁶ with tetramethylimidazolylidene (**33**) yielded bicyclic tetraphosphane **5** in a surprisingly good isomeric ratio (**5a** : **5b**) of 1 : 12 (Scheme 4). The isolated yield of pure **5b** was low (14% based on **32**), since the degradation of **32** did not proceed cleanly but rather gave a mixture of different products. Anyway, **5b** could be crystallized from the reaction mixture in large, block-shaped crystals, making isolation comparatively easy.

Selective synthesis of *exo-exo*-Mes*P₄Mes* (**5a**) by reduction

Concerning the synthesis of pure **5a**, the isomerisation at elevated temperatures certainly offered a viable possibility to increase the isomeric ratio in favour of the *exo-exo* isomer. Nevertheless, we found a much more straightforward way to synthesize pure **5a**: starting from **32**, reduction with stoichiometric amounts of Mg afforded **5a** in high yields (based on ³¹P NMR integrals: 95%; isolated substance: 73%) in a clean reaction (Scheme 5, top). For comparison, the original synthesis of **5a** published by Fluck *et al.* afforded the bicyclic phosphane in a yield of only 5.2%.²² Formally, the reduction of **32** with Mg can be compared to the reduction of dichloro-*cyclo*-diphosphadiazanes, $[\text{ClP}(\mu\text{-NR})_2]$, which results in the formation of *cyclo*-diphosphadiazanediyls, $[\text{P}(\mu\text{-NR})_2]$, provided that the substituent R is bulky enough to prevent dimerization (Scheme 5,



Scheme 5 Top: Reduction of *cyclo*-tetraphosphane **32** yields bicyclic phosphane **5a** selectively. Bottom: Reduction of homologous dichloro-*cyclo*-diphosphadiazanes results in singlet open-shell biradicals with a drastically different bonding situation.

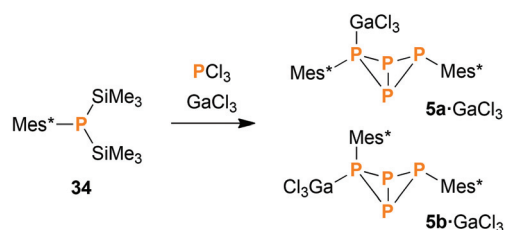
bottom).⁵² Yet, in contrast to the bicyclic tetraphosphane, the NP species comprise a planar ring system with singlet bi-radical character, as there is no classical bonding interaction between the transannular P atoms in this case.

Synthesis of Mes*P₄Mes*·GaCl₃ (**5**·GaCl₃) from P₁ units

When heating a solution of Mes*P(SiMe₃)₂ (**34**) in the presence of PCl₃, a mixture of various products was obtained. Interestingly, the *exo-exo*-isomer **5a** was found to be one of the major products. Other species that could be identified were Mes*PPMes* (**31**), Mes*PCl₂, P₄, *endo-exo*-isomer **5b** (minor amounts), and some higher aggregates of uncertain composition. However, the reaction was rather slow, so we decided to add a Lewis acid for activation purposes. Indeed, in the presence of GaCl₃, complete conversion was detected after one hour even at low temperatures (Scheme 6). Upon slow warming to ambient temperature, colourless crystals of **5a**·GaCl₃ or **5b**·GaCl₃ were obtained. Depending on the solvent, either one could be crystallized selectively, even though the ratio of both isomers in solution (7 : 5) remained unaffected by the choice of solvent.

Spectroscopic characterization

For both **5a**·GaCl₃ and **5b**·GaCl₃, an A₂MX spin system was expected due to unsymmetrical substitution of the bicyclic scaffold. Nonetheless, the room temperature ³¹P NMR spectrum of **5a**·GaCl₃ only displayed two resonances (formal A₂X₂ pattern; −246.4, −97.1 ppm; Fig. 4), which were shifted downfield by *ca.* 30 ppm with respect to non-coordinating **5a**. At −80 °C, though, the actual A₂MX spin system was resolved (−248.1, −114.0, −74.8 ppm), with a rather large ²J_{MX} coupling constant of +225 Hz (*cf.* **5b**: ²J_{MX} = −27 Hz). To investigate the nature of this dynamic effect, temperature dependent NMR spectra were recorded. Basically, either an *intramolecular* or an *intermolecular* exchange (*i.e.* dissociation or bimolecular exchange) of the GaCl₃ unit could be responsible for the observed line shapes, given that the concentration of free **5a** is much lower than the concentration of the adduct **5a**·GaCl₃ (approx. ratio of 10^{−2} or less). However, at such low concentrations, the free phosphane could well be below the detection limit and it might not be discernible in the spectrum even at slow exchange. Accordingly, we added an excess of **5a**, so the appearance of the NMR spectrum would change drastically if the free phosphane (*i.e.* dissociation) was involved in the



Scheme 6 Reacting **34** with PCl₃ and GaCl₃ leads to GaCl₃ adducts of the bicyclic tetraphosphane **5**, among other products.



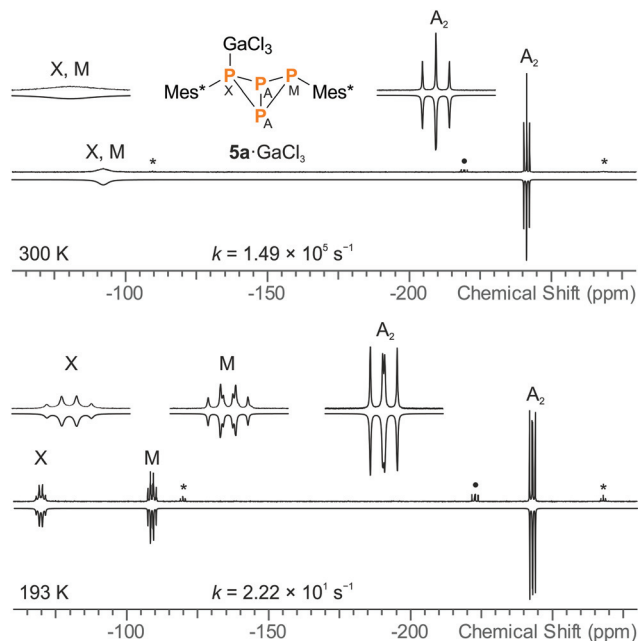


Fig. 4 Experimental (up) and simulated (down) ^{31}P NMR spectra of $5\text{a}\cdot\text{GaCl}_3$ at $27\text{ }^\circ\text{C}$ (top) and $-80\text{ }^\circ\text{C}$ (bottom), demonstrating the dynamic exchange of the GaCl_3 moiety in solution (* = 5a , • = impurity of $5\text{b}\cdot\text{GaCl}_3$). GaCl_3 was added to 5a in slightly sub-stoichiometric amounts (0.95 eq.) so the non-coordinating bicyclic phosphane was detectable in the NMR spectrum.

observed exchange.⁵³ However, the signals of the excess phosphane could be detected independently of those of the adduct and the signal pattern of $5\text{a}\cdot\text{GaCl}_3$ remained unchanged, regardless of the excess of phosphane, proving an intramolecular mechanism (Scheme 7). Still, at higher temperatures above the coalescence of the M and X signal of $5\text{a}\cdot\text{GaCl}_3$, slight broadening of the signals of free 5a was detected, hinting at an independent intermolecular exchange. Full line-shape analysis of the NMR signals (Fig. 4, ESI†) facilitated derivation of the rate constants k at different temperatures. Using the Eyring eqn (7), the Gibbs energy of activation of the intramolecular exchange could be determined.

$$k = \kappa \frac{k_{\text{B}}T}{h} \exp\left(-\frac{\Delta G^\ddagger}{RT}\right) \quad (7)$$

Least-squares fitting gave a mean Gibbs energy of activation $\Delta G^\ddagger = 39.5(4)\text{ kJ mol}^{-1}$, which compares, for example, to the activation barrier of the exchange of NH_3 in $\text{H}_3\text{N}\cdot\text{GaMe}_3$



Scheme 7 In case of $5\text{a}\cdot\text{GaCl}_3$, a fast intramolecular exchange of the GaCl_3 unit was observed. The Gibbs energy of activation for this process was determined to be 39.5 kJ mol^{-1} .

(35.6 kJ mol^{-1}).⁵⁴ According to the linearized Eyring plot, the enthalpy of activation ΔH^\ddagger was found to be $39.5(4)\text{ kJ mol}^{-1}$ and the entropy of activation $\Delta S^\ddagger = -0.20(2)\text{ J mol}^{-1}\text{ K}^{-1}$, indicating a monomolecular transition state in agreement with the discussed intramolecular exchange reaction. The NMR data at slow exchange ($-80\text{ }^\circ\text{C}$) correspond well with calculated NMR shifts and coupling constants (ESI†).

The *endo-exo* isomer $5\text{b}\cdot\text{GaCl}_3$ showed an A_2MX spin system ($-224.5, -114.5, -50.0\text{ ppm}$), which resembled the NMR spectrum of free 5b . Like in $5\text{a}\cdot\text{GaCl}_3$, the A part was broadened due to coupling with Ga. Owing to the arrangement of the Mes^* substituents, no intramolecular exchange was observed; the linewidths did not change significantly upon cooling to $-80\text{ }^\circ\text{C}$. Nonetheless, upon addition of an excess of 5b the ^{31}P NMR spectrum revealed a dynamic exchange between free phosphane and adduct, which is most likely caused by a bimolecular exchange of the type $5\cdot\text{GaCl}_3 + 5' \rightleftharpoons 5'\cdot\text{GaCl}_3 + 5$ (ESI†).

Both isomers were nicely distinguishable in the solid state Raman spectra, due to the different positions of the “breathing mode” bands, similar to the non-coordinating tetraphosphabicyclo[1.1.0]butanes 5a and 5b . In contrast to the latter, the most intense Raman signal was caused by the Ga–Cl stretching at 343 ($5\text{a}\cdot\text{GaCl}_3$) or 348 cm^{-1} ($5\text{b}\cdot\text{GaCl}_3$). P–C valence modes could be identified at 613 (Mes^* at coordinating P, $5\text{a}\cdot\text{GaCl}_3$) and 618 cm^{-1} (*endo-Mes**, $5\text{b}\cdot\text{GaCl}_3$), the other ones were superimposed by the intense “breathing mode” signals. Important vibrational modes of the P_4 scaffold are summarized in Table 1.

Molecular structure

Lewis acid adduct $5\text{a}\cdot\text{GaCl}_3$ crystallized in the orthorhombic space group $Pnma$ as *n*-hexane solvate (Fig. 5). The PP bond lengths lie within the range of typical single bonds, however the P3–P2 (or P3–P2′) bond is slightly shortened ($2.1805(9)\text{ \AA}$); therefore, the bicyclic structure with two longer and two shorter bonds actually resembles the bicyclic scaffold in 5b .

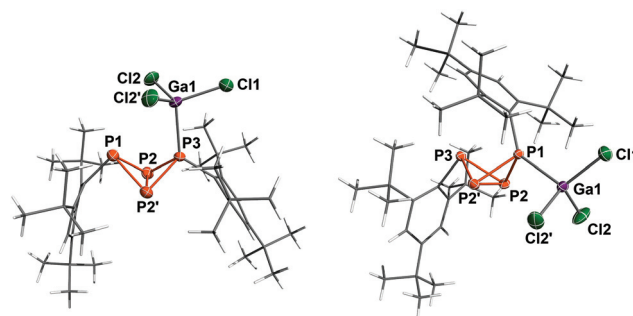


Fig. 5 Molecular structure of $5\text{a}\cdot\text{GaCl}_3$ (left) and $5\text{b}\cdot\text{GaCl}_3$ (right). Ellipsoids are set at 50% probability (173 K). Selected bond lengths [\AA] and angles [$^\circ$]: $5\text{a}\cdot\text{GaCl}_3$ P1–P2 2.228(1), P2–P3 2.1805(9), P2–P2′ 2.200(1), Ga1–P3 2.4206(8), P1–P2–P2′–P3 98.96(3); $5\text{b}\cdot\text{GaCl}_3$ P1–P2 2.1854(5), P2–P3 2.2365(6), P2–P2′ 2.2074(8), P1–Ga1 2.3966(5); P1–P2–P2′–P3 102.64(2).



The transannular bond (P2–P2': 2.200(1) Å), on the other hand, is noticeably longer than in **5a** or **5b**. In comparison with the sum of covalent radii (2.35 Å),⁵⁰ the P3–Ga1 bond is somewhat elongated (2.4206(8) Å), most likely due to Pauli repulsion between the *ortho-tert*-butyl groups of the neighbouring Mes* moiety and the GaCl₃ unit. The bonding angles at the coordinating P atom (P3) are considerably flattened, so one of the Mes* substituents is bent further outwards. Moreover, the fold angle of the bicyclic system amounts to 98.69(3)° and is therefore 3° larger than in **5a**.

Compound **5b**·GaCl₃ crystallized in the monoclinic space group *P*₂₁/*m* either as toluene or CH₂Cl₂ solvate with similar cell parameters and molecular structure. Hence only the toluene solvate shall be discussed in the following; again, the bonds between the bridgehead atoms and the coordinating P atom (P2–P1 and P2'–P1: 2.1854(5) Å) are shortened in comparison with **5b**, whereas the transannular bond is somewhat widened (P2–P2': 2.2074(8) Å). The P–Ga bond length (2.3699(5) Å) is shorter than in **5a**·GaCl₃ and compares well to the sum of covalent radii. The angle of the P3–P2–P2' plane to the P3–C13 bond axis (96.92(6)°) is about 8° smaller than in **5b**, so the Mes* substituent moves closer to the bicyclic scaffold. In contrast to **5a**·GaCl₃, the fold angle of **5b**·GaCl₃ lessens with respect to the free bicyclic tetraphosphane by 3° (102.64(2)°).

In both isomers, the substitution pattern at the bicyclic P₄ scaffold is comparable to the borane adduct TerP₄Me·B(C₆F₅)₃ (23-B(C₆F₅)₃) or the bicyclic phosphino-phosphonium cation [Mes*P₄(Cl)Mes*]⁺ (**29**).^{12,45}

Computational study

NBO analysis revealed that the partial charges of the P atoms in **5a**·GaCl₃ and **5b**·GaCl₃ (bridgehead P: +0.10e, coordinating P: +0.24e, non-coordinating P: +0.31e) changed only slightly in

comparison with **5a** and **5b** (bridgehead P: 0.00e, P(Mes*): +0.27e), implying a similar distribution of the electron density. Inspection of the molecular orbitals (MOs) showed that the principal bonding orbitals of the P₄ scaffold remained intact. According to the electron localization function (ELF), the P–Ga bond is strongly polarized towards phosphorus (Fig. 6). The natural Lewis description actually suggests a non-bonding situation with a lone pair (LP) at phosphorus and an empty p-type orbital at Ga, with low P–Ga bond indices (NLMO: 0.34, Wiberg: 0.50). However, a second order perturbation analysis revealed a strong donor–acceptor interaction between the LP at P and the empty p-type orbital at Ga (**5a**·GaCl₃: 530.5 kJ mol⁻¹, **5b**·GaCl₃: 555.2 kJ mol⁻¹); thus, the P–Ga bonding can be described as a classical dative bond. At the PBE0/aug-cc-pVDZ level of theory, the *exo-exo* isomer **5a**·GaCl₃ was calculated to be energetically favoured by 8.03 kJ mol⁻¹ (Δ*G*²⁹⁸); therefore the energetic difference between *exo-exo* and *endo-exo*-isomer slightly decreased in comparison to non-coordinating **5a** and **5b**. This is reflected in the calculated Gibbs energies (Δ*RG*²⁹⁸) for the association of **5a** or **5b** and GaCl₃, which amount to –46.7 kJ mol⁻¹ or –47.4 kJ mol⁻¹, respectively.

Equilibrium between **5a**·GaCl₃ and **5b**·GaCl₃

Similar to the free phosphanes, the GaCl₃ adducts **5a**·GaCl₃ and **5b**·GaCl₃ were found to interconvert slowly in solution at ambient temperature. Over a period of several weeks, the establishment of equilibrium was monitored by ³¹P NMR spectroscopy. Interestingly, the equilibrium constant was found to be 1.6(2), thus the amount of *endo-exo* isomer at equilibrium was significantly higher than in case of the free phosphanes. This is in agreement with the calculations, although the actual effect is even more pronounced. According to the experiment, the energetic difference between both isomers is just 1.2(4) kJ mol⁻¹ (Δ*G*).

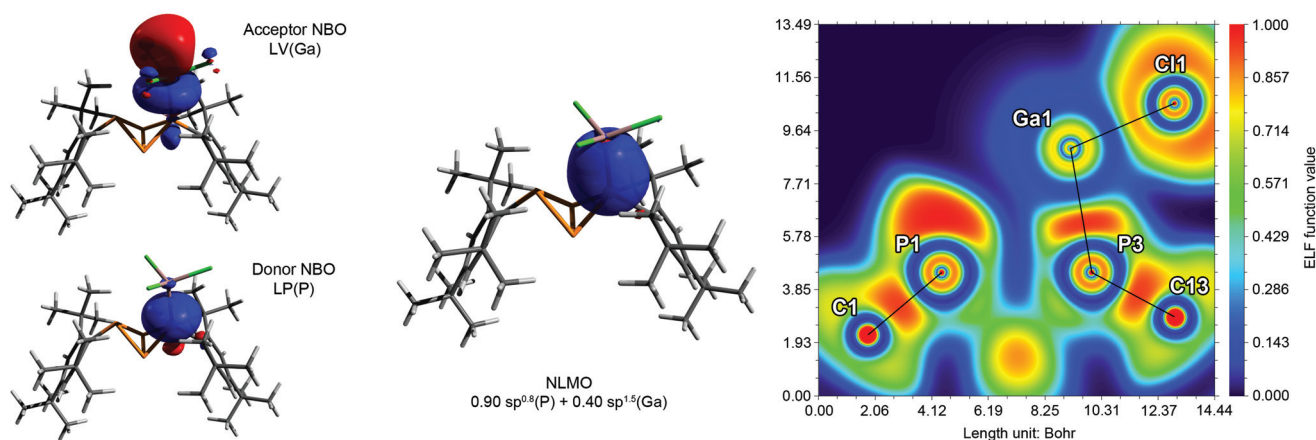
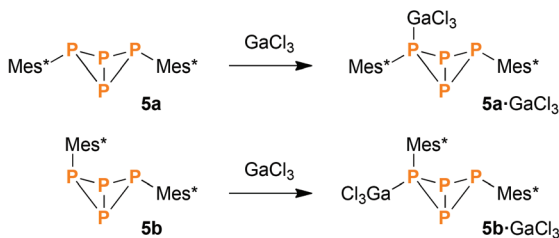


Fig. 6 Exemplary description of the bonding in **5a**·GaCl₃. Left: Donor and acceptor NBOs describing the dative bond from P to Ga. Middle: P–Ga bond in the natural localized MO (NLMO) picture. Right: Electron localization function (ELF) depicted in a plane through atoms P1, P3 and Ga1. The P–Ga and Ga–Cl bonds are strongly polarized and exhibit partly ionic character. The deformation of the LP at P1 is due to Pauli repulsion with Cl2 and Cl2' (out of plane).





Scheme 8 Rational synthesis of **5a**·GaCl₃ and **5b**·GaCl₃.

Direct synthesis of Mes*P₄Mes*·GaCl₃ (5·GaCl₃)

As expected, **5a**·GaCl₃ and **5b**·GaCl₃ could be synthesized from pure **5a** and **5b** by treatment with equimolar amounts of GaCl₃. Mixing solutions of both reactants and subsequent evaporation of the solvent led to quantitative yield of the respective GaCl₃ adduct (Scheme 8). Due to the short reaction time (*ca.* 5 min), isomerization could be avoided.

Conclusions

We present new insights into the chemistry of tetraphosphacyclo[1.1.0]butanes: various synthetic approaches were investigated, involving precursor molecules with one, two or four phosphorus atoms. Thereby, the *endo-exo* isomer of Mes*P₄Mes* (**5b**) could be fully characterized for the first time and the interconversion of both isomers could be studied in detail. Furthermore, the hitherto unknown GaCl₃ adducts of both *exo-exo* and *endo-exo* isomer (**5a**·GaCl₃, **5b**·GaCl₃) were thoroughly investigated, including experimental assessment of dynamic behaviour in solution and computational studies of the bonding situation.

Due to isomerization in solution, it is difficult to obtain either isomer purely; ideally, synthetic strategies should be designed to (a) minimize the reaction time and (b) take place at low temperatures to avoid thermodynamic equilibrium.

Experimental

All manipulations were carried out under oxygen- and moisture-free conditions under argon using standard Schlenk or Drybox techniques. All starting materials containing the Mes* moiety were synthesized according to modified literature procedures; other reactants and solvents were obtained from commercial sources and thoroughly dried. Detailed information concerning experimental procedures, data acquisition and processing, as well as purification of chemicals can be found in the ESI.†

Synthesis of **5a**

A solution of [ClP(μ-PMes*)]₂ (206 mg, 0.30 mmol) in THF (3 mL) is added to magnesium turnings (10 mg, 0.42 mmol) and stirred at ambient temperature overnight. Subsequently,

the solvent is removed *in vacuo* and the solid residue is extracted with *n*-hexane (5 mL). After filtration, the filtrate is concentrated and stored at 5 °C, resulting in crystallization of colourless *exo-exo*-Mes*P₄Mes*. Yield: 135 mg (0.22 mmol, 73%). CHN calc. (found) in %: C 70.34 (70.32), H 9.51 (9.35). ³¹P{¹H} NMR (CD₂Cl₂, 121.5 MHz): δ = -273.2 (t, ¹J_{AX}(³¹P,³¹P) = -177 Hz, 2 P, P_{bridgehead}), -128.3 (t, ¹J_{AX}(³¹P,³¹P) = -177 Hz, 2 P, PMes*). ¹H NMR (CD₂Cl₂, 300.1 MHz): δ = 1.19 (s, 18 H, *p-t*-Bu), 1.63 (s, 36 H, *o-t*-Bu), 7.07 (m, 4 H, *m*-H). Raman (633 nm, 15 s, 10 scans, cm⁻¹): $\tilde{\nu}$ = 3075 (1), 2963 (2), 2924 (2), 2903 (3), 2863 (1), 2777 (1), 2709 (1), 1588 (1), 1527 (1), 1473 (1), 1461 (1), 1442 (1), 1396 (1), 1365 (1), 1292 (1), 1281 (1), 1241 (1), 1208 (1), 1201 (1), 1175 (1), 1152 (1), 1128 (1), 1033 (2), 1020 (1), 934 (1), 921 (1), 891 (1), 822 (2), 775 (1), 637 (1), 592 (10), 563 (1), 490 (1), 475 (1), 463 (1), 447 (1), 432 (1), 412 (1), 387 (1), 351 (4), 294 (1), 259 (2), 211 (1), 191 (1), 177 (1), 136 (1), 125 (2), 107 (3), 86 (3).

Synthesis of **5b**

Method 1: HOTf (180 mg, 1.12 mmol) is condensed onto a degassed solution of Mes*PPN(i-Pr)₂ (489 mg, 1.12 mmol) in CH₂Cl₂ (8 mL) at -196 °C. The reaction mixture is slowly warmed to ambient temperature overnight. The solvent is removed *in vacuo* and the residue is extracted with *n*-hexane (5 mL). Insoluble solids are filtered off. The clear orange filtrate is concentrated, resulting in crystallization of a mixture of *exo-exo* and *endo-exo*-Mes*P₄Mes* (1 : 4 ratio). Yield: 120 mg (0.20 mmol, 35%). Re-crystallization yields pure *endo-exo*-Mes*P₄Mes*. Method 2: A mixture of [ClP(μ-PMes*)]₂ (835 mg, 1.22 mmol) and Me₄C₃N₂ (302 mg, 2.44 mmol) is dissolved in CH₂Cl₂ (10 mL) at -80 °C, resulting in a dark red solution. The reaction vessel is warmed to ambient temperature over a period of one hour, whereupon the solution is concentrated and stored at 5 °C, resulting in the crystallization of orange, block shaped crystals that were identified as Mes*PPMes*. The supernatant is separated and concentrated. Storage at 5 °C affords large colourless crystals of *endo-exo*-Mes*P₄Mes*. Yield: 105 mg (0.17 mmol, 14%). CHN calc. (found) in %: C 70.34 (70.04), H 9.51 (9.47). ³¹P{¹H} NMR (CD₂Cl₂, 121.5 MHz): δ = -220.4 (dd, ¹J_{AX}(³¹P,³¹P) = -234 Hz, ¹J_{AM}(³¹P,³¹P) = -213 Hz, 2 P, P_{bh}), -94.8 (td, ¹J_{AM}(³¹P,³¹P) = -213 Hz, ²J_{MX}(³¹P,³¹P) = -27 Hz, 1 P, P_{exo}), -54.7 (td, ¹J_{AX}(³¹P,³¹P) = -234 Hz, ²J_{MX}(³¹P,³¹P) = -27 Hz, 1 P, P_{endo}). ¹H NMR (CD₂Cl₂, 300.1 MHz): δ = 1.19 (s, 9 H, *exo*-Mes*, *p-t*-Bu), 1.30 (s, 9 H, *endo*-Mes*, *p-t*-Bu), 1.49 (s, 18 H, *exo*-Mes*, *o-t*-Bu), 1.66 (m, 18 H, *endo*-Mes*, *o-t*-Bu), 7.02 (m, 2 H, *exo*-Mes*, *m*-H), 7.05 (m, 2 H, *endo*-Mes*, *m*-H). Raman (633 nm, 15 s, 20 scans, cm⁻¹): $\tilde{\nu}$ = 3168 (1), 3074 (1), 3055 (1), 2959 (4), 2924 (4), 2902 (5), 2865 (2), 2778 (1), 2712 (1), 1584 (3), 1520 (1), 1475 (1), 1466 (2), 1444 (2), 1399 (1), 1392 (1), 1360 (1), 1283 (2), 1251 (1), 1203 (1), 1186 (1), 1182 (1), 1173 (1), 1148 (1), 1132 (2), 1033 (3), 1017 (2), 932 (1), 919 (2), 897 (1), 877 (1), 822 (4), 772 (1), 744 (1), 740 (1), 647 (1), 638 (1), 591 (2), 584 (2), 568 (10), 500 (2), 490 (1), 473 (1), 435 (1), 419 (2), 412 (2), 381 (4), 363 (2), 330 (1),



309 (1), 295 (1), 256 (2), 200 (1), 177 (1), 143 (4), 139 (3), 103 (7), 78 (6).

Synthesis of 5a-GaCl₃

Method 1: Solutions of PCl₃ (130 mg, 0.95 mmol) and GaCl₃ (168 mg, 0.95 mmol) in *n*-hexane (2 mL each) are added consecutively to a stirred solution of Mes*P(SiMe₃)₂ (403 mg, 0.95 mmol) in *n*-hexane (5 mL) at -80 °C. The mixture is warmed to ambient temperature, resulting in the deposition of an intensively red oil. Overnight, large colourless crystals grow at the phase interface at ambient temperature. Yield: 45 mg (0.07 mmol, 8%). Method 2: A solution of GaCl₃ (10 mg, 0.057 mmol) in CH₂Cl₂ (1 mL) is added to a solution of *exo-exo*-Mes*P₄Mes* (35 mg, 0.057 mmol) in CH₂Cl₂ (2 mL). The mixture is stirred for ten minutes and the solvent is removed *in vacuo*, yielding an analytically pure powder of *exo-exo*-Mes*P₄Mes*.GaCl₃. Yield: 30 mg (0.038 mmol, 67%). CHN calc. (found) in %: C 54.68 (53.97), H 7.39 (6.89). ³¹P{¹H} NMR (CD₂Cl₂, 121.5 MHz): δ = -246.4 (t, ¹J_{AX}(³¹P,³¹P) = -198 Hz, 2 P, P_{bridgehead}), -97.1 (broad, 2 P, PMes*). ³¹P{¹H} NMR (CD₂Cl₂, 121.5 MHz, -80 °C): δ = -248.1 (dd, ¹J_{AM}(³¹P,³¹P) = -182 Hz, ¹J_{AX}(³¹P,³¹P) = -216 Hz, 2 P, P_{bridgehead}), -114.0 (dt, ¹J_{AM}(³¹P,³¹P) = -182 Hz, ²J_{MX}(³¹P,³¹P) = +225 Hz, 1 P, PMes*), -74.8 (dt, ¹J_{AX}(³¹P,³¹P) = -216 Hz, ²J_{MX}(³¹P,³¹P) = +225 Hz, 1 P, P(Ga)Mes*). ¹H NMR (CD₂Cl₂, 300.1 MHz): δ = 1.20 (s, 18 H, Mes*, *p*-*t*-Bu), 1.68 (s, 36 H, *o*-*t*-Bu), 7.24 (s, 4 H, *m*-H). Raman (785 nm, 30 s, 4 scans, cm⁻¹): $\tilde{\nu}$ = 3064 (1), 2976 (1), 2960 (2), 2928 (2), 2904 (3), 2869 (1), 2786 (1), 2717 (1), 1593 (3), 1582 (2), 1536 (1), 1477 (2), 1465 (3), 1443 (2), 1393 (2), 1362 (1), 1284 (3), 1250 (2), 1208 (2), 1176 (3), 1031 (3), 1025 (3), 1016 (2), 920 (2), 891 (1), 819 (5), 772 (1), 747 (1), 638 (1), 613 (3), 597 (9), 561 (4), 502 (1), 497 (1), 480 (2), 470 (1), 451 (2), 436 (2), 406 (3), 395 (4), 385 (3), 366 (4), 343 (10), 294 (2), 260 (4).

Synthesis of 5b-GaCl₃

Method 1: A solution of PCl₃ (131 mg, 0.95 mmol) in CH₂Cl₂ (1 mL) and a solution of GaCl₃ (168 mg, 0.95 mmol) in CH₂Cl₂/toluene (1:1, 2 mL) are added consecutively to a stirred solution of Mes*P(SiMe₃)₂ (403 mg, 0.95 mmol) in CH₂Cl₂ (5 mL) at -80 °C. The mixture is warmed to -50 °C, whereupon the solution turns red. After further stirring at -50 °C for two hours, the solution is concentrated and subsequently warmed to ambient temperature overnight, resulting in crystallization of *endo-exo*-Mes*P₄Mes*.GaCl₃ (CH₂Cl₂ solvate) in colourless, block-shaped crystals. The solvent is removed by drying *in vacuo*. Yield: 50 mg (0.08 mmol, 9%). Method 2: A solution of GaCl₃ (15 mg, 0.085 mmol) in CH₂Cl₂ (1 mL) is added to a solution of *endo-exo*-Mes*P₄Mes* (52 mg, 0.085 mmol) in CH₂Cl₂ (2 mL). The mixture is stirred for ten minutes and the solvent is removed *in vacuo*, yielding an analytically pure powder of *endo-exo*-Mes*P₄Mes*.GaCl₃. Yield: 51 mg (0.064 mmol, 75%). CHN calc. (found) in %: C 54.68 (54.15), H 7.39 (7.15). ³¹P{¹H} NMR (CD₂Cl₂, 121.5 MHz): δ = -224.5 (dd, ¹J_{AM}(³¹P,³¹P) = -192 Hz, ¹J_{AX}(³¹P,³¹P) = -249 Hz, 2 P, P_{bridgehead}), -114.5 (td, ¹J_{AM}(³¹P,³¹P) = -192 Hz, ¹J_{MX}(³¹P,³¹P) = +24 Hz, 1 P, P_{exo}), -50.0 (broad, 1 P, P_{endo}). ¹H NMR (CD₂Cl₂,

300.1 MHz): δ = 1.21 (s, 9 H, *exo*-Mes*, *p*-*t*-Bu), 1.33 (s, 9 H, *endo*-Mes*, *p*-*t*-Bu), 1.49 (s, 18 H, *exo*-Mes*, *o*-*t*-Bu), 1.70 (m 18 H, *endo*-Mes*, *o*-*t*-Bu), 7.11 (d, *J*(¹H,³¹P) = 1.9 Hz, 2 H, *exo*-Mes*, *m*-H), 7.32 (d, *J*(¹H,³¹P) = 5.0 Hz, 2 H, *endo*-Mes*, *m*-H). Raman (633 nm, 10 s, 4 scans, cm⁻¹): $\tilde{\nu}$ = 3055 (2), 3035 (1), 2973 (5), 2966 (6), 2905 (7), 2866 (3), 2782 (1), 2714 (1), 1603 (1), 1582 (4), 1525 (1), 1463 (2), 1441 (2), 1394 (1), 1362 (1), 1284 (2), 1208 (2), 1173 (1), 1133 (2), 1029 (3), 1011 (2), 1002 (3), 924 (1), 818 (3), 784 (2), 741 (2), 618 (3), 567 (7), 518 (1), 508 (1), 438 (3), 407 (2), 391 (2), 372 (2), 348 (10), 302 (1), 258 (3), 213 (1).

Detailed analytical data for all compounds, including low temperature NMR data, can be found in the ESI.†

Acknowledgements

We thank Dr Dirk Michalik for the measurement of low-temperature NMR spectra, Dr Alexander Hinz for a gift of tetramethylimidazolyliene, and the Fonds der Chemischen Industrie (JB) as well as the Deutsche Forschungsgemeinschaft (SCHU 1170/11-1) for financial support.

Notes and references

- 1 L. Stahl, *Coord. Chem. Rev.*, 2000, **210**, 203–250.
- 2 M. S. Balakrishna, D. J. Eisler and T. Chivers, *Chem. Soc. Rev.*, 2007, **36**, 650–664.
- 3 G. He, O. Shynkaruk, M. W. Lui and E. Rivard, *Chem. Rev.*, 2014, **114**, 7815–7880.
- 4 O. J. Scherer, *Comments Inorg. Chem.*, 1987, **6**, 1–22.
- 5 M. Baudler and K. Glinka, *Chem. Rev.*, 1993, **93**, 1623–1667.
- 6 M. Scheer, G. Balázs and A. Seitz, *Chem. Rev.*, 2010, **110**, 4236–4256.
- 7 B. M. Cossairt, N. A. Piro and C. C. Cummins, *Chem. Rev.*, 2010, **110**, 4164–4177.
- 8 N. A. Giffin and J. D. Masuda, *Coord. Chem. Rev.*, 2011, **255**, 1342–1359.
- 9 J. D. Masuda, W. W. Schoeller, B. Donnadiou and G. Bertrand, *Angew. Chem., Int. Ed.*, 2007, **46**, 7052–7055.
- 10 S. Heintl, S. Reisinger, C. Schwarzmaier, M. Bodensteiner and M. Scheer, *Angew. Chem., Int. Ed.*, 2014, **53**, 7639–7642.
- 11 S. Heintl and M. Scheer, *Chem. Sci.*, 2014, **5**, 3221–3225.
- 12 J. E. Borger, A. W. Ehlers, M. Lutz, J. C. Slootweg and K. Lammertsma, *Angew. Chem., Int. Ed.*, 2014, **53**, 12836–12839.
- 13 E. Niecke, R. Rieger and B. Krebs, *Angew. Chem., Int. Ed. Engl.*, 1982, **21**, 544–545.
- 14 A. H. Cowley, P. C. Knueppel and C. M. Nunn, *Organometallics*, 1989, **8**, 2490–2492.
- 15 H.-P. Schrödel, H. Nöth, M. Schmidt-Amelunxen, W. W. Schoeller and A. Schmidpeter, *Chem. Ber.*, 1997, **130**, 1801–1805.
- 16 P. Jutzi and T. Wippermann, *J. Organomet. Chem.*, 1985, **287**, C5–C7.



- 17 P. Jutzi and U. Meyer, *J. Organomet. Chem.*, 1987, **333**, C18–C20.
- 18 P. Jutzi, R. Kroos, A. Müller and M. Penk, *Angew. Chem.*, 1989, **101**, 628–629.
- 19 P. Jutzi and N. Brusdeilins, *Z. Anorg. Allg. Chem.*, 1994, **620**, 1375–1380.
- 20 L. Weber, G. Meine, R. Boese and N. Niederprün, *Z. Naturforsch., B: Chem. Sci.*, 1988, **43**, 415–721.
- 21 V. D. Romanenko, V. L. Rudzevich, E. B. Rusanov, A. N. Chernega, A. Senio, J.-M. Sotiropoulos, G. Pfister-Guilouzo and M. Sanchez, *J. Chem. Soc., Chem. Commun.*, 1995, 1383–1385.
- 22 R. Riedel, H.-D. Hausen and E. Fluck, *Angew. Chem., Int. Ed. Engl.*, 1985, **24**, 1056–1057.
- 23 E. Fluck, R. Riedel, H.-D. Hausen and G. Heckmann, *Z. Anorg. Allg. Chem.*, 1987, **551**, 85–94.
- 24 M. Baudler, C. Adamek, S. Opiela, H. Budzikiewicz and D. Ouzounis, *Angew. Chem., Int. Ed. Engl.*, 1988, **27**, 1059–1061.
- 25 M. Baudler and B. Wingert, *Z. Anorg. Allg. Chem.*, 1992, **611**, 50–55.
- 26 M. B. Power and A. R. Barron, *Angew. Chem., Int. Ed. Engl.*, 1991, **30**, 1353–1354.
- 27 A. R. Fox, R. J. Wright, E. Rivard and P. P. Power, *Angew. Chem., Int. Ed.*, 2005, **44**, 7729–7733.
- 28 I. Krossing and I. Raabe, *Angew. Chem., Int. Ed.*, 2001, **40**, 4406–4409.
- 29 M. H. Holthausen and J. J. Weigand, *J. Am. Chem. Soc.*, 2009, **131**, 14210–14211.
- 30 J. J. Weigand, M. H. Holthausen and R. Fröhlich, *Angew. Chem., Int. Ed.*, 2009, **48**, 295–298.
- 31 D. Holschumacher, T. Bannenberg, K. Ibrom, C. G. Daniliuc, P. G. Jones and M. Tamm, *Dalton Trans.*, 2010, **39**, 10590–10592.
- 32 S. Khan, R. Michel, J. M. Dieterich, R. A. Mata, H. W. Roesky, J. P. Demers, A. Lange and D. Stalke, *J. Am. Chem. Soc.*, 2011, **133**, 17889–17894.
- 33 J.-P. Bezombes, P. B. Hitchcock, M. F. Lappert and J. E. Nycz, *Dalton Trans.*, 2004, 499–501.
- 34 N. A. Giffin, A. D. Hendsbee, T. L. Roemmele, M. D. Lumsden, C. C. Pye and J. D. Masuda, *Inorg. Chem.*, 2012, **51**, 11837–11850.
- 35 C. Rotter, M. Schuster and K. Karaghiosoff, *Inorg. Chem.*, 2009, **48**, 7531–7533.
- 36 A. Sidiropoulos, B. Osborne, A. N. Simonov, D. Dange, A. M. Bond, A. Stasch and C. Jones, *Dalton Trans.*, 2014, **43**, 14858–14864.
- 37 M. Baudler and B. Wingert, *Z. Anorg. Allg. Chem.*, 1993, **619**, 1977–1983.
- 38 P. Jutzi, N. Brusdeilins, H.-G. Stammer and B. Neumann, *Chem. Ber.*, 1994, **127**, 997–1001.
- 39 O. J. Scherer, G. Schwarz and G. Wolmershäuser, *Z. Anorg. Allg. Chem.*, 1996, **622**, 951–957.
- 40 O. J. Scherer, T. Hilt and G. Wolmershäuser, *Organometallics*, 1998, **17**, 4110–4112.
- 41 P. Barbaro, C. Bazzicalupi, M. Peruzzini, S. Seniori Costantini and P. Stoppioni, *Angew. Chem., Int. Ed.*, 2012, **51**, 8628–8631.
- 42 S. Pelties, D. Herrmann, B. de Bruin, F. Hartl and R. Wolf, *Chem. Commun.*, 2014, 7014–7016.
- 43 N. Wiberg, A. Wörner, H.-W. Lerner and K. Karaghiosoff, *Z. Naturforsch., B: Chem. Sci.*, 2002, **57**, 1027–1035.
- 44 M. Donath, E. Conrad, P. Jerabek, G. Frenking, R. Fröhlich, N. Burford and J. J. Weigand, *Angew. Chem., Int. Ed.*, 2012, **51**, 2964–2967.
- 45 J. Bresien, K. Faust, A. Schulz and A. Villinger, *Angew. Chem., Int. Ed.*, 2015, **54**, 6926–6930.
- 46 J. Bresien, C. Hering, A. Schulz and A. Villinger, *Chem. – Eur. J.*, 2014, **20**, 12607–12615.
- 47 M. Yoshifuji, I. Shima, N. Inamoto, K. Hirotsu and T. Higuchi, *J. Am. Chem. Soc.*, 1981, **103**, 4587–4589.
- 48 M. Yoshifuji, I. Shima, N. Inamoto, K. Hirotsu and T. Higuchi, *J. Am. Chem. Soc.*, 1982, **104**, 6167.
- 49 Y. M. Bosworth, R. J. H. Clark and D. M. Rippon, *J. Mol. Spectrosc.*, 1973, **46**, 240–255.
- 50 P. Pyykkö and M. Atsumi, *Chem. – Eur. J.*, 2009, **15**, 12770–12779.
- 51 E. D. Glendening, J. K. Badenhop, A. E. Reed, J. E. Carpenter, J. A. Bohmann, C. M. Morales, C. R. Landis and F. Weinhold, *NBO 6.0*, Theoretical Chemistry Institute, University of Wisconsin, Madison, 2013.
- 52 T. Beweries, R. Kuzora, U. Rosenthal, A. Schulz and A. Villinger, *Angew. Chem., Int. Ed.*, 2011, **50**, 8974–8978.
- 53 H. Schmidbaur, A. Shiotani and H. F. Klein, *J. Am. Chem. Soc.*, 1971, **93**, 1555–1557.
- 54 J. B. DeRoos and J. P. Oliver, *J. Am. Chem. Soc.*, 1967, **89**, 3970–3977.



7 Appendix

7.1 $[\text{ClP}(\mu\text{-PMes}^*)]_2$ – A Versatile Reagent in Phosphorus Chemistry

Jonas Bresien, Axel Schulz, and Alexander Villinger

Phosphorus, Sulfur and Silicon **2016**, accepted.

DOI: 10.1080/10426507.2015.1128915

This article contains an overview of the reactivity of $[\text{ClP}(\mu\text{-PMes}^*)]_2$ and will be published as part of the IRIS-14 (International Symposium on Inorganic Ring Systems) proceedings. The manuscript was written by me, my own contribution amounts to approx. 90 %.

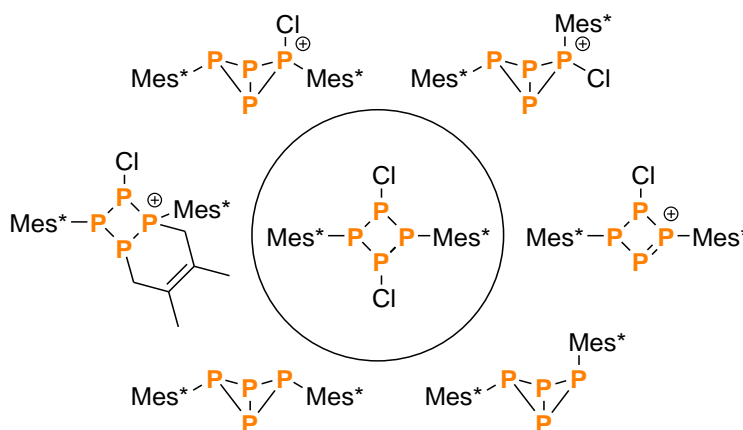
[CIP(μ -PMes*)]₂ – A Versatile Reagent in Phosphorus Chemistry

Jonas Bresien,¹ Axel Schulz,^{1,2*} Alexander Villinger¹

¹ Institut für Chemie, Universität Rostock, Albert-Einstein-Straße 3a, 18059 Rostock, Germany

² Leibniz-Institut für Katalyse e.V. an der Universität Rostock, Albert-Einstein-Straße 29a, 18059 Rostock, Germany

GRAPHICAL ABSTRACT



Abstract The synthesis and some key reactions of the cyclotetraphosphane [CIP(μ -PMes*)]₂ (**2**, Mes* = 2,4,6-tri-*tert*-butylphenyl) with Lewis acids and reducing agents are discussed. All products were fully characterized, including single crystal X-ray diffraction, spectroscopic methods as well as computational studies.

Keywords Ring systems; phosphorus chemistry; *cyclo*-phosphanes; ³¹P NMR spectroscopy; DFT calculations

Received xx yyyy 2015; accepted xx yyyy 2015

The authors wish to thank the Fonds der Chemischen Industrie (scholarship for JB) and the Deutsche Forschungsgemeinschaft (SCHU 1170/11-1) for financial support.

Address correspondence to Axel Schulz, axel.schulz@uni-rostock.de

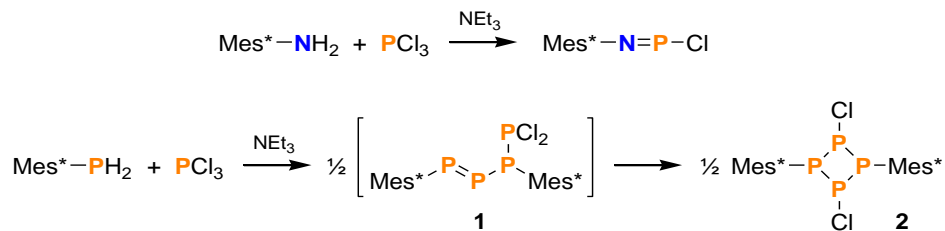
INTRODUCTION

Ring systems composed of group 15 elements (pnictogens, Pn) are an interesting and widely investigated field of main group chemistry.^{1–3} Especially, phosphorus based ring systems have received increasing attention,^{4,5} since various types of mono- and polycyclic phosphanes were prepared by direct activation of white phosphorus (P₄).^{6–13} However, selective functionalization of such ring systems was not studied in detail, which is why we set out to prepare a suitable functionalized P₄ precursor and investigate its reactivity. In analogy to the well explored chemistry of dichloro-*cyclo*-diphosphadiazanes,^{1–3} the homologous dichloro-*cyclo*-tetraphosphanes seemed a worthwhile target for further chemistry. Known examples of such halogen substituted *cyclo*-tetraphosphanes comprised [ClP(μ -PSi(*t*-Bu)₃)]₂ and [ClP(μ -PSi(*t*-Bu)₃)]₂; yet we found their preparation unsuitable for synthetic scale.^{14,15}

RESULTS AND DISCUSSION

Preparation of [ClP(μ -PMes*)]₂

In analogy to the synthesis of Mes**N*PCl (Scheme 1, top; Mes* = 2,4,6-tri-*tert*-butylphenyl),¹⁶ treatment of Mes**P*H₂ with PCl₃ in the presence of NEt₃ led to P–P coupling under elimination of [HNEt₃]Cl. In the first step, the tetraphosphene Mes**P*=P–P(Mes*)PCl₂ (**1**) was formed, which underwent rearrangement to [ClP(μ -PMes*)]₂ (**2**) in polar solvents (Scheme 1, bottom).¹⁷ After optimization of the reaction conditions, compound **2** could be prepared in 50–60 % yield (5 g scale), which facilitated the investigation of its reactivity.¹⁸



Scheme 1 Top: Synthesis of Mes**N*PCl. Bottom: Synthesis of [ClP(μ -PMes*)]₂ (**2**).

Compound **2** was characterized by an A_2X_2 spin system in the ^{31}P NMR spectrum ($\delta_{\text{exptl}} = -8.1, +131.1$ ppm; $\delta_{\text{calcd}} = -1.6, 119.9$ ppm). Its solid state structure was determined by single crystal X-ray diffraction. The four membered ring system adopts a puckered conformation, all substituents are arranged in the equatorial position (Figure 1). The experimental structural data correspond nicely with calculated structural parameters (PBE0/6-31g(d,p) level of theory).¹⁷

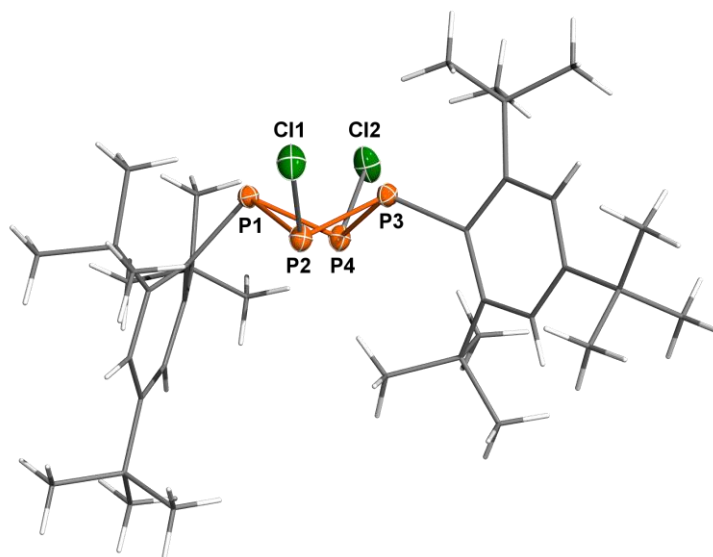
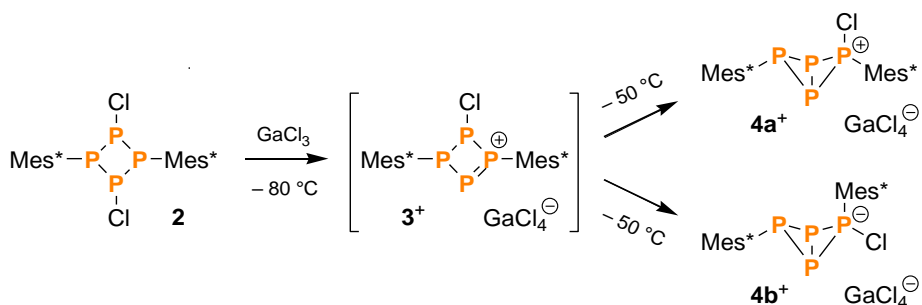


Figure 1 Molecular structure of **2** in the crystal ($P2_1/c$). Ellipsoids are set at 50% probability (173 K). Selected bond lengths [Å] and angles [°]: P1–P2 2.2731(5), P1–P4 2.2596(5), P2–P3 2.1905(5), P2–Cl1 2.0967(5), P3–P4 2.2026(5), P4–Cl2 2.1061(6); P1–P2–P3 80.54(2), P1–P2–Cl1 106.45(2), P3–P2–Cl1 97.97(2), P2–P3–P4 84.65(2), P3–P4–P1 80.58(2), P3–P4–Cl2 97.32(2), P1–P4–Cl2 104.47(2); P1–P2–P4–P3 119.45(3), Cl1–P2–P4–Cl2 $-1.06(5)$ Cl1–P1–P3–C19 $-17.9(1)$.

Reaction with GaCl_3

When **2** was treated with GaCl_3 at -80 °C, the intermediate formation of a highly reactive tetraphosphenium cation (**3**⁺) could be detected by *in situ* ^{31}P NMR spectroscopy (Scheme 2).¹⁸ Upon warming to -50 °C, a formal 1,2-Cl shift was observed, resulting in the formation of two isomers of an unprecedented bicyclic triphosphino-phosphonium cation (**4**⁺; Figure 2, left).



Scheme 2 The reaction of **2** with GaCl_3 leads to the highly reactive intermediate **3⁺**, which rearranges to the bicyclic cation **4⁺**. The latter is observed as *exo-exo* (**4a⁺**) and *endo-exo* isomer (**4b⁺**).

In the ^{31}P NMR spectrum, both isomers of **4⁺** were characterized by A_2MX patterns (**4a⁺**: $\delta_{\text{exptl}} = -214.5, -89.5, +51.2$ ppm; $\delta_{\text{calcd}} = -220.3, -103.8, +24.6$ ppm; **4b⁺**: $\delta_{\text{exptl}} = -226.4, -123.6, +9.0$ ppm; $\delta_{\text{calcd}} = -227.8, -135.7, -12.0$ ppm). The molecular structure of **4a**[GaCl_4] was elucidated by single crystal X-ray diffraction.¹⁸ The bicyclic P_4 scaffold adopts a butterfly conformation with a fold angle of 102° , which is comparable to other bicyclic tetraphosphanes.^{13,19–25} According to NBO analysis,²⁶ the positive charge is mostly localized at the formal phosphonium centre ($+0.76 e$), while the whole P_4 scaffold bears a positive charge of $+1.37 e$.

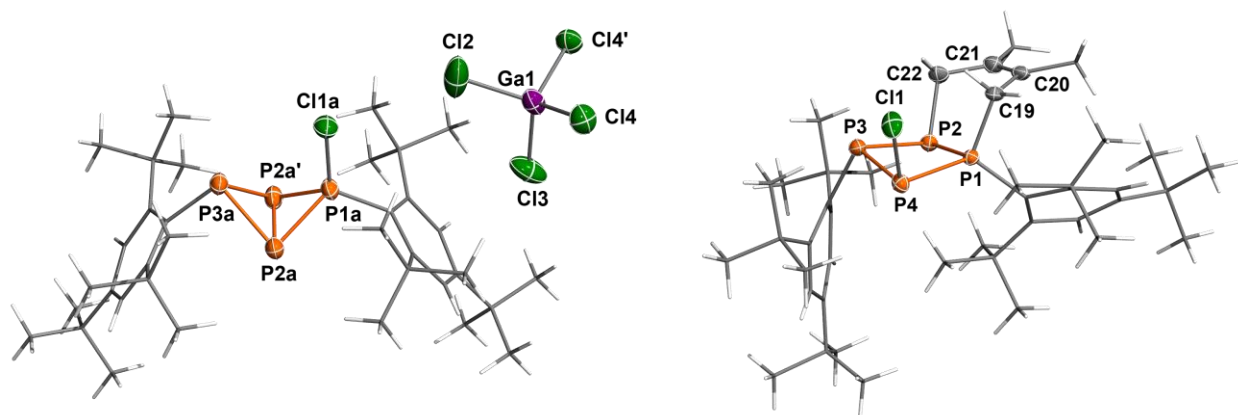


Figure 2 Molecular structure of **4**[GaCl_4] (left) and **5⁺** (right) in the crystal. Ellipsoids are set at 50% probability (173 K). Selected bond lengths [\AA] and angles [$^\circ$]: **4⁺** P1a–P2a 2.150(2), P1a–Cl1a 2.009(2), P2a–P2a' 2.244(2), P2a–P3a 2.244(2); Cl1a–P1a–P2a 117.65(7), Cl1–P1a–Cl1a 118.7(2), P2a'–P1a–P2a 62.91(7), P1a–P2a–P2a' 58.55(3), P3a–P2a–P2a' 59.99(3), P1a–P2a–P3a 83.60(6), P2a'–P3a–P2a 60.02(7); P1a–P2a–P2a'–P3a $-101.68(3)$; **5⁺** P1–P2 2.195(1), P1–C19 1.846(3), C19–C20 1.514(4), C20–C21 1.334(4), C21–C22 1.500(4), P2–C22 1.871(3), P4–C11 2.068(1); P2–P1–P4 91.78(4), C19–P1–P2 102.3(1), C19–P1–P4 116.1(1); P1–P2–P4–P3 159.03(1).

Received xx yyyy 2015; accepted xx yyyy 2015

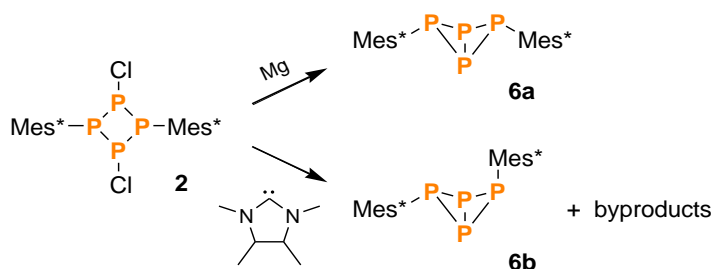
The authors wish to thank the Fonds der Chemischen Industrie (scholarship for JB) and the Deutsche Forschungsgemeinschaft (SCHU 1170/11-1) for financial support.

Address correspondence to Axel Schulz, axel.schulz@uni-rostock.de

The intermediate 3^+ could be trapped by a formal [4+2] cycloaddition reaction with dimethylbutadiene (dmb), resulting in a bicyclic tetraphosphaoctenium cation (5^+ ; Figure 2, right), which is comparable to previously reported cyclic phosphino-phosponium cations.^{27–29}

Reduction reactions

Reduction of **2** with Mg selectively afforded the *exo-exo* isomer of the bicyclic tetraphosphane $\text{Mes}^*\text{P}_4\text{Mes}^*$ (**6a**; Scheme 3, top) in good yields (73 %).³⁰ Compound **6** had previously been prepared by reacting a mixture of Mes^*Br and Mes^*Li with white phosphorus, though merely in low yields (5 %).^{21,31} Intriguingly, the carbene promoted degradation of **2** gave rise to the elusive *endo-exo* isomer of $\text{Mes}^*\text{P}_4\text{Mes}^*$ (**6b**; Scheme 3, bottom),³⁰ which had previously only been characterized spectroscopically.³²



Scheme 3 Starting from **2**, both isomers of the bicyclic tetraphosphane **6** can be obtained selectively.

Both isomers of **6** were fully characterized. In the ^{31}P NMR spectrum, **6a** is characterized by an A_2X_2 pattern ($\delta_{\text{exptl}} = -273.2, -128.3$ ppm; $\delta_{\text{calcd}} = -271.5, -138.0$ ppm), while **6b** displays an A_2MX spin system ($\delta_{\text{exptl}} = -220.4, -94.8, -54.7$ ppm; $\delta_{\text{calcd}} = -217.8, -100.2, -68.0$ ppm). The molecular structure was determined by single crystal X-ray diffraction. In both isomers, the overall structure of the P_4 scaffold is rather similar. The fold angle of the bicyclus in the *endo-exo* isomer is significantly larger (108°) than in the *exo-exo* isomer (96°), presumably due to Pauli repulsion between the *endo*- Mes^* substituent and the *ortho*-*t*-Bu groups of the *exo*- Mes^* group (Figure 3).

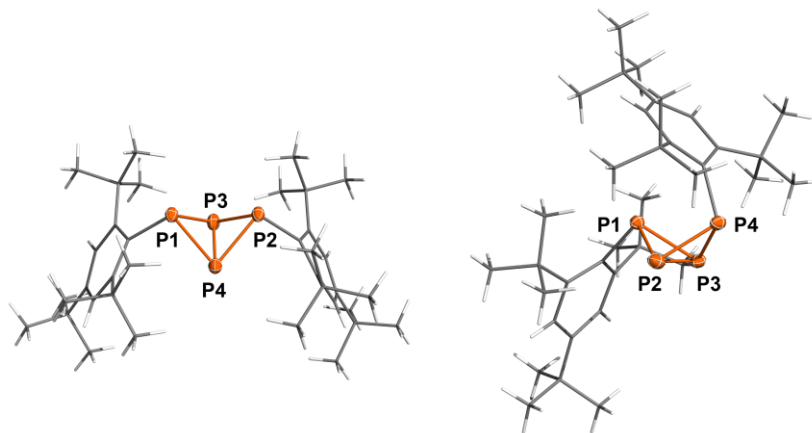


Figure 3 Molecular structure of **6a** (left) and **6b** (right) in the crystal. Ellipsoids are set at 50% probability (173 K).

Selected bond lengths [Å] and angles [°]: **6a** P1–P3 2.2310(7), P1–P4 2.2171(7), P2–P3 2.2294(7), P2–P4 2.2236(7), P3–P4 2.1634(8); P1–P3–P4–P2 –95.66(3); **6b** P1–P2 2.2244(7), P1–P3 2.2326(8), P2–P4 2.2131(8), P3–P4 2.2101(8), P2–P3 2.1773(8); P1–P2–P3–P4 107.78(3).

In conclusion, the synthesis of the *cyclo*-phosphane **2** was newly developed and subsequently improved to make it readily available for synthetic use. The introduction of reactive P–Cl bonds directly at the ring system gave rise to fascinating follow-up chemistry by abstraction or reductive elimination of the Cl atoms, affording new preparative routes to known as well as unprecedented phosphorus ring systems. This nicely demonstrates the potential of our synthetic approach. To extend the product spectrum, the reactivity of **2** towards Lewis bases and transition metals is currently under investigation.

REFERENCES

- 1 Stahl, L. *Coord. Chem. Rev.* **2000**, 210, 203.
- 2 Balakrishna, M. S.; Eisler, D. J.; Chivers, T. *Chem. Soc. Rev.* **2007**, 36, 650.
- 3 He, G.; Shynkaruk, O.; Lui, M. W.; Rivard, E. *Chem. Rev.* **2014**, 114, 7815.
- 4 Scherer, O. J. *Comm. Inorg. Chem.* **1987**, 6, 1.
- 5 Baudler, M.; Glinka, K. *Chem. Rev.* **1993**, 93, 1623.
- 6 Scheer, M.; Balázs, G.; Seitz, A. *Chem. Rev.* **2010**, 110, 4236.
- 7 Giffin, N. A.; Masuda, J. D. *Coord. Chem. Rev.* **2011**, 255, 1342.
- 8 Cossairt, B. M.; Piro, N. A.; Cummins, C. C. *Chem. Rev.* **2010**, 110, 4164.
- 9 Masuda, J. D.; Schoeller, W. W.; Donnadiou, B.; Bertrand, G. *Angew. Chem. Int. Ed.* **2007**, 46, 7052.
- 10 Masuda, J. D.; Schoeller, W. W.; Donnadiou, B.; Bertrand, G. *J. Am. Chem. Soc.* **2007**, 129, 14180.

Received xx yyyy 2015; accepted xx yyyy 2015

The authors wish to thank the Fonds der Chemischen Industrie (scholarship for JB) and the Deutsche Forschungsgemeinschaft (SCHU 1170/11-1) for financial support.

Address correspondence to Axel Schulz, axel.schulz@uni-rostock.de

A VERSATILE REAGENT IN PHOSPHORUS CHEMISTRY

- 11 Heintl, S.; Reisinger, S.; Schwarzmaier, C.; Bodensteiner, M.; Scheer, M. *Angew. Chem. Int. Ed.* **2014**, *53*, 7639.
- 12 Heintl, S.; Scheer, M. *Chem. Sci.* **2014**, *5*, 3221.
- 13 Borger, J. E.; Ehlers, A. W.; Lutz, M.; Slootweg, J. C.; Lammertsma, K. *Angew. Chem. Int. Ed.* **2014**, *53*, 12836.
- 14 Wiberg, N.; Wörner, A.; Lerner, H.-W.; Karaghiosoff, K. *Z. Naturforsch. B* **2002**, *57*, 1027.
- 15 Lorbach, A.; Nadj, A.; Tüllmann, S.; Dornhaus, F.; Schödel, F.; Sänger, I.; Margraf, G.; Bats, J. W.; Bolte, M.; Holthausen, M. C.; Wagner, M.; Lerner, H. *Inorg. Chem.* **2009**, *48*, 1005.
- 16 Niecke, E.; Nieger, M.; Reichert, F. *Angew. Chem. Int. Ed. Engl.* **1988**, *27*, 1715.
- 17 Bresien, J.; Hering, C.; Schulz, A.; Villinger, A. *Chem. Eur. J.* **2014**, *20*, 12607.
- 18 Bresien, J.; Faust, K.; Schulz, A.; Villinger, A. *Angew. Chem. Int. Ed.* **2015**, *54*, 6926.
- 19 Holthausen, M. H.; Surmiak, S. K.; Jerabek, P.; Frenking, G.; Weigand, J. J. *Angew. Chem. Int. Ed.* **2013**, *52*, 11078.
- 20 Niecke, E.; Rüger, R.; Krebs, B. *Angew. Chem. Int. Ed. Engl.* **1982**, *21*, 544.
- 21 Riedel, R.; Hausen, H.-D.; Fluck, E. *Angew. Chem. Int. Ed. Engl.* **1985**, *24*, 1056.
- 22 Power, M. B.; Barron, A. R. *Angew. Chem. Int. Ed. Engl.* **1991**, *30*, 1353.
- 23 Bezombes, J.-P.; Hitchcock, P. B.; Lappert, M. F.; Nycz, J. E. *Dalton Trans.* **2004**, 499.
- 24 Fox, A. R.; Wright, R. J.; Rivard, E.; Power, P. P. *Angew. Chem. Int. Ed.* **2005**, *44*, 7729.
- 25 Donath, M.; Conrad, E.; Jerabek, P.; Frenking, G.; Fröhlich, R.; Burford, N.; Weigand, J. J. *Angew. Chem. Int. Ed.* **2012**, *51*, 2964.
- 26 Glendening, E. D.; Badenhop, J. K.; Reed, A. E.; Carpenter, J. E.; Bohmann, J. A.; Morales, C. M.; Weinhold, F. *NBO 5.9*, Theoretical Chemistry Institute, University of Wisconsin, Madison, **2011**.
- 27 Burford, N.; Dyker, C. A.; Lumsden, M.; Decken, A. *Angew. Chem. Int. Ed.* **2005**, *44*, 6196.
- 28 Dyker, C. A.; Burford, N.; Menard, G.; Lumsden, M. D.; Decken, A. *Inorg. Chem.* **2007**, *46*, 4277.
- 29 Weigand, J. J.; Burford, N.; Davidson, R. J.; Cameron, T. S.; Seelheim, P. *J. Am. Chem. Soc.* **2009**, *131*, 17943.
- 30 Bresien, J.; Faust, K.; Hering-Junghans, C.; Rothe, J.; Schulz, A.; Villinger, A. *Dalt. Trans.* **2016**, DOI: 10.1039/C5DT02757H.
- 31 Fluck, E.; Riedel, R.; Hausen, H.-D.; Heckmann, G. *Zeitschrift fuer Anorg. und Allg. Chemie* **1987**, *551*, 85.
- 32 Jutzi, P.; Meyer, U. *J. Organomet. Chem.* **1987**, *333*, C18.

Received xx yyyy 2015; accepted xx yyyy 2015

The authors wish to thank the Fonds der Chemischen Industrie (scholarship for JB) and the Deutsche Forschungsgemeinschaft (SCHU 1170/11-1) for financial support.

Address correspondence to Axel Schulz, axel.schulz@uni-rostock.de

7.2 Source Code of the Submission Script

The script presented in the following uses the application programming interface (API) of the SLURM workload manager to queue Gaussian jobs and should therefore work on any cluster computer with that software after slight modifications (paths, resource limits, environment variables etc.)

```
#!/bin/bash

# Script created by Jonas Bresien
# Department of Chemistry, Lab 114, Tel. 6392
# Script version: 3.2
# Last update: 2015-06-09

Script_Name="$(/bin/basename "$0")"
Script_FullPath="$(/bin/readlink -e "$0")"

# Function definitions

esc_sed() {
    local str=$@
    echo -n "$( /bin/sed -r 's/\\/\\/\\/\\/ig;s/\\/\\/\\/\\/ig' <<< "$str")"
}

in_array() {
    local str2="$1"
    local array="$2"

    for str1 in "${array[@]}"; do
        test "$str1" = "$str2" && echo 0 && return 0
    done
    echo 1 && return 1
}

trim() {
    local var=$@
    var="${var%${var%[![:space:]]*}}" # remove leading whitespace ↴
                                     characters
    var="${var%${var##*[![:space:]]}}" # remove trailing whitespace ↴
                                     characters
    echo -n "$var"
}

#####
#                                     #
# Input processing - interactive part #
#                                     #
#####
```

```

if [ ! -n "$SLURM_JOB_ID" ] ; then

    # Default values (do not change)

    email=""           # E-mail address
    proc=1             # Number of processor cores
    proc_max=20        # Max. number of processor cores
    mem=0              # RAM (MB)
    mem_max_cpu=3150   # Max. RAM per core (MB)
    tcpu=72            # Time limit (h)
    tcpu_max=72        # Max. time limit (h)
    tsig=20            # Signal before time limit (min)
    after_job=""       # Execute only if the specified job terminated
                        # successfully (#ID)

    # Get options

    while getopts ":a:e:s:t:h" opt ; do
        case $opt in
            a)
                if [[ "$OPTARG" =~ ^[0-9]+$ ]] ; then after_job="$OPTARG" ; fi
                ;;
            e)
                email="$OPTARG"
                ;;
            s)
                if [ "$OPTARG" -ge 10 -a "$OPTARG" -le 120 ] ; then
                    tsig=$OPTARG
                else
                    echo -e "\n $Script_Name -s: Please enter a value between 10 ↵
                    and 120 minutes.\n"
                    exit 1
                fi
                ;;
            t)
                if [ "$OPTARG" -ge 1 -a "$OPTARG" -le $tcpu_max ] ; then
                    tcpu=$OPTARG
                else
                    echo -e "\n $Script_Name -t: Maximum time is $tcpu_max ↵
                    hours.\n"
                    exit 1
                fi
                ;;
            h)
                echo -e "\n $Script_Name: Usage\n\n -e Specify your e-mail ↵
                address (e.g. -e name@provider.org)\n        Alternatively, you ↵
                may save your e-mail address in ~/email_addr\n -t CPU time in ↵
                hours (unfinished jobs will be resubmitted automatically)\n ↵
                -s Signal time in minutes (time frame for all checkpointing ↵
                operations, default is 20)\n -a Execute only AFTER successful ↵
                completion of the specified job (ID)\n -h Show this help\n\n ↵
                Example: $Script_Name -e name@provider.org -t 24 input.com\n\n ↵

```

```

        To check the progress of running jobs, use the command ↵
        'check_g09'\n"
    exit 1
    ;;
\?)
    echo -e "\n $Script_Name:  Invalid option: -$OPTARG\n"
    exit 1
    ;;
:)
    echo -e "\n $Script_Name:  Option -$OPTARG requires an ↵
    argument.\n"
    exit 1
    ;;
esac
done

shift $(( $OPTIND - 1 ))

if [ $# -ne 1 ] ; then
    echo -e "\n Usage: $Script_Name [options] <input file>\n Type ↵
    $Script_Name -h for more information.\n"
    exit 1
fi

# Signal time ($tsig) must be less than 1/3 of the time limit ($tcpu)

if [ $tsig -gt $(( $tcpu * 20 )) ] ; then
    echo -e "\n $Script_Name:  The signal time (-s) cannot be larger ↵
    than a third of the time limit (-t).\n"
    exit 1
fi

# Locate input file on disk

INP_FILE="$(/bin/readlink -e "$1")"

if [ ! -n "$INP_FILE" ] ; then
    echo -e "\n $Script_Name:  The specified file \"$1\" does not exist!\n"
    exit 1
fi

INP_NAME="$(/bin/basename "$INP_FILE")"
INP_DIR="$(/usr/bin/dirname "$INP_FILE")"
shopt -s extglob
INP_NAME="${INP_NAME%.*?(com|gjf|inp|restart)}"
shopt -u extglob
INP_SCRIPT="$INP_DIR/$INP_NAME.qsub"

# Get e-mail address (may be saved in ~/email_addr)

Email_File="$(/bin/readlink -e ~/email_addr)"

if [ ! -n "$email" -a -e "$Email_File" ] ; then
    email="$(<"$Email_File")"

```

```

elif [ ! -n "$email" ] ; then
    echo -e "\n $Script_Name: No e-mail address specified. Please do!\n"
    exit 1
fi

# Load input file and convert Windows line breaks (\r\n) to Linux/Unix ↵
format (\n)

Inp_Content="$(<"$INP_FILE")"
Inp_Content="$(/bin/sed -r 's/\r//ig' <<< "$Inp_Content")"

# "Restart" implemented in Gaussian does not support multi step jobs ↵
(--Link1--)
# => Exit if multi step job was submitted

if [ -n "$(/bin/grep -i "\-Link1\-" <<< "$Inp_Content")" ] ; then
    echo -e "\n $Script_Name: Unfortunately, multi step jobs (--Link1--) ↵
are not supported\n at the moment due to limitations of Gaussian's ↵
RESTART functionality.\n"
    exit 1
fi

# Read %nproc and %mem

inp_nproc="$(/bin/sed -n -r
's/^\s*%nproc(s|shared)?\s*=\s*(\w+)\s*$/\2/ip' <<< "$Inp_Content")"

if [ -n "$inp_nproc" ] ; then
    if [ "$inp_nproc" -ge 1 -a "$inp_nproc" -le $proc_max ] ; then
        proc=$inp_nproc
    else
        echo -e "\n $Script_Name: Number of processors must be between 1 ↵
and $proc_max.\n"
        exit 1
    fi
fi

inp_mem="$(/bin/sed -n -r 's/^\s*%mem\s*=\s*(\w+)\s*$/\1/ip' <<< ↵
"$Inp_Content")"

if [ -n "$inp_mem" ] ; then
    # Values are only interpreted if given in KB, MB or GB
    inp_mem="$(/bin/sed -n -r 's/^(.+)\s*(gb|mb|kb)$/1:\2/ip' <<< ↵
"$inp_mem")"

    if [ -n "$inp_mem" ] ; then
        inp_mem_unit="$(/bin/cut -d: -f2 <<< $inp_mem)"
        inp_mem_unit="{inp_mem_unit^^}"
        inp_mem="$(/bin/cut -d: -f1 <<< $inp_mem)"

        # Convert to MB
        case "$inp_mem_unit" in
            GB) inp_mem=$(( $inp_mem * 1024 )) ;;
            KB) inp_mem=$(( $inp_mem / 1024 )) ;;
        esac
    fi
fi

```

```

    esac

    # Test if requested RAM complies to mem-per-cpu limit
    if [ "$inp_mem" -ge 1 -a "$(((($inp_mem+2048)/$proc))" -le ↓
$mem_max_cpu ] ; then
        mem=$inp_mem
    else
        echo -e "\n $Script_Name: Error: Requested amount of RAM ↓
($inp_mem MB) exceeds available memory.\n          RAM ↓
available for $proc CPU(s): $((($mem_max_cpu*$proc-2048)) MB.\n"
        exit 1
    fi
else
    echo -e "\n $Script_Name: The memory requirement in the input ↓
file (%mem) must be given in KB, MB or GB.\n"
    exit 1
fi
else
    echo -e "\n $Script_Name: No memory requirement specified.\n"
    exit 1
fi

# Save SLURM script
# #SBATCH --mem-per-cpu=$(((($mem+2048)/$proc))

echo "#!/bin/bash
#SBATCH -J \"g09_{$INP_NAME}_$$\"
#SBATCH -e \"g09_{$INP_NAME}.slurm_%j\"
#SBATCH -o \"g09_{$INP_NAME}.slurm_%j\"
#SBATCH -D \"{$INP_DIR}\"
#SBATCH -p shared_mem
#SBATCH -N1
#SBATCH -n1
#SBATCH --open-mode=append
#SBATCH --cpus-per-task=$proc
#SBATCH --mem-per-cpu=$mem_max_cpu
#SBATCH --time=$((($tcpu*60))
#SBATCH --mail-type=ALL
#SBATCH --mail-user=$email
#SBATCH --signal=B:USR1@$(($tsig*60))
$(test -n "$after_job" && echo "#SBATCH -d afterok:$after_job")

INP_FILE=\"{$INP_FILE}\"
INP_NAME=\"{$INP_NAME}\"
INP_DIR=\"{$INP_DIR}\"
INP_SCRIPT=\"{$INP_SCRIPT}\"

INP_MEM=\"{$mem}\"
INP_PROC=\"{$proc}\"

. $Script_FullPath" > "{$INP_SCRIPT"

sbatch "{$INP_SCRIPT"

```

```

#####
#                               #
# Run Gaussian - static part #
#                               #
#####

else

Local_Directory="/local/$USER.$SLURM_JOB_ID"
Scratch_Directory="/local/$USER.$SLURM_JOB_ID/scratch"

Inp_INP="$Local_Directory/$INP_NAME.com"
Out_File="$Local_Directory/$INP_NAME.log"

# Load input file and convert Windows line breaks (\r\n) to Linux/Unix ↵
format (\n)

if [ ! -e "$INP_FILE" ] ; then
    echo "$Script_Name: No input file found"
    exit 1
fi

Inp_Content="$(<"$INP_FILE")"
Inp_Content="$(/bin/sed -r 's/\r//ig' <<< "$Inp_Content")"

# Find checkpoint file

inp_chk="$(/bin/sed -n -r 's/^\s*%chk\s*=\s*"?(["^"]+)"?\s*$/\1/ip' <<< ↵
"$Inp_Content")"
inp_chk="$(trim "$inp_chk")"
if [ -n "$inp_chk" ] ; then

    # Locate checkpoint file on disk
    if [ -e "$inp_chk" ] ; then

        # Save absolute path
        Inp_Chk_File="$(/bin/readlink -e "$inp_chk")"
        Out_Chk_File="$Inp_Chk_File"
        Local_Chk_File="$Local_Directory/$(/bin/basename "$inp_chk")"

    # Create new chk file if non-existent
    else
        Out_Chk_File="$INP_DIR/$(/bin/basename "$inp_chk")"
        Local_Chk_File="$Local_Directory/$(/bin/basename "$inp_chk")"
    fi

    # Update chk path(s) in input
    local_chk="$(esc_sed "$Local_Chk_File")"
    Inp_Content="$(/bin/sed -r 's/%chk\s*=\s*.\s*%/chk='"$local_chk"' ↵
/ig' <<< "$Inp_Content")"

# Create checkpoint file if none is specified
# Needed to enable RESTART functionality

```

```

else
    Out_Chk_File="$INP_DIR/$INP_NAME.chk"
    Local_Chk_File="$Local_Directory/$INP_NAME.chk"
    Inp_Content="%chk=$Local_Chk_File\n%nosave\n$Inp_Content"
fi

# Find read-write file (RWF)

inp_rwf="$(/bin/sed -n -r 's/^\s*%rwf\s*=\s*"?([\^"]+)"?\s*$/\1/ip' <<< ↵
"$Inp_Content")"
inp_rwf="$(trim "$inp_rwf")"
if [ -n "$inp_rwf" ] ; then

    # Locate RWF on disk
    if [ -e "$inp_rwf" ] ; then

        # Save absolute path
        Inp_Rwf_File="$(/bin/readlink -e "$inp_rwf")"
        Out_Rwf_File="$Inp_Rwf_File"
        Local_Rwf_File="$Local_Directory/$(/bin/basename "$inp_rwf")"

    # Create new RWF if non-existent
    else
        Out_Rwf_File="$INP_DIR/$(/bin/basename "$inp_rwf")"
        Local_Rwf_File="$Local_Directory/$(/bin/basename "$inp_rwf")"
    fi

    # Update RWF path(s) in input
    local_rwf="$(esc_sed "$Local_Rwf_File")"
    Inp_Content="$(/bin/sed -r 's/%rwf\s*=\s*.\s*/%rwf='"$local_rwf"' ↵
/ig' <<< "$Inp_Content")"

# Create read-write file if none is specified
# Needed to enable RESTART functionality

else
    Out_Rwf_File="$INP_DIR/$INP_NAME.rwf"
    Local_Rwf_File="$Local_Directory/$INP_NAME.rwf"
    Inp_Content="%rwf=$Local_Rwf_File\n%nosave\n$Inp_Content"
fi

# Some more infos needed for RESTART ...
# Determine whether CHK and RWF should be saved after job completion ↵
(%nosave) as defined by user

ln_nosave="$(/bin/grep -ni '%nosave' <<< "$Inp_Content" | ↵
/usr/bin/tail -n1 | /bin/cut -d: -f1)"
ln_chk="$(/bin/grep -ni '%chk' <<< "$Inp_Content" | /bin/cut -d: -f1)"
ln_rwf="$(/bin/grep -ni '%rwf' <<< "$Inp_Content" | /bin/cut -d: -f1)"

test ! -n "$ln_nosave" && ln_nosave=0

if [ "$ln_nosave" -gt "$ln_chk" ] ; then save_chk=0 ; else save_chk=1

```

```

fi
if [ "$ln_nosave" -gt "$ln_rwf" ] ; then save_rwf=0 ; else save_rwf=1
fi

#####
# Copy all necessary files to the node ... #
#####

# Create temporary local directory on the node filesystem

/bin/mkdir -m 700 "$Local_Directory"
cd "$Local_Directory"

# Create appropriate Gaussian input (i.e. INPUT or RESTART file)

if [ ! -n "$SLURM_RESTART_COUNT" ] ; then
  # Create new temporary input file including local paths
  echo -e "$Inp_Content\n" > "$Inp_INP"
else
  # Save RESTART input
  echo -e "%rwf=\"$Local_Rwf_File\" ↵
          $(test "$save_rwf" -eq 0 && echo -e "\n%nosave")
          %chk=\"$Local_Chk_File\" ↵
          $(test "$save_chk" -eq 0 && echo -e "\n%nosave")
          %nproc=$INP_PROC
          %mem=${INP_MEM}MB
          #P Restart\n" > "$Inp_INP"
  Out_File="$Local_Directory/$INP_NAME-$SLURM_RESTART_COUNT.log"
  Inp_Rwf_File="$Out_Rwf_File"
  Inp_Chk_File="$Out_Chk_File"
fi

sig=0
err=0

# Requeue if time limit is exceeded

trap "sig=1 ; echo \"$Script_Name: Time limit exceeded\"
      cd /local
      /bin/rm -rf \"$Scratch_Directory\"           # This will cause ↵
                                                  Gaussian to terminate

      /bin/rm -f \"$Inp_INP\"
      test -n \"$Inp_Chk_File\" && /bin/mv -f \"$Local_Chk_File\" ↵
      \"$Inp_Chk_File\"
      test -n \"$Inp_Rwf_File\" && /bin/mv -f \"$Local_Rwf_File\" ↵
      \"$Inp_Rwf_File\"
      /bin/mv -f $Local_Directory/* \"$INP_DIR\"
      /bin/rm -rf \"$Local_Directory\"
      scontrol requeue $SLURM_JOB_ID && echo \"$Script_Name: Job ↵
      #$SLURM_JOB_ID was requeued\"
      exit 1" USR1

# Delete local data if job is cancelled by user (scancel)

```

```

trap "sig=1 ; echo \"\$Script_Name: Terminated by SIGTERM\"
      cd /local
      /bin/rm -rf \"\$Local_Directory\"
      exit 1" TERM

trap "sig=1 ; echo \"\$Script_Name: Terminated by SIGKILL\" ; cd ↵
      /local ; /bin/rm -rf \"\$Local_Directory\" ; exit 1" KILL

# Copy CHK and RWF files to local directory

test -n "$Inp_Chk_File" && /bin/cp -f "$Inp_Chk_File" "$Local_Chk_File"
test -n "$Inp_Rwf_File" && /bin/cp -f "$Inp_Rwf_File" "$Local_Rwf_File"

# Set up Gaussian environment and execute Gaussian job

/bin/mkdir -m 700 "$Scratch_Directory"
export g09root=/apps/Gaussian
export GAUSS_SCRDIR="$Scratch_Directory"
. /apps/Gaussian/g09/bsd/g09.profile

cd "$Local_Directory"
g09 <"$Inp_INP" 1>"$Out_File" || err=1

# Move results back to /data directory

if [ $sig -eq 0 ] ; then

    /bin/rm -rf "$Scratch_Directory"
    /bin/rm -f "$Inp_INP"

    if [ -n "$Inp_Chk_File" -a "$save_chk" -eq 1 ] ; then
        /bin/mv -f "$Local_Chk_File" "$Inp_Chk_File"
    elif [ "$save_chk" -eq 0 ] ; then
        test ! -e "$Local_Chk_File" -a -e "$Out_Chk_File" && /bin/rm -f ↵
        "$Out_Chk_File"
    fi

    if [ -n "$Inp_Rwf_File" -a "$save_rwf" -eq 1 ] ; then
        /bin/mv -f "$Local_Rwf_File" "$Inp_Rwf_File"
    elif [ "$save_rwf" -eq 0 ] ; then
        test ! -e "$Local_Rwf_File" -a -e "$Out_Rwf_File" && /bin/rm -f ↵
        "$Out_Rwf_File"
    fi

    /bin/mv -f $Local_Directory/* "$INP_DIR"

# Delete all temporary files on node and in input directory

cd /local
/bin/rm -rf "$Local_Directory"
/bin/rm -f "$INP_SCRIPT"

fi

```

```
# Return exit code 1 if Gaussian ran into a problem

if [ $err -eq 1 ] ; then
    echo "$Script_Name: Calculation failed; please check the Gaussian09 ↵
    log file for further information"
    exit 1
fi

fi
```